

# UC Berkeley

## Sustainability, Whole Building Energy and Other Topics

### Title

Performance, Prediction and Optimization of Night Ventilation across Different Climates

### Permalink

<https://escholarship.org/uc/item/6n99w3bx>

### Author

Landsman, Jared

### Publication Date

2016-04-01

Performance, Prediction and Optimization of Night Ventilation across  
Different Climates

By  
Jared Paul Landsman

A thesis submitted in partial satisfaction of the  
requirements for the degree of  
Master of Science  
in  
Architecture  
in the  
Graduate Division  
of the  
University of California, Berkeley

Committee in charge:  
Professor Gail S. Brager, Chair  
Professor Stefano Schiavon  
Professor Scott Moura

Spring 2016



## Abstract

### Performance, Prediction and Optimization of Night Ventilation across Different Climates

by

Jared Paul Landsman

Master of Science in Architecture

University of California, Berkeley

Professor Gail S. Brager, Chair

Night ventilation, or night flushing, is a passive cooling technique that utilizes the outdoor diurnal temperature swing and the building's thermal mass to pre-cool a building through increased outdoor airflow at night, allowing radiant cooling to take place during the day when the building is occupied. Previous studies have demonstrated a potential reduction in cooling load and improvement in comfort from the implementation of night ventilation. However, very few field studies have been done looking at the impact of location and climate on night ventilation performance.

This thesis describes the performance, in terms of indoor environmental conditions, of three buildings from both the U.S. and India that use night ventilation as their primary cooling method. The analysis is based on monitored data collected from each building (ranging in duration from two months to one year), including indoor and outdoor air temperature, mass temperature, supply temperature, and airflow rate. The first building, located in Oakland, California, uses forced ventilation at night to increase the airflow. The second building, located in Sunnyvale, California, uses natural ventilation by means of automated windows. The third building, in Auroville, India, uses natural ventilation by means of occupant-controlled windows. The research methods used the following approach: 1) Assess the cooling strategy by comparing indoor conditions from days that did and did not use night ventilation, specifically in relation to the adaptive comfort model; 2) Develop a hybrid model, using both first principle equations and the collected data, to predict the instantaneous air and mass temperatures within each building; 3) Determine an optimized ventilation control strategy for each building to minimize energy and maintain comfortable temperatures.

The study yielded the following results: 1) The buildings in the mild climate are successfully keeping the indoor temperature low, but also tend to be overcooling; 2) The night ventilation strategy has very little impact on the indoor conditions of the buildings in the mild climate; 3) The impact of night ventilation is less significant when there is low internal loads and heavy mass; 4) The building in the hot and humid climate is keeping the indoor temperature within the comfort bounds for 88% of the year; 5) The night ventilation strategy has advantageous impact on indoor conditions of the building in the hot and humid climate, but not enough to cool the space on its own; 6) Model predictive control has the potential to further improve the performance of night ventilation.

# Table of Contents

List of figures.....	iv
List of tables.....	vi
List of equations .....	vii
List of acronyms.....	viii
Acknowledgements .....	ix
<b>1. Introduction.....</b>	<b>1</b>
1.1 Background.....	1
1.2 Problem statement.....	1
<b>2. Research objective .....</b>	<b>2</b>
<b>3. Literature review .....</b>	<b>3</b>
<b>3.1 Night ventilation as a cooling strategy .....</b>	<b>3</b>
3.1.1 Fundamentals of night ventilation .....	3
3.1.2 Types of night ventilation.....	3
3.1.3 Parameters that impact night ventilation .....	4
3.1.4 Benefits of night ventilation .....	5
<b>3.2 Approaches for assessing night ventilation .....</b>	<b>6</b>
3.2.1 Approaches for night ventilation field studies.....	6
3.2.2 Approaches for night ventilation model generation, validation, and optimization.....	8
3.2.3 Approaches for night ventilation performance analysis .....	9
<b>3.3 Findings from previous night ventilation field studies &amp; simulation studies .....</b>	<b>11</b>
<b>4. Methods.....</b>	<b>14</b>
<b>4.1 Building descriptions.....</b>	<b>14</b>
4.1.1 La Escuelita Elementary School.....	14
4.1.2 Indio Building.....	17
4.1.3 Blessing House .....	19
<b>4.2 Data collection &amp; designer/operator interviews.....</b>	<b>20</b>
4.2.1 La Escuelita Elementary School.....	21
4.2.2 Indio Building.....	21
4.2.3 Blessing House .....	22
4.2.4 Interview procedure.....	23
<b>4.3 Model generation .....</b>	<b>25</b>
4.3.1 First principles equations.....	25
4.3.2 Parameter identification.....	26
4.3.3 Model validation.....	30
<b>4.4 Comfort and energy analysis .....</b>	<b>31</b>
4.4.1 Baseline data analysis.....	31
4.4.2 Comparison of night ventilation vs non-night ventilation using real data.....	32
4.4.3 Comparison to comfort standards.....	33
4.4.4 Comparison of night ventilation vs non-night ventilation using model .....	34
<b>4.5 Optimization.....</b>	<b>34</b>
4.5.1 LEES optimization .....	34
4.5.2 BH & IND optimization .....	35

<b>5. Results .....</b>	<b>36</b>
<b>5.1 Baseline data analysis .....</b>	<b>36</b>
5.1.1 La Escuelita Elementary School.....	36
5.1.2 Indio Building.....	40
5.1.3 Blessing House .....	43
<b>5.2 Comparison to comfort standards .....</b>	<b>47</b>
5.2.1 La Escuelita Elementary School.....	47
5.2.2 Indio Building.....	48
5.2.3 Blessing House .....	48
<b>5.3 Comparison of night ventilation vs non-night ventilation using real data .....</b>	<b>49</b>
5.3.1 La Escuelita Elementary School.....	49
5.3.2 Indio Building.....	53
5.3.3 Blessing House .....	54
<b>5.4 Model selection.....</b>	<b>56</b>
5.4.1 La Escuelita Elementary School.....	56
5.4.2 Indio Building.....	58
5.4.3 Blessing House .....	59
<b>5.5 Comparison of night ventilation vs non-night ventilation using model data .....</b>	<b>60</b>
5.5.1 La Escuelita Elementary School.....	60
5.5.2 Indio Building.....	61
5.5.3 Blessing House .....	61
<b>5.6 Optimization.....</b>	<b>63</b>
5.6.1 La Escuelita Elementary School.....	63
5.6.2 Indio Building.....	63
5.6.3 Blessing House .....	63
<b>5.7 Designer &amp; operator interviews .....</b>	<b>67</b>
5.7.1 La Escuelita Elementary School.....	67
5.7.2 Indio Building.....	68
5.7.3 Blessing House .....	68
<b>Discussion.....</b>	<b>70</b>
6.1 Performance of night ventilation in LEES .....	70
6.2 Performance of night ventilation in IND .....	71
6.3 Performance of night ventilation in BH.....	72
6.4 Comparison of case studies .....	72
6.5 Limitations to study.....	74
<b>7. Conclusions.....</b>	<b>76</b>
<b>8. Future work.....</b>	<b>77</b>
8.1 Daytime ventilation.....	77
8.2 Ceiling fans.....	77
8.3 Morning warmup.....	77
8.4 Impact of high humidity.....	77
8.5 Applicability of ACS.....	77
8.6 Critical internal loads.....	78
8.6 Implement new control strategy .....	78
<b>9. References.....</b>	<b>79</b>
<b>10. Appendices.....</b>	<b>82</b>
10.1 Matlab code.....	82
10.1.1 Window state data conversion.....	82

10.1.2 Persistence of excitation .....	83
10.1.3 Gradient descent method .....	86
10.1.4 Nonlinear least squares method .....	93
10.1.5 Model simulation .....	96
10.1.6 Model error calculation .....	97
10.1.7 K-fold cross validation .....	99
10.1.8 LEES Optimization with comfort as constraint.....	104
10.1.9 LEES Optimization with comfort as objective.....	106
10.1.10 BH & IND Optimization .....	109
<b>10.2 R code .....</b>	<b>114</b>
10.2.1 Heatmap generation.....	114
10.2.2 Boxplot generation .....	115
10.2.3 T-tests .....	118

# List of figures

Figure 1. Oakland annual outdoor air temperature profile .....	14
Figure 2. LEES classroom .....	15
Figure 3. LEES wall construction .....	15
Figure 4. LEES classroom cooling schematic .....	16
Figure 5. Sunnyvale annual outdoor air temperature profile .....	17
Figure 6. IND open-plan office .....	18
Figure 7. IND wall construction .....	18
Figure 8. Auroville annual outdoor air temperature profile .....	19
Figure 9. A) BH roof/ceiling construction; B) BH wall construction .....	20
Figure 10. BH window used for natural ventilation .....	20
Figure 11. Data collection in BH .....	23
Figure 12. Performance metric visualization .....	32
Figure 13. LEES room 233 temperature and airflow profile during and after night ventilation ..	36
Figure 14. LEES room 233 temperature and airflow profile over one week .....	37
Figure 15. LEES room 233 instantaneous damping over one week .....	37
Figure 16. LEES daily maximum indoor air temperature .....	38
Figure 17. LEES daily maximum damping .....	38
Figure 18. LEES daily indoor air temperature range .....	39
Figure 19. LEES daily decrement factor .....	39
Figure 20. LEES area normalized daily energy removed .....	40
Figure 21. LEES daily potential energy efficiency .....	40
Figure 22. IND temperature and window state profile during and after night ventilation .....	41
Figure 23. IND temperature and window state profile over one week .....	42
Figure 24. IND instantaneous damping over one week .....	42
Figure 25. A) IND daily maximum indoor air temperature; B) IND daily maximum damping; C) IND time lag .....	42
Figure 26. A) IND daily indoor air temperature range; B) IND daily decrement factor .....	43
Figure 27. BH temperature and window state profile during and after night ventilation .....	43
Figure 28. BH temperature and window state over one week .....	44
Figure 29. BH instantaneous damping over one week .....	44
Figure 30. BH daily maximum indoor air temperature by season .....	45
Figure 31. BH daily maximum damping by season .....	45
Figure 32. BH daily time lag by season .....	46
Figure 33. BH indoor air temperature range by season .....	46
Figure 34. BH decrement factor by season .....	47
Figure 35. BH energy removed by season .....	47
Figure 36. LEES room 233 operative temperature with ACS limits .....	48
Figure 37. IND operative temperature with ACS limits .....	48
Figure 38. BH operative temperature with ACS & IMAC comfort limits .....	49
Figure 39. LEES daily maximum indoor air temperature with & without night ventilation .....	50
Figure 40. LEES daily maximum damping with & without night ventilation .....	51
Figure 41. LEES daily indoor air temperature range with & without night ventilation .....	51
Figure 42. LEES daily decrement factor with & without night ventilation .....	52
Figure 43. LEES daily energy removed with & without night ventilation .....	52



Figure 44. LEES daily potential energy efficiency with & without night ventilation .....	53
Figure 45. LEES daily discomfort degree hours below minimum ACS limit with & without night ventilation .....	53
Figure 46. IND daily time lag with & without night ventilation .....	54
Figure 47. BH daily maximum indoor air temperature with & without night ventilation.....	55
Figure 48. Real and simulated data in LEES room 110.....	58
Figure 49. BH simulation daily maximum indoor air temperature with & without night ventilation .....	62
Figure 50. BH simulation daily maximum damping with & without night ventilation.....	62
Figure 51. BH simulation daily discomfort degree hours above maximum ACS limit with & without night ventilation .....	63
Figure 52. BH measured, optimized, & no NV operative temperature .....	64
Figure 53. BH daily maximum indoor air temperature, measured, optimized, & no NV .....	65
Figure 54. BH daily maximum damping, measured, optimized, & no NV .....	65
Figure 55. BH daily discomfort degree hours above maximum ACS limit, measured, optimized, & no NV.....	66
Figure 56. BH daily indoor air temperature range, measured, optimized, & no NV .....	66
Figure 57. BH daily decrement factor, measured, optimized, & no NV .....	67
Figure 58. Daily maximum damping for each case study .....	73
Figure 59. Daily time lag for each case study.....	74

## List of tables

Table 1. LEES classroom physical and system parameters .....	17
Table 2. Model nomenclature .....	25
Table 3. Differences and p-values for LEES real data performance metrics.....	50
Table 4. Differences and p-values for IND real data performance metrics .....	54
Table 5. Differences and p-values for BH real data performance metrics.....	55
Table 6. Final parameters for LEES model .....	57
Table 7. LEES model error for training data .....	57
Table 8. LEES model error for validation data.....	57
Table 9. Final parameters for IND model .....	59
Table 10. IND model error.....	59
Table 11. Final parameters for BH model .....	60
Table 12. BH model error .....	60
Table 13. Differences and p-values for BH simulated data performance metrics .....	61
Table 14. Differences and p-values for BH optimized data performance metrics.....	64
Table 15. Differences and p-values across case study measured data performance metrics .....	73

# List of equations

Equation 1. Climatic Cooling Potential .....	10
Equation 2. General form of dynamical equations .....	26
Equation 3. Persistence of excitation formula .....	26
Equation 4. Gradient descent normalization value .....	27
Equation 5. Gradient descent normalized estimation error.....	27
Equation 6. Gradient descent cost criteria .....	27
Equation 7. Gradient descent update law.....	27
Equation 8. Nonlinear least squares P matrix calculation.....	27
Equation 9. Nonlinear least squares cost criteria .....	27
Equation 10. Nonlinear least squares update law .....	27
Equation 11. General formula for model simulation .....	27
Equation 12. MAE & SDAE calculation .....	28
Equation 13. MAPE & SDAPE calculation.....	28
Equation 14. RMSE calculation.....	28
Equation 15. CVRMSE calculation .....	28
Equation 16. Base case dynamical equations .....	29
Equation 17. Airflow/supply temperature case replacement term.....	29
Equation 18. Stacked room case additional terms .....	29
Equation 19. Solar radiation case additional terms.....	29
Equation 20. Internal load case additional terms .....	30
Equation 21. Linearization formula .....	30
Equation 22. Linearized dynamical equations with inputs of airflow and supply temperature....	30
Equation 23. Instantaneous Damping .....	31
Equation 24. Daily maximum damping .....	31
Equation 25. Daily indoor temperature range.....	31
Equation 26. Decrement factor .....	31
Equation 27. Time lag.....	32
Equation 28. A) Daily energy removed, B) Area normalized daily energy removed .....	32
Equation 29. Potential energy efficiency .....	32
Equation 30. Area weighted surface temperature .....	33
Equation 31. Discomfort degree hours .....	33
Equation 32. Prevailing mean outdoor air temperature .....	33
Equation 33. ACS 80% acceptability limits .....	34
Equation 34. IMAC 80% acceptability limits.....	34
Equation 35. LEES objective function with comfort as constraint.....	34
Equation 36. Optimization constraints.....	35
Equation 37. LEES objective function with comfort as objective.....	35
Equation 38. BH & IND objective function .....	35
Equation 39. BH & IND additional constraint.....	35
Equation 40. Final dynamical equations for LEES model.....	56
Equation 41. Final dynamical equations for IND model .....	58
Equation 42. Final dynamical equations for BH model.....	59

# List of acronyms

Adaptive Comfort Standard (ACS)  
Blessing House (BH)  
Building Management System (BMS)  
Climatic Cooling Potential (CCP)  
Cubic Feet per Minute (CFM)  
Coefficient of Variation of the Root Mean Square Error (CVRMSE)  
Coefficient of Performance (COP)  
Discomfort Degree Hours (DDH)  
Heating, Ventilation, and Air Conditioning (HVAC)  
India Model for Adaptive Comfort (IMAC)  
Indio Building (IND)  
La Escuelita Elementary School (LEES)  
Mean Absolute Error (MAE)  
Mean Absolute Percent Error (MAPE)  
Model predictive control (MPC)  
Persistence of Excitation (PE)  
Pounds per Cubic Foot (PCF)  
Predicted Mean Vote (PMV)  
Predicted Percent Dissatisfied (PPD)  
Root Mean Square Error (RMSE)  
Standard Deviation of Absolute Error (SDAE)  
Standard Deviation of Absolute Percent Error (SDAPE)  
Variable Air Volume (VAV)

# Acknowledgements

I would like to thank the Center for the Built Environment and the Center for Building Energy Research and Development for providing me with funding and provision for this project. Special thanks to Professor Gail Brager for all of her guidance and support throughout the process, and to Professor Stefano Schiavon and Scott Moura for their invaluable technical advice. This thesis is possible due to the insightful and constructive feedback I received from my committee.

My thanks also goes to all of the researchers and staff at the Center for the Built Environment for making themselves available and offering guidance at a moments notice, especially Fred Bauman for sharing his expertise on field study methodology, Paul Raftery for his assistance in data analysis, Frank Chuang for his facilitation of modeling and model optimization, and Carlos Duarte for helping me whenever I was struggling with a problem in R. I also extend my thanks to the researchers at the Energy, Controls, and Applications Lab, especially Eric Burger for guiding me through model generation techniques. Additionally, I want to thank the team at the Centre for Advanced Research in Building Science and Energy for welcoming me with open arms during my visit to Ahmedabad, especially Rajan Rawal and Sanyogita Manu.

Finally, this thesis was made possible thanks to all of the individuals who helped bring these case studies to my attention and collect data for these buildings. This includes Glenn Friedman and Brent Eubanks for the La Escuelita Elementary School, Neil Burger, Shannon Allison, and Eric Sande for 435 Indio Way, and Mona Doctor-Pingel and Vijai Devijai for the Blessing House.

# 1. Introduction

## 1.1 Background

Many developing countries currently undergoing economic growth and urbanization are also experiencing increased energy consumption due to the following of western design practices, such as mechanical cooling. For example, the number of households in Malaysia with air conditioning increased from 13,000 to 775,000 between 1970 and 2000, while sales of air conditioners in China doubled from 2009 to 2014, and air conditioner sales are growing at 20% each year in India. (Kubota, Chyee, and Ahmad 2009; Davis and Gertler 2015; McNeil and Letschert 2008). In the developed world, cooling demands have also been on the rise, especially in commercial buildings. These high cooling demands have occurred, in part, as a result of trends towards increased glazing in buildings, allowing higher solar loads (Artmann, Manz, and Heiselberg 2007). While improvements in glazing properties have helped reduce solar loads, there has also been a rise in internal gains in commercial buildings as a result of an increase in computer use and other plug loads, and higher occupant densities. The prevalence of air conditioning in both the developed and developing world has led to a reliance on mechanical cooling, which in turn has the consequence of increased comfort expectations. As the developing world, especially areas with a hot climate, continues to urbanize and their energy regulations continue to get more stringent, it will become even more necessary to find low-energy solutions to cooling before the use of mechanical cooling becomes the norm all over the world, which would inevitably increase global energy consumption.

There are a number of passive design strategies that have been used for centuries that have the ability to maintain occupant comfort without the use of any mechanical cooling, in a range of suitable climate conditions. Passive strategies use favorable outdoor conditions to provide comfortable interiors through climate-responsive design. It is well known that passive building design can reduce energy consumption. For low- or zero-net energy buildings, passive architectural design is an essential part of load-reduction, and these are critical first steps before consideration of efficient mechanical equipment or renewable sources of energy. As such, passive design can pave the path for low-carbon development.

## 1.2 Problem statement

Although passive design has been used for centuries, it remains an underutilized strategy for contemporary western designers. To promote passive design for this group, it must first be more universally understood. Most practitioners in the field know very little about how these strategies influence energy consumption and occupant comfort. The performance of passive design strategies has been studied for decades, but mostly using simulations of varying sophistication. Of the limited field studies that have taken place, there has been little focus on how these systems were designed or expected to perform. Practitioners are now increasingly incorporating these strategies into their design with the technical capability of doing long term monitoring, specifically with the interest of determining how the systems are performing. This thesis focuses on the performance of one specific passive design strategy, night ventilation, in three real case studies.

## 2. Research objective

The first objective of this study is to understand the control strategy and performance expectations of three real buildings using different night ventilation control strategies (automated mechanical, automated natural, and manual natural) coupled with thermal mass.

The second objective is to make generalizable statements about the performance of night ventilation that can help engineers and architects effectively design for the strategy, specifically with regard to climate, program, level of mass, and type of ventilation system. This is done by assessing the actual performance of each building using measured data with respect to the adaptive comfort model, and by assessing the effect of the strategy on indoor conditions within each building using both measured data and a temperature prediction model.

The third objective is to optimize the ventilation control strategy for each building to minimize the amount of time outside of the comfort bounds.

### 3. Literature review

This literature review focuses on the current state of research on night ventilation as a cooling strategy and how its performance has been assessed in past studies. The section begins with a general overview of the fundamentals, uses, benefits, and different types of night ventilation strategies. It then describes the findings from past studies that are most crucial to the design and practice of night ventilation. Finally, this section goes on to explain the methodology used in previous experiments, specifically covering approaches taken for field studies, model generation, model verification, optimization, and performance analysis.

#### 3.1 Night ventilation as a cooling strategy

##### 3.1.1 Fundamentals of night ventilation

One passive design strategy that has been of interest to researchers for the last 30 years or so is night ventilation, also known as night flushing, night cooling, or nocturnal convective cooling. Night ventilation is a passive or semi-passive cooling technique that utilizes the outdoor diurnal temperature swing and the building's thermal mass to pre-cool a building through increased outdoor airflow at night. At night, when the outdoor air temperature is lower than during the daytime, the increased airflow cools down the mass by convective heat loss, allowing it to release the heat that was stored inside it during the previous day. During the following day, because the surfaces of thermal mass are colder than the surfaces of occupants and equipment inside the space, the cooler mass serves as a heat sink to absorb the heat present in the space from solar and internal loads (Givoni 1992a; M. Santamouris et al. 1996; Artmann, Manz, and Heiselberg 2007).

This strategy differs from the more commonly used direct ventilation, or comfort ventilation, which provides higher indoor air speeds during the day to enhance cooling sensations of building occupants (Givoni 1992a). Night ventilation is indirect in that the building occupants are not cooled directly from the increased airflow, but rather from the cooled mass surfaces. Additionally, this strategy differs from free cooling, which is used as part of an economizer cycle in the mechanical system to assist in chilling water at night, to be used the following day for cooling air, in that night ventilation cools down the thermal mass of a building.

##### 3.1.2 Types of night ventilation

There are three categories of night ventilation, the first of which is natural, or passive, night ventilation. This is the most basic form of the strategy, which simply ventilates the spaces by naturally induced airflow through openings in the building's envelope, typically windows or air vents (Geros et al. 1999). Natural night ventilation can be induced by wind-driven (cross ventilation) or temperature-driven (stack ventilation) pressure differences between the indoor and outdoor environment. This strategy requires the least amount of energy to move the air and requires no mechanical systems, but it is also subject to the most unsystematic patterns of airflow due to its reliance on naturally induced airflow. Natural night ventilation can be done through



automated windows/vents (which require a small amount of energy for actuators) or completely passively through manual occupant control.

The second category is mechanical night ventilation. This form of the strategy utilizes air ducts along with supply and exhaust fans to provide airflow in the space (Geros et al. 1999). During the day, air is supplied into the space at a code-required minimum airflow rate. Although mechanical night ventilation does require a small amount of energy for fan use, it is also a much more controlled and predictable system. The system is completely automated so there is no manual control required from the occupants on a daily basis.

The final category of night ventilation is hybrid ventilation, which is some combination of natural and mechanical night ventilation. This can include the use of natural and mechanical ventilation at different times of the day or year in the same space, at the same time in different rooms, or at the same time in the same space. Hybrid night ventilation can be done by inducing airflow through openings in the envelope in addition to supply and exhaust fans (Geros et al. 1999; Artmann, Manz, and Heiselberg 2007). In some instances, these are two different systems acting in tandem (i.e., fans for ducted ventilation), or one singular system (i.e. fans placed in the envelope openings). A hybrid night ventilation system allows for more flexibility in the control of the system and associated energy usage. When the climatic conditions are suitable, natural night ventilation can be used on its own. When the climatic conditions cannot provide sufficient airflow, mechanical night ventilation can be added.

### 3.1.3 Parameters that impact night ventilation

There are numerous parameters that have a strong effect on the successful performance of night ventilation. The first category are those parameters associated with the physical characteristics of the space. This includes the size of the building or space, the magnitude of loads inside the building, and most importantly the features of the thermal mass inside the space. The larger the thermal mass, the larger the heat storage capacity of the zone (Givoni 1992a; Kolokotroni and Aronis 1999a; Shaviv, Yezioro, and Capeluto 2001; Pfafferott, Herkel, and Jäschke 2003)). This allows the space to heat up or cool down slower. In addition to its physical size, the thermal properties of the thermal mass, such as the Biot number (the ratio of heat transfer resistances inside, and at the surface of, an object), have a significant impact on the heat transfer between the thermal mass and the loads inside the space (Pfafferott, Herkel, and Jäschke 2003). The placement of thermal mass inside the space, in addition to the mechanism of activation of the thermal mass, specifically the area of surface exposed to loads and airflow, can also modify how much heat can be absorbed and released from the mass. Finally, the window placement is important to the performance of the strategy in that it affects the amount of natural wind entering the space, and the direction of the airflow within the interior, and can raise issues of security if windows are too low to the ground.

The next category of parameters important to the design of night ventilation is related to the ventilation system being utilized in the space, including the type and the associated control strategy. This category is discussed in more detail in the Types of Night Ventilation section. Most importantly, the ventilation system typically dictates the airflow rate achieved in the space. The higher the airflow rate, the faster the heat can be released from the thermal mass.

The third category of parameters includes those connected to the environment or climate. Studies have suggested that the two most significant environmental parameters for night ventilation are the relative difference between indoor and outdoor air temperature, and the diurnal temperature swing (the difference between maximum daytime and minimum nighttime temperature) (Givoni 1992a; M. Santamouris et al. 1996). The strategy is most effective in hot and arid climates with low night-time temperatures during the cooling season (Artmann, Manz, and Heiselberg 2007).

Another environmental parameter important to the practice of night ventilation is air quality. If the outdoor pollutant concentration is above a safe level, this can limit the amount of time that windows are allowed to be open into the space. In addition to air quality, the building location and usage can also have a serious impact on when the strategy can be used. Depending on the type of facility, operable windows can sometimes raise security issues. This strategy is of particular interest for commercial spaces in which windows cannot be opened during the day due to noise levels or elevated wind speeds. Because these types of spaces are typically only occupied during the day, noise and elevated wind speeds are not an issue at night, making it an ideal candidate for night ventilation (Kolokotroni and Aronis 1999a; Artmann, Manz, and Heiselberg 2007). Because there are so many different parameters that affect the performance of night ventilation, architects and engineers are hesitant to incorporate the strategy into current building design (Artmann, Manz, and Heiselberg 2008).

### 3.1.4 Benefits of night ventilation

The first and foremost benefit of night ventilation is a reduction in indoor daytime temperature while reducing or eliminating the need for energy-intensive mechanical cooling. With regard to temperature reduction, for buildings with high amount of thermal mass and effective solar control that are using night ventilation, the maximum indoor temperature can fall significantly below the outdoor maximum temperature (Givoni 1992a; Kolokotroni and Aronis 1999a). With a diurnal swing of 15-20 °C, the indoor maximum temperature can be about 6-8 °C below the maximum outdoor temperature (Givoni 1992a). In addition to an air temperature reduction, the strategy also has the potential to lower the mass slab temperature, which in turn can lower the mean radiant temperature, and create a time lag between the occurrence of maximum outdoor air temperature and maximum indoor air temperature (Kolokotroni and Aronis 1999a). The temperature reductions and time lag can both have a strong impact on the occupant comfort inside the space.

If the climatic conditions are appropriate, night ventilation can be implemented allowing mechanical cooling to be reduced or eliminated during the day, thus reducing the cooling energy (Artmann, Manz, and Heiselberg 2008). If the strategy does not completely eliminate the need for mechanical cooling, the time lag in peak temperature created by night ventilation allows for a time shift and peak shave of the load. This means that the remainder of mechanical cooling necessary to keep the occupants comfortable is then taking place later in the day, when energy is typically cheaper.

## 3.2 Approaches for assessing night ventilation

There are numerous methods for assessing the performance of night ventilation. Of the research that has been conducted in the past, the methods used include field studies, chamber studies, simulation studies, and development of mathematical models. The majority of studies include some component of simulation or modelling. Below is a summary of methods that have been used in previous studies with a focus on field studies and model use. The section then goes on to describe approaches that have been taken to analyze big data sets pertaining to night ventilation, specifically looking at comfort and energy. Finally, this section covers the most commonly used metrics for assessing the performance of night ventilation.

### 3.2.1 Approaches for night ventilation field studies

Givoni (1998) coordinated a field study in the summer of 1993 looking at the performance of night ventilation with regard to size of thermal mass. The study was comprised of monitoring three buildings, each having an identical floor plan, but with different levels of thermal mass. Measurements of indoor air temperature, black globe temperature, interior wall surface temperatures and ceiling temperature were taken at intervals of 10 s and later averaged for hourly values. Surface temperatures were captured using thermocouples glued to surfaces and covered with tape. Meteorological data, including outdoor air temperature, relative humidity, wind speed, wind direction, and horizontal global solar radiation, were retrieved from a weather station on top of one of the buildings. The measurements were taken under four different conditions that varied the shading, time of window opening, and use of fan-assisted ventilation.

Blondeau et al. (1997) conducted a field study in the summer of 1994 looking at the performance of night ventilation in a three-level office and classroom building. To complete the study, four rooms were monitored over a one-month period, three of which under night ventilation and one of which was not night ventilated, to be used as a reference room. Each of the rooms was monitored using a thermocouple that measured the air temperature, operative temperature, wall surface temperature, and outgoing air temperature every 2 min, with a measurement error of 0.5 °C. The energy consumption due to fan use was measured using an electricity meter. In addition, climatic data, including solar radiation, outdoor air temperature, and relative humidity, was retrieved from a meteorological center 1 km away.

In the summer of 1995 and 1996, Geros et al. (1999) executed a field study looking at the performance of night ventilation in two air conditioned buildings and one free floating building. Each of the buildings was monitored for a period of one to three weeks under four different conditions of varying night ventilation usage and mechanical systems usage (free floating vs. thermostatically controlled). Indoor temperature was measured throughout the experiments in addition to air-flow rates during the nighttime period, using the tracer gas method.

From 2000 to 2002, Pfafferott et al. (2004) conducted a field study looking at the efficiency of night ventilation in an office building in Germany. The study was conducted in 12 rooms over a period of 2 years, with measurements of energy demand, internal loads, operative temperature, airflow rate, and outdoor air temperature, collected every 5 min, and later averaged to hourly values. Temperature readings were taken using PT 100 sensors mounted on the wall. In addition

to the long-term measurements, short term measurements were taken of air temperature and air leakage. In the summer of 2002, Pfafferoth et al. (2003) led another field study in order to determine the relationship between night ventilation efficiency and air change rate, solar gains, and internal gains. The study was conducted in 21 rooms of two office buildings during a three-month period, half of the time with night ventilation and half of the time without night ventilation. Measurements included outdoor temperature, indoor air temperature, surface temperature, operative room temperature, and air change rate.

In the summer of 2003, Finn et al. (2007) ran a field study in a night-ventilated library, looking at the impact of different design and operational parameters on the strategy's success. The study was conducted over 4 weeks between May and June and consisted of building monitoring using HOBO H8 temperature data loggers to track indoor air temperature and internal wall surface temperature, collected at 30-minute intervals. Although the mean radiant temperature was not directly measured, the parameter was estimated using an area weighted surface temperature. In addition to indoor conditions, internal occupancy levels and internal gains were also measured. External weather conditions, including outdoor temperature, relative humidity, wind speed, wind direction, and total direct and diffuse solar radiation were obtained from the closest weather station, approximately 20 km away, at 1-hour time intervals. Finally, airflow rates were measured using a hot wire anemometer at different locations within the air ducts.

In the summer of 2007, Kubota et al. (2009) conducted a field study looking at the performance of night ventilation in a hot-humid climate. The study took place from June to August in two unoccupied homes of identical size, design and construction. Monitoring of the two homes was done with Innova AirTech Instruments data loggers, measuring indoor air temperature, relative humidity, air velocity, and globe temperature every 10 minutes, within an accuracy of  $\pm 0.3$  °C,  $\pm 2\%$  RH, and  $\pm 0.02$  m/s respectively. Climatic data, including outdoor temperature, relative humidity, wind speed, wind direction, and horizontal global solar radiation, was also collected from a nearby weather station.

In 2010, a paper was published by Santamouris et al. (2010) on a recent field study they conducted, analyzing the relationship between cooling load and the energy contribution of night ventilation. The study consisted of 214 residential buildings, all of which were high in thermal mass, used mechanical air conditioning, and were located in a similar climate. While general information regarding energy consumption was collected for all 214 buildings, ten of the buildings were monitored over a three-year period, measuring airflow rate and indoor environmental quality.

Finally, in summer of 2011, Gagliano et al. (2014) led a field study to evaluate the thermal behavior under natural ventilation and high mass construction. The study was done in a historical building over five periods from July to September, totaling 17 days. Measurements were taken for indoor air temperature, outdoor air temperature, inner and outer wall surface temperature, at 15-minute time intervals. The measurements were collected in two rooms, each with an external wall having different orientation. A nearby weather station was used to retrieve global solar irradiance and wind velocity.

### 3.2.2 Approaches for night ventilation model generation, validation, and optimization

Model predictive control (MPC) is an emerging topic in the field of building automation due to its enabling of effective control systems that can operate without expert intervention (García, Prett, and Morari 1989). To successfully execute model predictive control, one must obtain data, develop a model to predict interior conditions, train the model and then implement that model in a control sequence. MPC is especially of interest for those buildings being pre-cooled through night ventilation. Previous research on night ventilation has included some work in the field of model generation. In one of the field studies conducted by Pfafferott et al. (2004), a model was generated to determine the potential for optimization and to determine how complex a simulation tool must be to accurately reflect reality. The key to model generation is finding a model that is simple enough to minimize computation time but complex enough to minimize error. This balance is often very difficult to achieve.

There are two approaches to developing a model for MPC. The first method is black-box, meaning the model is based solely on historical data from building monitoring and does not reflect the physical properties of the building construction or systems (Vidrih, Arkar, and Medved 2016). The second method is white-box, meaning the model relies only on physical properties of the building and not on historical data. There are also approaches to model generation that combine black-box and white box methods. To generate a hybrid black-box/white-box model for MPC, first a set of first-principles equations must be chosen to represent the dynamics of the space. Zhang et al. (2014) used simplified resistance/capacitance equations to represent the heat transfer between the thermal mass, indoor air, and exterior. Once a set of dynamical equations is chosen, the model parameters must be identified. Pfafferott et al. (2004) identified its model parameters, such as thermal properties of walls and windows, using previously collected short-term data and a sensitivity analysis. There are numerous approaches to identifying parameters including, but not limited to, the gradient descent method and the nonlinear least squares method, described in detail in the Methodology section. It is standard practice to use a portion of collected data, referred to as training data, for parameter identification and leave the other portion of data, referred to as test data, for model validation. Although the test data set cannot be examined during model generation, a method known as K-fold cross validation, discussed in detail in the Methodology section, can be implemented using only training data to simulate model validation.

Once all parameters are identified, the model must be validated against measured data. The acceptable error between model values and actual values varies depending on the type of data and purpose of the model. In previous studies modeling night ventilation, the following have been considered acceptable errors for temperature data: 0.5 °C maximum error, 0.3 °C mean error, 0.46 °C mean bias deviation with 0.88 °C root mean square difference, and 1.14 °C mean bias deviation with 1.35 °C root mean square difference (Blondeau et al., 1997; Finn et al., 2007; Geros et al., 1999). Pfafferott et al. (2004) went a step further and conducted a Monte Carlo simulation to assess the uncertainty of the model parameters. To run the Monte Carlo simulation, more than 20 input parameters, including building capacity, heat loss coefficient, and solar aperture, were varied in the range of 25%, 20%, and 20% respectively. This showed the researchers how sensitive the model parameters were to outdoor conditions and user behavior.

Pfafferott et al. (2004) subsequently performed a Fourier analysis of the operative temperature and ceiling temperature to quantify the building's dynamic response. This Fourier analysis showed that the frequency spectrum of simulated data and actual data were in agreement, which suggests that the model is accurately calculating the conditions.

After the model is validated, it can then be paired with weather forecasts to predict future conditions inside the building. Medved et al. (2014) used a TRNSYS simulation, along with weather forecasts of outdoor air temperature, global solar radiation, and wind velocity for the following 24-h period, to predict the time-dependent night cooling potential and cooling load for the following day. Because the forecasted weather data was from an off-site location, six days of data were collected onsite and used to set the bias for a Kalman Filter, which allowed the weather station data to be adjusted to represent outdoor conditions at the building site (Medved et al., 2014).

In addition to the forecasting of future indoor conditions, the model can also be used to optimize the night ventilation strategy, helping determine when the building should enter and exit night ventilation mode. To optimize the model, a cost function must be determined to minimize a specific state variable. Additionally, constraints must be set to keep the state variables within a certain range. Zhang et al. (2014) optimized their model by minimizing the energy consumed by cooling coils and fans, while setting constraints of minimum airflow rate equal to the ASHRAE 62.1 acceptable indoor air quality limit, and supply temperature greater than 16 °C, to reduce local discomfort.

### 3.2.3 Approaches for night ventilation performance analysis

When analyzing the performance of night ventilation, the first step is to determine under what conditions the strategy is to be assessed. As discussed in 3.3.1. Approaches for night ventilation field studies, the following conditions have been compared in previous field studies: air conditioned vs. free-floating, fan-assisted ventilation vs. natural ventilation, only daytime ventilation vs. nighttime ventilation, full day ventilation vs. nighttime ventilation, no ventilation vs. nighttime ventilation, and low thermal mass vs. high thermal mass (Geros et al., 1999; Givoni, 1998; Kubota et al., 2009).

Once it has been decided what conditions are being compared, a method of performance assessment must be chosen. The two areas of night ventilation analysis conducted in previous studies are energy performance and comfort performance. The most common energy metrics across all studies are percent energy savings, heat removed, and cooling load, while the most common comfort metrics are indoor air temperature, maximum daily indoor air temp, and discomfort degree hs. In field studies, comfort metrics are much more prevalent than energy metrics, probably because indoor condition data is easier to obtain than energy data.

Criterion for comfort performance can be very simple, using metrics such as daily indoor maximum air temperature, its reduction below outdoor maximum air temperature, daily indoor temperature range, or ratio of daily indoor temperature range to outdoor temperature range (also known as decrement factor) (Gagliano et al., 2014; Givoni, 1998). Slightly more complex, an alternative comfort criterion can be the annual percentage of time above a specific temperature

(often called “exceedance”). In studies conducted by Pfafferott et al. (2003, 2004) and Artmann et al. (2008), the exceedance comfort criterion were the percentage of time with operative room temperatures above 25 °C and 26 °C, respectively, with a value lower than 10% of working hours considered a success. This value is taken from the 2003 German standard on thermal protection and energy economy in buildings.

Percentage of time above a temperature gives a good indication of the amount of time that is out of the comfort range, but it does not designate how far outside of the comfort range those points lie. Another exceedance metric that considers this is discomfort degree hours, which is the sum of the difference between the indoor temperature and a specified temperature threshold across all time steps, multiplied by the time step. One specific case of discomfort degree hours is the climatic cooling potential (CCP) (see equation 1), in which the specified temperature threshold is the outdoor air temperature (Artmann et al., 2007). CCP is used as a simplified metric for the potential of night ventilation for a specific climate. Another aspect of comfort not covered by any of the aforementioned metrics is the delay in heat escalation within the space. This characteristic is covered by the daily time lag, or the difference in time between the daily peaks of the outdoor air/surface temperature and the indoor air/surface temperature (Gagliano et al., 2014).

$$CCP = \sum_{t=1}^N h_t (T_{indoor,t} - T_{outdoor,t}) \begin{cases} h_t = 1 & \text{if } T_{indoor,t} \geq T_{outdoor,t} \\ h_t = 0 & \text{if } T_{indoor,t} < T_{outdoor,t} \end{cases}$$

*Equation 1. Climatic Cooling Potential*

The most complex criteria for comfort are the prescribed thermal comfort models. The most common comfort model used today is the predicted mean vote (PMV)/predicted percentage dissatisfied (PPD) model, developed by Fanger (1970), which incorporates six parameters of thermal comfort: air temperature, mean radiant temperature, relative humidity, air speed, metabolic rate, and clothing level. Blondeau et al. (1997) used the PMV/PPD model to assess thermal comfort in a night ventilated building using collected temperature data along with the following inputs: a 70 kg man wearing light summer clothing (0.4 clo) at moderate standing activity (1.4 met) with air velocity of 0.2 m/s. Zhang et al. (2014) used the PMV model for their comfort analysis in a building with night ventilation, with their comfort criterion being a PMV between -0.5 and +0.5, equivalent to a PPD below 10%. Similar to the PMV model, the standard effective temperature (SET\*), proposed by Gagge et al. (1986), is another index that combines all six parameters of thermal comfort. Kubota et al. (2009) used SET\* with collected temperature values and the following assumptions: occupants are seated, doing quiet activity (1.0 met) wearing typical summer attire (0.5 clo).

In addition to the PMV model, a newer comfort model exists specifically for spaces that are naturally ventilated. This model, now part of ASHRAE standard 55, is known as the adaptive comfort model, or adaptive comfort standard (ACS) (de Dear and Brager 1998). This standard is based on experiments conducted all over the world, including tropical regions, and is a function of running mean outdoor air temperature. Typically, as done by Kubota et al. (2009), the comfort criterion used for the ACS are 80% or 90% acceptability limits of indoor operative temperature. The ACS is very appropriate for night ventilation because most spaces using the strategy are at least somewhat naturally ventilated during the day as well.

Although comfort metrics are more common amongst field studies, there are also a variety of metrics used in previous night ventilation studies looking at energy performance. This can be a challenge when energy consumption is not directly measured, but there are a number of ways around this, the most common of which is to calculate the hourly or daily energy removal from the building during the nighttime period. This metric can be computed by integrating the difference between the outdoor and indoor air temperature, multiplied by the specific heat of air and the mass flow rate, over the night ventilation period (Blondeau et al., 1997; Medved et al., 2014; Pfafferott et al., 2003). Heat removed can also be calculated by multiplying the specific heat of air and mass flow rate with the CCP (Artmann et al., 2007). When data for energy consumption is available, the ratio of utilized thermal energy to electrical energy, or the coefficient of performance (COP) for night ventilation can be calculated (Blondeau et al., 1997; Medved et al., 2014; Pfafferott et al., 2003).

### 3.3 Findings from previous night ventilation field studies & simulation studies

Numerous studies have been conducted looking at the impact that each of the aforementioned parameters has on the performance of night ventilation. The first category of parameters to discuss is those associated with physical building characteristics. With regards to the influence of cooling load on night ventilation performance, a consensus has not yet been reached amongst researchers. Comfort improvement is strongly dependent on good control over heat gains from solar loads, equipment, occupants, and conduction through building fabric (Blondeau et al., 1997). Some studies had findings that suggest that lower internal loads allow for improved night ventilation performance, whereas other studies had findings that would propose that as the internal load increases, the potential for energy conservation by night ventilation also increases. Kolokotroni et al. (1999a) conducted an experiment that showed increasing heat gains diminished the effectiveness of night ventilation. Geros et al. (1999) showed that night ventilation efficiency increased during an experimental period with lower convective and radiative internal gains. Artmann et al. (2008) ran a study in which overheating degree hours increased by a factor of 2-2.5 when heat gains from office equipment increased from 50 to 150 W per person. On the other hand, Santamouris et al. (2010) found a linear relationship between initial cooling load and energy contribution of night ventilation, indicating that the higher the cooling load, the higher the potential energy reduction due to night ventilation. The results of these studies seem to be suggesting an inverse relationship between cooling load and night ventilation performance. However, it is also possible that while the strategy is more effective with lower cooling loads, at the same time it is more necessary as the cooling load increases.

In addition to cooling load, past studies have arrived at significant (and more consistent) conclusions regarding the impact of room size and orientation on night ventilation effectiveness. Experiments in different sized rooms showed that the night ventilation efficiency decreases when room size increases, due to the fact that an increase in room volume also means a lower volume to surface area ratio and therefore less efficient convective heat transfer, in addition to less homogenous airflow distribution inside the space (Blondeau et al., 1997).

Experiments in rooms with thermal mass walls at different orientations indicated that indoor temperature is greater in rooms with thermal mass on the east than with thermal mass on the west



because heat stored in the east wall from solar radiation has more time to enter the space during the day, whereas heat in the west wall from solar radiation is released sooner by night ventilation (Gagliano et al., 2014).

The effect of thermal mass size on the performance of night ventilation is fairly unanimous amongst researchers regarding high mass conditions, but there is some disagreement regarding low mass conditions. On the whole, it is believed that night ventilation improves as exposed thermal mass increases (Kolokotroni and Aronis, 1999). This has been seen during experiments in which night ventilation lowered the indoor maximum temperature more so in a high-mass building than in a low-mass building (Finn et al., 2007; Givoni, 1998; Shaviv et al., 2001). However, there is disagreement about whether or not lightweight buildings help or hurt the effectiveness of night ventilation. Some argue that even lightweight construction can benefit night ventilation, whereas others observed that a light structure can actually trap heat inside the building (Kolokotroni and Aronis, 1999; Shaviv et al., 2001). Interestingly, when thermal mass is present in the walls, the magnitude of its effect on night ventilation changes depending on the size of the room. As the room volume decreases and the ratio of wall to floor area decreases, the size of the thermal mass becomes less significant (Artmann et al., 2008).

Another parameter that has been investigated is level of glazing and shading. The consequence of reducing window-to-wall ratio is improved night ventilation performance (Finn et al., 2007; Kolokotroni and Aronis, 1999). That being said, the energy consumption of a space using night ventilation sees very little effect from a change in the amount of solar protection (Kolokotroni and Aronis, 1999).

The next category of parameters that has been studied encompasses those associated with system and control. One of the most critical parameters in this category is airflow rate or air speed. It is universally agreed upon that increased airflow corresponds to increased night ventilation performance. Experiments have shown that higher airflow rates lead to increased energy savings for all forms of natural ventilation and that an increase in air change rate increases the cooling effect of night ventilation (Kolokotroni and Aronis, 1999; Pfafferott et al., 2003). That being said, there is some disagreement on the returns of an incremental escalation in airflow rate. Some studies did not note any comfort improvement beyond 10 air changes per hour (Blondeau et al., 1997; Finn et al., 2007), while one study saw significant improvements in comfort up to 20 air changes per hour (Artmann et al., 2008). Some studies found that an increase from 10 to 30 air changes per hour led to an average decrease of peak indoor temperature from 1.8 °C to 2.2 °C (Geros et al. 1999). On the other hand, one study perceived a plateau of maximum indoor air temperature by the airflow rate of 20 air changes per hour (Shaviv, Yezioro, and Capeluto 2001).

The most significant control parameters are setpoint temperature and hours of night ventilation operation. These are both crucial components of all mechanical night ventilation systems. One study found that an increase of setpoint temperature from 24 °C to 27 °C led to an increase of energy savings due to night ventilation from 5% to 8%, and that five extra hours of night ventilation operation increased energy savings from 5% to 7% (Kolokotroni and Aronis, 1999). Another study saw a reduction in overheating hours due to night ventilation of 39-51% at a setpoint temperature of 25 °C, 69-79% at a setpoint temperature of 27 °C, and 92-96% at a setpoint temperature of 29 °C (Geros et al., 1999). Interestingly, one experiment has shown

increased energy usage from no night ventilation to mechanical night ventilation in a medium weight office building, due to the increased operation of fans (Kolokotroni and Aronis 1999a).

The most crucial parameters are those related to climate. Experiments have shown that a reduction of outdoor night-time temperature corresponds with an increase in night ventilation system capacity and lower internal morning temperatures (Artmann et al., 2008; Kolokotroni et al., 1998; Pfafferott et al., 2003; Santamouris and Asimakopoulos, 1996). Research has shown that this relationship between internal temperature and outdoor temperature in warm climates is stronger when the outdoor temperature is high and weaker when outdoor temperature is low, suggesting that user behavior and internal loads have a stronger effect on internal temperature at lower outdoor temperatures (Pfafferott et al., 2004). It has also been seen that lower outdoor temperature amplitude, or diurnal swing, leads to a lower cooling potential for night ventilation (Geros et al., 1999).

In addition to the investigation of parameter influence on night ventilation performance, many studies compared spaces using night ventilation, no night ventilation or only daytime ventilation, holding all other parameters constant. In almost every case, night ventilation outperformed the other ventilation strategies with regard to comfort and energy. Although each case had different variations of physical, systems, and environmental parameters, it was seen that night ventilation has the ability to decrease indoor air temperature by anywhere from 1°C to 6 °C, delay peak indoor air temperature by 3 hours, lower PMV by 0.75, and diminish energy consumption by 5% (Blondeau et al., 1997; Geros et al., 1999; Kolokotroni et al., 1998; Kolokotroni and Aronis, 1999; Pfafferott et al., 2003). The only case in which night ventilation has not always outperformed other types of ventilation is in hot and humid climates. It was found that night ventilation did not help improve the indoor conditions in studies conducted in Shanghai and Singapore compared to daytime ventilation (da Graça et al., 2002; Liping and Hien, 2007). However, a study conducted in Malaysia saw a reduction of maximum indoor air temperature of about 2.5 °C between daytime ventilation and nighttime ventilation, and about 2 °C between no ventilation and night ventilation (Kubota et al., 2009). That being said, the nighttime ventilated space had 13% higher minimum relative humidity than a daytime ventilated space and 21% higher minimum relative humidity than a space with no ventilation (Kubota et al., 2009).

Finally, previous studies have made significant findings regarding the savings associated with optimization of night ventilation systems using model predictive control versus typical rule-based control. Experimenters have observed energy savings from 15%-40% between schemes with pre-defined night ventilation control and optimized operation strategies. (Vidrih et al., 2016; Zhang et al., 2014)

## 4. Methods

### 4.1 Building descriptions

This thesis focuses on three different case studies. Each case study is of a building that uses a different night ventilation control strategy and different physical, system, and environmental parameters. This section describes each of these buildings in detail regarding their construction, control sequence, and climate.

#### 4.1.1 La Escuelita Elementary School

The first case study, La Escuelita Elementary School (LEES), is an elementary school that is part of the Oakland Unified School District. The school is located in Oakland, CA, which has a fairly mild climate. As seen in figure 1, the temperature ranges from about -1 °C (30 °F) to 32 °C (90 °F) throughout the year, only 20 days of which go above 27 °C (80 °F). Oakland sees an average diurnal swing of about 8 °C (15 °F), sometimes going as high as 20 °C (36 °F). Although there is not much seasonal variation in weather, Fall and Summer tend to have slightly higher temperatures and Fall days tend to have the highest diurnal swing. Even when the outdoor air temperature does get high, Oakland has fairly low humidity.

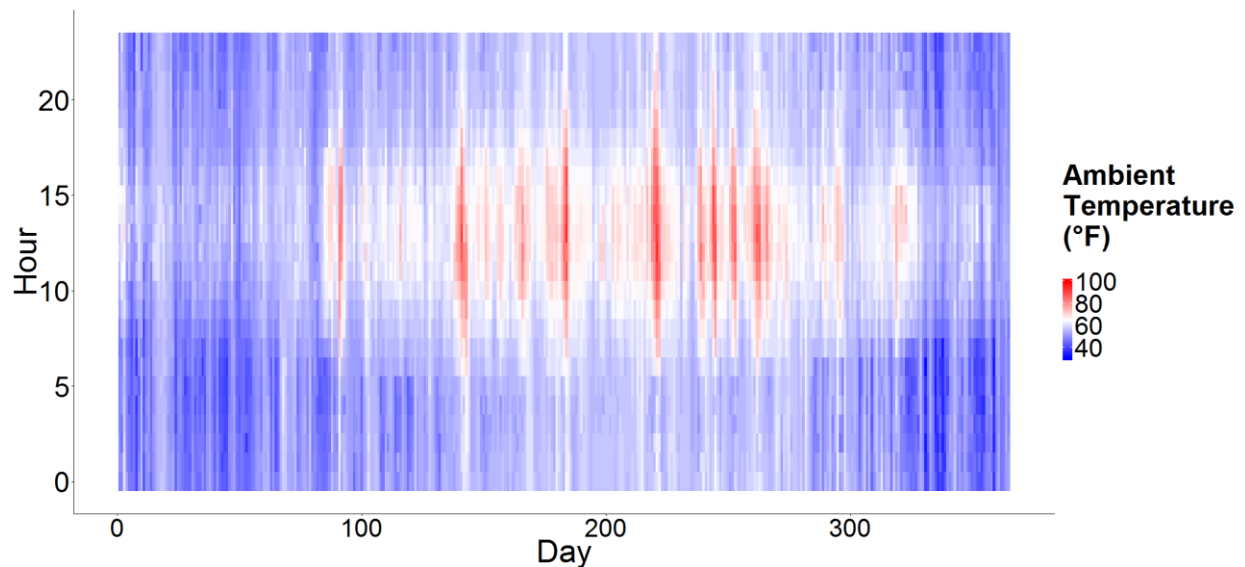


Figure 1. Oakland annual outdoor air temperature profile



Figure 2. LEES classroom

Each classroom contains thermal mass in the form of a 4-inch concrete slab (145 pcf) and 2-inch cement plaster walls (95 pcf). The floor and walls both have embedded temperature sensors and varying depths, unknown to the designer. Of the classrooms studied here, two are located on the ground floor and six are located on the second floor, each with varying area and position (see Table 1 for values).

**THERMAL MASS MATERIAL DENSITY:**  
 1/2" USG DUROCK® BRAND CEMENT BOARD - APPROX. DENSITY 72#/C.F.  
 1 1/8" PORTLAND CEMENT PLASTER - APPROX. DENSITY 116#/C.F. W/ SAND AGGREGATE

## EXTERIOR

UL# U404, SIMILAR.

## INTERIOR

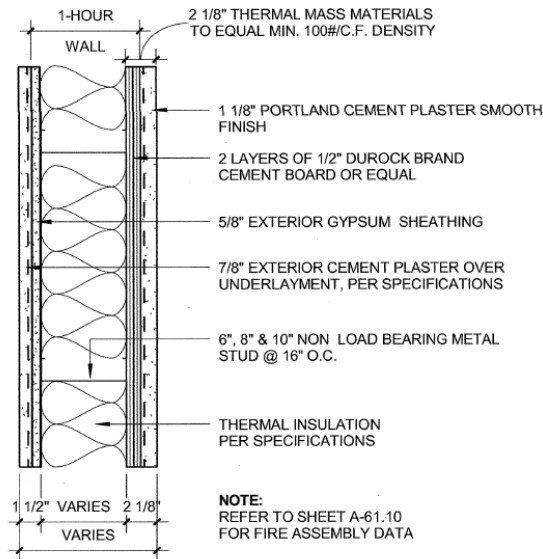


Figure 3. LEES wall construction

The controls for LEES were designed by Taylor Engineering. The facility uses fan-assisted mechanical ventilation for cooling. During occupied hours (8AM – 4 PM), the variable air volume (VAV) box for each classroom will supply the room with the minimum amount of airflow to meet the code requirements,  $V_{min}$ , through displacement ventilation (see Table 1 for values). The displacement diffusers provide 100% outdoor air from central air handling units. When windows are opened in a space, a switch disables the heating, ventilation and air

conditioning (HVAC) system, allowing passive natural ventilation into the space. If the outdoor air temperature is low, the room is ventilated by displacement ventilation, which creates a temperature stratification in the space. If the indoor air temperature exceeds the cooling setpoint (23.3 °C (74 °F) in perimeter rooms, 22.8 °C (73 °F) in interior rooms), the system relies on increased airflow to cool its occupants. When the space overheats, the airflow rate will ramp up to the occupied cooling airflow setpoint,  $V_{cool,occ}$  (see Table 1 for values) and ceiling fans are activated.

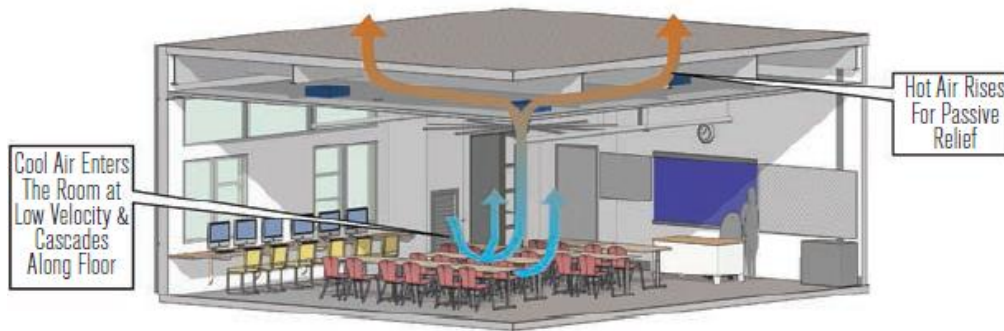


Figure 4. LEES classroom cooling schematic

The mechanical system is designed to enter night ventilation mode, which consists of ramping up the airflow to the unoccupied cooling airflow setpoint,  $V_{cool,unocc}$  (see Table 1 for values), when the following conditions are met:

1. The classroom is unoccupied
2. The classroom is within 8 hours of the expected start of occupancy the following day
3. The floor surface temperature is at least 0.56 °C (1 °F) higher than the mass temperature setpoint
4. The outdoor air temperature is at least 5.6 °C (10 °F) below the floor temperature

As per design, the mass temperature setpoint is set equal to the heating setpoint of 21.1 °C (70 °F) in order to avoid unnecessary warmup after night ventilation. After occupancy, the building operator had the opportunity to offset the mass temperature setpoint. In its current state, the mass temperature setpoint has been adjusted by +1.1 °C (2 °F) for classrooms 120 and 234. During night ventilation, the zone's heating coil and/or parallel box fan are locked out. The system will leave night ventilation mode when the floor temperature falls below the mass temperature setpoint. The system will sometimes enter a "warm-up mode" the morning after night ventilation if the indoor air temperature is below the heating setpoint. When the space was designed, models showed a classroom using night ventilation to maintain an indoor air temperature at or below 23.3 °C (74 °F) for 88% of a typical weather year (Eubanks 2014).

Classroom	Story	Position	Area (ft <sup>2</sup> )	V <sub>min</sub> (CFM)	V <sub>cool,occ</sub> (CFM)	V <sub>cool,unocc</sub> (CFM)
110	1st	N	1240	215	1800	1800
120	1st	NE	1185	230	1900	1900
233	2nd	NW	930	175	1500	1500
234	2nd	NW	930	140	1100	1100
235	2nd	W	960	145	1200	1200
240	2nd	S	1050	140	1100	1100
241	2nd	SE	1020	140	1100	1100
242	2nd	SE	1020	185	1500	1500

Table 1. LEES classroom physical and system parameters

#### 4.1.2 Indio Building

The second case study is 435 Indio Way (IND), an open-plan office located in Sunnyvale, CA, which also has a mild climate. The climate in Sunnyvale is very similar to that of Oakland, but with just slightly higher temperatures. As seen in figure 5, the temperature ranges from about -1 °C (30 °F) to 37.8 °C (100 °F) throughout the year, only 44 days of which go above 27 °C (80 °F). Sunnyvale sees an average diurnal swing of about 9.4 °C (17 °F), sometimes going as high as 17.8 °C (32 °F). Although there is not much seasonal variation in weather, Fall and Summer tend to have slightly higher temperatures and Fall days tends to have the highest diurnal swing. Like Oakland, Sunnyvale has fairly low humidity.

The facility, which was recently renovated to become net zero energy, is approximately 3,000 m<sup>2</sup> (32,000 ft<sup>2</sup>). The structure of the building is comprised of 12-inch thick concrete walls and exposed concrete slab, both of which are left over from the existing building structure. IND also makes use of electrochromic windows to block solar radiation, in addition to solar PV panels as a renewable source of energy.

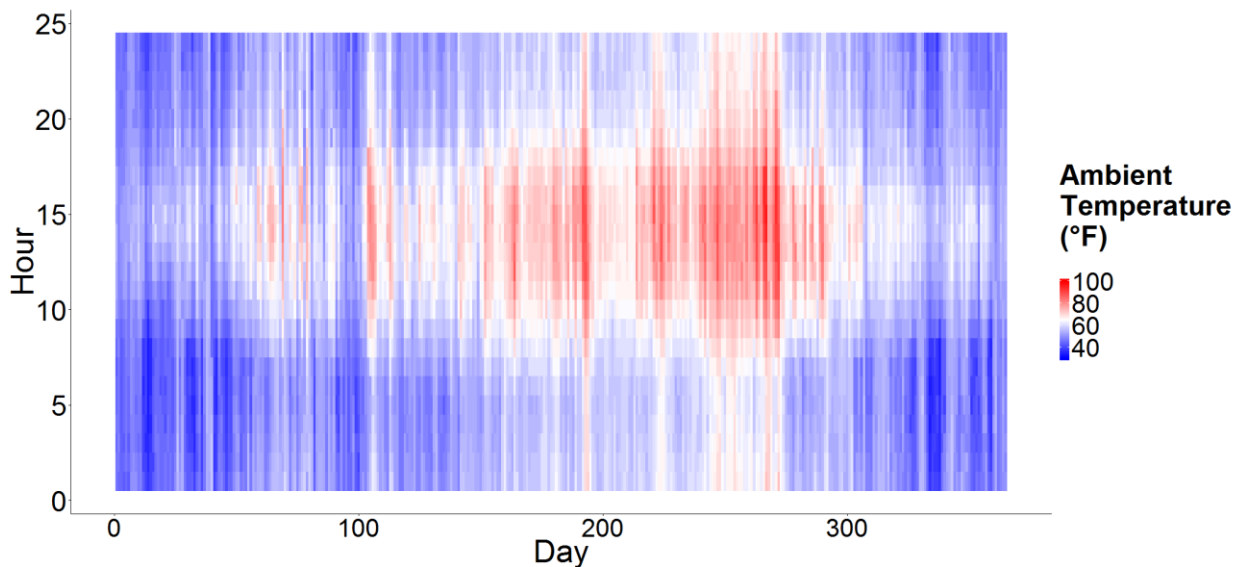


Figure 5. Sunnyvale annual outdoor air temperature profile



Figure 6. IND open-plan office

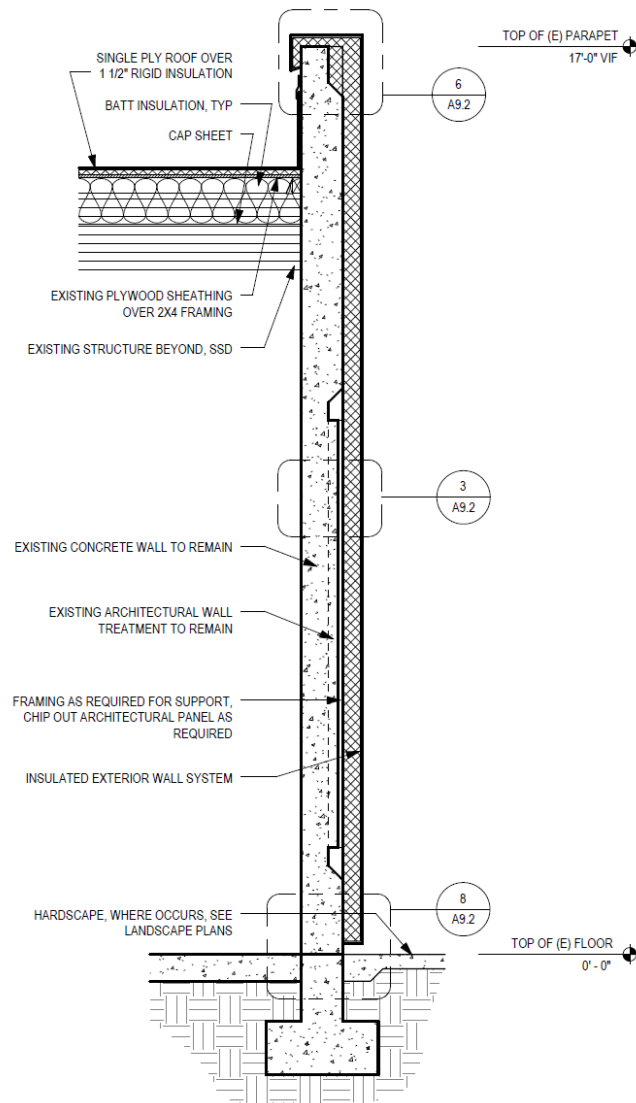


Figure 7. IND wall construction

IND uses automated natural night ventilation to pre-cool the building. During occupied hours (6AM-8PM), the space is almost never cooled mechanically. The system enters night ventilation mode by opening up the windows and skylights under the following conditions:

1. The space is unoccupied
2. The indoor air temperature is greater than 21.1 °C (70 °F)
3. The outdoor air temperature is less than 20 °C (68 °F)

These thresholds were chosen by the building operator based on trial and error. Unlike LEES, mass temperature is not one of the criteria for the operating algorithm. Air temperature was chosen as a threshold rather than mass temperature because there were no embedded mass temperature sensors in the original design. The system leaves night ventilation mode when the indoor air temperature falls below 20.6 °C (69 °F).

### 4.1.3 Blessing House

The third case study is called the Blessing House (BH), a residential building located in Auroville, India, which has a hot and humid climate. As seen in figure 8, the temperature ranges from about 16 °C (60.8 °F) to 40 °C (104 °F) throughout the year, almost all of which go above 28 °C (82.4 °F). Auroville sees an average diurnal swing of about 9 °C (16.2 °F), sometimes going as high as 15 °C (27 °F). The Pre-Monsoon and Monsoon seasons tend to have higher temperatures (averaging 30 °C (86 °F)) and higher diurnal swing (averaging 10 °C (18 °F)) than Post-Monsoon and Winter seasons. In addition to the heat, Auroville also has an average relative humidity of 60%.

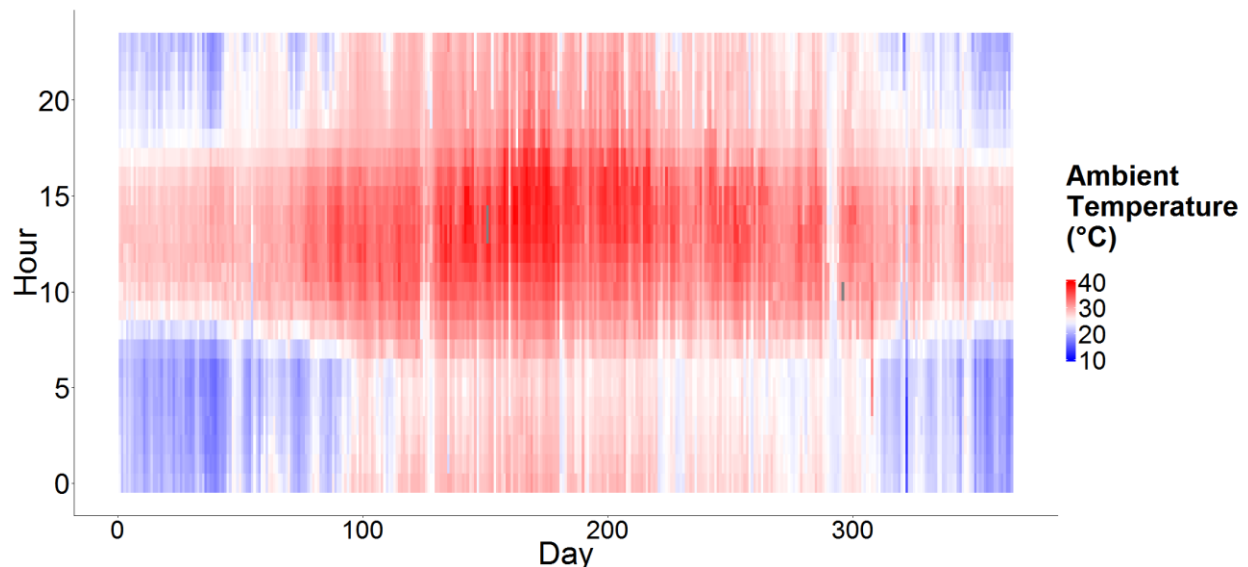


Figure 8. Auroville annual outdoor air temperature profile

BH is a two story home containing thermal mass in its floor, roof, and walls. The building's walls consist of compressed earth blocks (290x140x90 mm), Aerocon blocks (600x200x75 mm) and a layer of cement plaster (20 mm thick). The building's ceiling/roof construction consists of white reflective ceramic tiles, Aerocon blocks (300x300x50 mm), Hurdi terra cotta hollow



blocks, and a layer of cement plaster (20 mm thick). The space of interest to this case study is a room on the second floor, 24 m<sup>2</sup> in area, with a ceiling slanting from 3 m to 4.6 m.

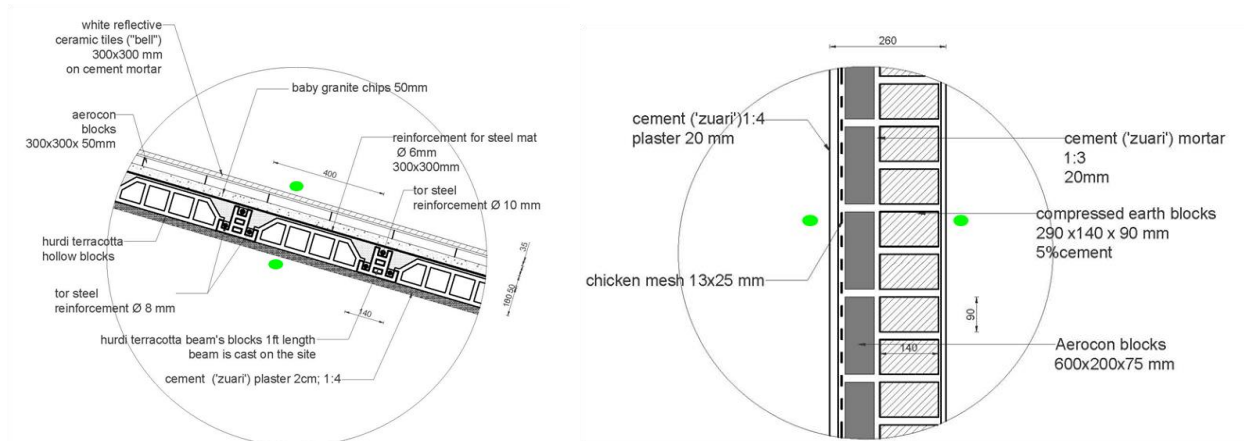


Figure 9. A) BH roof/ceiling construction; B) BH wall construction

This facility uses occupant controlled natural night ventilation to pre-cool the house. This means the occupants manually open their windows at night and close them in the morning at their own discretion. The occupants typically open their windows when the outdoor air temperature is equal to the indoor air temperature. The space studied for this case study has a window facing north, spanning from the floor to 2.5 m above the floor. This space is approximately 24 m<sup>2</sup> (255 ft<sup>2</sup>).



Figure 10. BH window used for natural ventilation

## 4.2 Data collection & designer/operator interviews

The following section describes the methods used to retrieve data for each case study and consolidate each data set. This section also outlines the procedure taken for interviewing building designers and operators.

#### 4.2.1 La Escuelita Elementary School

Indoor conditions from LEES were collected through the building management system (BMS), which retrieved temperature data from PreCon Encapsulated Thermistor Sensors, with an accuracy of  $\pm 0.2^{\circ}\text{C}$  ( $0.36^{\circ}\text{F}$ ). The following data was available for all eight classrooms being studied for the dates of July 2<sup>nd</sup>, 2015 to Oct 6<sup>th</sup> 2015:

1. Indoor air temperature ( $^{\circ}\text{F}$ )
2. Embedded mass floor temperature ( $^{\circ}\text{F}$ )
3. Supply temperature ( $^{\circ}\text{F}$ )
4. Airflow rate (CFM)
5.  $\text{CO}_2$  concentration (ppm)
6. Window state (open/closed)
7. Warmup mode (on/off)
8. Night ventilation mode (on/off)
9. Occupied indoor air temperature setpoint ( $^{\circ}\text{F}$ )
10. Night ventilation air temperature setpoint ( $^{\circ}\text{F}$ )
11. Night ventilation mass temperature setpoint ( $^{\circ}\text{F}$ )

This data was available in 15-min to hourly time intervals, depending on the parameter. In addition to these parameters, embedded mass wall temperature was also available for half of the classrooms. Using the National Oceanic and Atmospheric Association's Climatic data center, hourly outdoor air temperature ( $^{\circ}\text{F}$ ) was downloaded from the quality controlled local climatological data being recorded at the Oakland airport, the closest weather station to LEES. Although the weather station data did not include solar radiation, these values were estimated based on the direct normal solar radiation values ( $\text{Wh}/\text{m}^2$ ) in the TMY3 file for Oakland, CA. After the building data and weather data was collected, the data was combined and consolidated using the Universal Translator, set to an hourly time interval.

#### 4.2.2 Indio Building

Indoor conditions from IND were also collected through the BMS, using Veris CW sensors, with an accuracy of  $\pm 0.5^{\circ}\text{C}$  ( $1^{\circ}\text{F}$ ) from  $10^{\circ}\text{C}$  ( $50^{\circ}\text{F}$ ) to  $35^{\circ}\text{C}$  ( $95^{\circ}\text{F}$ ). The following data was available for the open-plan office for the dates of Sept 1<sup>st</sup>, 2015 to Oct 31<sup>st</sup>, 2015 in 30 min time intervals:

1. Outdoor air temperature ( $^{\circ}\text{F}$ )
2. Indoor air temperature ( $^{\circ}\text{F}$ )
3. Embedded mass wall temperature ( $^{\circ}\text{F}$ )
4. Window state (open/closed)

Although the BMS was not measuring solar radiation, these values were estimated based on the direct normal solar radiation values ( $\text{Wh}/\text{m}^2$ ) in the TMY3 file for Sunnyvale, CA. In addition, daily energy loads were obtained for year, broken down by submeter. Hourly loads were estimated based on this data. After the building data, weather data, and energy data was collected, the data was combined and consolidated using the Universal Translator, set to an hourly time interval.

### 4.2.3 Blessing House

Indoor conditions from BH were collected through HOBO U12 data loggers. These data loggers measure temperature with an accuracy of  $\pm 0.35$  °C (0.63 °F) from 0 °C (32 °F) to 50 °C (122 °F) and relative humidity with an accuracy of  $\pm 2.5$  % from 10 % to 90 %. The data was subsequently cross-checked with spot measurements using an Extech HT 30 globe temperature meter. The following data was collected for the dates of Oct 22<sup>nd</sup>, 2013 to Oct 14<sup>th</sup>, 2014 in hourly time intervals:

1. Indoor air temperature (°C)
2. Relative humidity (%)
3. Mass wall indoor surface temperature (°C)
4. Mass wall outdoor surface temperature (°C)

An additional parameter being recorded by HOBO data loggers was window state (open/closed). However, the data logger only recorded instances in which the window state changed (i.e., opened or closed), not window state during all hours. Therefore, this data had to be converted to hourly values using Matlab (see Appendix 1.1).

In addition to building data, weather data was pulled from the Auroville weather station at hourly intervals including the following parameters:

1. Outdoor air temperature (°C)
2. Relative humidity (%)
3. Sun duration (min/day above threshold)
4. Wind speed (m/s)
5. Wind direction (N/S/E/W)

Because airflow rate data was not collected on site, this parameter was estimated based on the wind speed, wind direction, room dimensions, window dimensions, window direction, building height, and site topography. Because the solar radiation data was collected as sun duration rather than actual solar radiation, a proxy was used for this parameter. Using the TMY3 file for Pondicherry, India, average monthly direct normal solar radiation values (Wh/m<sup>2</sup>) were calculated. These monthly averages were then used as the sun duration threshold, allowing a rough conversion to solar radiation. After the building data and weather data was collected, the data was combined and consolidated using the Universal Translator, set to an hourly time interval.



Figure 11. Data collection in BH

#### 4.2.4 Interview procedure

Interviews were setup with the designers and operators of each building. Prior to conducting the interviews, a list of questions was prepared for consistency. The following questions were administered to all building designers:

1. What is the designed night ventilation control sequence for this building?
  - a. Threshold for entering night ventilation?
  - b. Threshold for exiting night ventilation?
  - c. How were these thresholds chosen? (i.e. air temperature versus mass temperature)
  - d. Did the control sequence differ for spaces of different size/location/orientation?
2. Why was this type of night ventilation chosen (i.e. automated natural vs manual natural vs mechanical)?
  - a. Was this decision based on the climate, building function, building construction, etc.?
3. Where/how deep are the embedded mass temperature sensors located?
4. How did you expect the strategy to perform?
  - a. With regard to indoor air temperature?
  - b. With regard to mass temperature?
  - c. Why?
5. Is the strategy performing as expected?
  - a. Why or why not?
  - b. How could the strategy/control sequence be improved?
6. What have you learned from this experience for future projects?

The following questions were administered to all building operators:

1. What is the operating night ventilation control sequence for this building?
  - a. Threshold for entering night ventilation?
  - b. Threshold for exiting night ventilation?
  - c. Has the control sequence been adjusted since design?
    - i. If so, why?

2. How is the strategy performing?
  - a. With regard to indoor air temperature?
  - b. With regard to mass temperature?
  - c. Why is it performing this way?
3. Is the strategy performing differently depending on building features?
  - a. Occupancy?
  - b. Construction?
  - c. Room size/location/orientation?
4. How could the strategy/control sequence be improved?

## 4.3 Model generation

In order to implement model predictive control, models needed to be generated for each building/room to capture the physical and thermal characteristics of the building construction and HVAC system. Hybrid (part black-box and part white-box) models were generated in Matlab by using collected data along with simplified resistance/capacitance dynamical equations. Once the first principles equations were established, model parameters were identified using the gradient descent method and the non-linear least squares method. Different model variations were tested using the k-fold cross validation technique. Finally, each model was validated against real building data.

### 4.3.1 First principles equations

$t$	Time step [hr]
$T$	Temperature [ $^{\circ}\text{F}$ or $^{\circ}\text{C}$ ]
$R$	Thermal resistance [ $^{\circ}\text{F}\cdot\text{hr}/\text{BTU}$ or $^{\circ}\text{C}\cdot\text{hr}/\text{J}$ ]
$C$	Thermal capacitance [ $\text{BTU}/^{\circ}\text{F}$ or $\text{J}/^{\circ}\text{C}$ ]
$V$	Ventilation rate [ $\text{ft}^3/\text{hr}$ or $\text{m}^3/\text{sec}$ ]
$s$	Window or ventilation state [0/1]
$r$	Solar radiation [BTU or J]
$int$	Internal load [BTU or J]
$\rho$	Density [ $\text{lb}/\text{ft}^3$ or $\text{kg}/\text{m}^3$ ]
$c$	Specific heat [ $\text{BTU}/\text{lb}\cdot^{\circ}\text{F}$ or $\text{J}/\text{kg}\cdot^{\circ}\text{C}$ ]
$P$	Power [BTU J]
$N$	# of data points
<i>Subscript</i>	
$I$	Indoor air
$O$	Outdoor air
$W$	Wall
$F$	Floor
$V$	Supply

Table 2. Model nomenclature

Numerous variations of dynamical equations were formulated to model the heat transfer for each case study. The dynamical equations for each building use some combination of the following:

1. Uncontrollable inputs of outdoor air temperature and solar radiation
2. Controllable inputs of supply temperature and airflow rate or window state
3. Outputs (or state variables) of indoor air temperature and mass temperature

The basic form of the dynamical equations takes the material capacitance multiplied by the time derivative of that material's temperature and sets it equal to the sum of the temperature difference of each material divided by their respective resistance (see equation 2). Material capacitance and resistance encapsulates the physical properties in a simplified manner via single

parameter values. Complete dynamical equations for each model variation can be seen in the parameter identification section.

$$C_i \dot{T}_i(t) = \sum_{j=1}^N \frac{1}{R_{ij}} [T_j(t) - T_i(t)]$$

*Equation 2. General form of dynamical equations*

### 4.3.2 Parameter identification

#### *Select training data*

The first step of parameter identification is choosing a portion of the data set as the training data for the model. The following portions of data were selected as training data for each building:

1. LEES
  - a. Room 110 & 120: 6/25/2015 12:00 PM – 7/25/2015 12:00 PM
  - b. Room 233, 234, 235, 240, 241, & 242: 8/1/2015 9:00 AM – 8/31/2015 9:00 AM
2. IND: 9/1/2015 12:00 AM – 9/30/2015 11:00 PM
3. BH: 10/22/2013 1:00 AM – 6/19/2014 12:00 AM

The training data sets are a different duration and time period for each building due to the availability and accuracy of each full data set.

#### *Test persistence of excitation*

The next step is to restructure the dynamical equations into theta-phi form, or into one vector of parameters ( $\theta$ ) and one vector of state variables and inputs ( $\phi$ ). Once in this form, the persistence of excitation (PE) can be calculated for each  $\phi$  vector using the training data and equation 3, where  $T$  is the final time step and  $\lambda_{min}$  is the minimum eigenvalue. If all PE values are above zero, this indicates that the parameters are identifiable. PE is calculated for each model in Matlab (see Appendix 1.2).

$$\lambda_{min} \left\{ \int_{t_1}^{t_N} \phi(t) \phi^T(t) dt \right\} > 0$$

*Equation 3. Persistence of excitation formula*

#### *Gradient descent method*

To identify the parameters, the first strategy used is the gradient descent method. This method begins by randomly choosing initial conditions for the estimated  $\theta$  vector and  $\Gamma$  matrix to satisfy equations 4 through 7, in which  $m^2$  is the normalization variable,  $\epsilon$  is the normalized estimation error,  $z$  is the actual measured value,  $\hat{z}$  is the estimated model value,  $\hat{\theta}$  is the parameter estimate,  $J$  is a cost criteria to be minimized, and  $\Gamma$  is a symmetric positive-definite matrix. This process is then iterated with varying values of  $\hat{\theta}$  initial conditions and  $\Gamma$  matrices. Initial conditions for  $\hat{\theta}$  were chosen based on the calculation of approximated real thermal and physical properties of each building. The gradient descent method is performed in Matlab (see appendix 1.3).

$$m^2 = 1 + \phi^T \phi$$

Equation 4. Gradient descent normalization value

$$\epsilon = \frac{z - \hat{z}}{m^2}$$

Equation 5. Gradient descent normalized estimation error

$$J(\hat{\theta}) = \frac{1}{2} \epsilon^2$$

Equation 6. Gradient descent cost criteria

$$\frac{d\hat{\theta}(t)}{dt} = \Gamma \epsilon \phi, \quad \hat{\theta}(0) = \hat{\theta}_0$$

Equation 7. Gradient descent update law

### Nonlinear least squares method

The next strategy used for identifying parameters is the nonlinear least squares method. This method minimizes the square error between the simulation results and the training data using equations 9 and 10, in which P is defined by equation 8 and J is a cost criteria to be minimized. To begin this method, first the final  $\hat{\theta}$  values from the gradient descent method are selected as initial conditions. The function then does 100 iterations for each parameter. Once a full set of iterations is complete, the initial conditions for  $\hat{\theta}$  are replaced with the final values from the previous iteration of the nonlinear least squares function. This process is done anywhere from one to ten times, depending on how many iterations are needed until the simulation produces no further improvements in reducing the error. The nonlinear least squares method is performed in Matlab (see appendix 1.4).

$$P(t) = \left[ \int_{t_1}^{t_N} \phi(t) \phi^T(t) dt \right]^{-1}$$

Equation 8. Nonlinear least squares P matrix calculation

$$J(\hat{\theta}) = \frac{1}{2} \int_{t_1}^{t_N} [z(t) - \hat{z}(t)]^2 dt$$

Equation 9. Nonlinear least squares cost criteria

$$\frac{d\hat{\theta}(t)}{dt} = P \epsilon \phi, \quad \hat{\theta}(0) = \hat{\theta}_0, \quad \frac{dP(t)}{dt} = -P(t) \phi(t) \phi^T(t) P(t), \quad P(0) = P_0$$

Equation 10. Nonlinear least squares update law

### Simulation with parameter estimates

Once parameters were identified, the model had to be simulated in order to calculate the model error. To simulate the model, the dynamical equations were rearranged into a system of linear state-space equations (see equation 11), where A is a matrix of state variable parameters, B is a matrix of input variable parameters, x is a vector of state variables, and u is a vector of input variables. The state-space equations were then solved using initiation conditions chosen from the actual data set. This process was completed in Matlab (see appendix 1.5).

$$\dot{x} = Ax + Bu, \quad x(0) = x_0$$

Equation 11. General formula for model simulation



Once the model was simulated, different types of error parameters were calculated, including mean absolute error (MAE), standard deviation of absolute error (SDAE), mean absolute percent error (MAPE), standard deviation of absolute percent error (SDAPE), root mean square error (RMSE), and the coefficient of variation of the root mean square error (CVRMSE) using equations 12 through 15. This process was completed in Matlab (see appendix 1.6). MAE and SDAE are the best error parameters to use for single data points. They are also the only parameters that have meaningful units. MAPE and SDAPE are very simple to understand, because they are a percentage. That being said, these two parameters are very sensitive to the scale of data, and if aggregated over many data points, they might be misleading if the data points are not all within the same scale. In addition, MAPE and SDAPE cannot be calculated if any of the actual data points have a value of zero. RMSE and CVRMSE are both scale independent. However, they are typically most appropriate for normally distributed data and they are very sensitive to outliers and large individual errors.

$$MAE = \frac{1}{N} \sum_{i=1}^N |z_i - \hat{z}_i|, \quad SDAE = \sqrt{\frac{1}{N} \sum_{i=1}^N (|z_i - \hat{z}_i| - MAE)^2}$$

*Equation 12. MAE & SDAE calculation*

$$MAPE = \frac{1}{N} \sum_{i=1}^N \frac{|z_i - \hat{z}_i|}{z_i}, \quad SDAPE = \sqrt{\frac{1}{N} \sum_{i=1}^N \left( \frac{|z_i - \hat{z}_i|}{z_i} - MAPE \right)^2}$$

*Equation 13. MAPE & SDAPE calculation*

$$RMSE = \sqrt{\frac{1}{N} \sum_{i=1}^N |z_i - \hat{z}_i|^2}$$

*Equation 14. RMSE calculation*

$$CVRMSE = \frac{RMSE}{\frac{1}{N} \sum_{i=1}^N z_i}$$

*Equation 15. CVRMSE calculation*

### *K-fold cross validation*

Although the validation data set is not to be used during model generation in order to avoid overfitting, a method known as K-fold cross validation can be executed using only the training data. K-fold cross validation is done by first dividing the training data set into K equal portions. For this study, the training set was broken into ten sets. Next, parameters are identified using the gradient descent method and nonlinear least squares method, but only using one tenth of the original training data. Finally, the model is simulated with the other nine tenths of the training data, which are now being used as validation data, and the model errors are calculated. This process is iterated with each tenth of the data set being used as training data and the other nine tenths being used as validation data. K-fold cross validation can give information about how a model will run with data that was not used for parameter identification prior to the actual model validation. This process was completed in Matlab (see appendix 1.7). The K-fold cross validation method is specifically useful for comparing the error amongst different model variations, described in the next section. It should be stated that K-fold cross validation is not used to obtain the final model parameters, but rather is only used to test model variations.

### Model variations

Numerous models were generated using different variations of dynamical equations and parameter identification techniques. Subsequently, K-fold cross validation was run for each model and the previously defined model errors were computed and compared. The base case model for this process uses the dynamical equations seen in equation 16A, 16B, and 16C, in which all variables are as defined in the model nomenclature. Whenever a model called for wall temperature or floor temperature but one was not available, the other was used as an estimated value.

$$\begin{aligned} \text{A. } C_I \dot{T}_I(t) &= \frac{1}{R_{OI}} [T_O(t) - T_I(t)] + \frac{1}{R_{WI}} [T_W(t) - T_I(t)] + \frac{1}{R_{FI}} [T_F(t) - T_I(t)] + P_V s(t) \\ \text{B. } C_W \dot{T}_W(t) &= \frac{1}{R_{OW}} [T_O(t) - T_W(t)] + \frac{1}{R_{WI}} [T_I(t) - T_W(t)] \\ \text{C. } C_F \dot{T}_F(t) &= \frac{1}{R_{FI}} [T_I(t) - T_F(t)] \end{aligned}$$

Equation 16. Base case dynamical equations

The first model variation tested was a model using airflow rate and supply temperature rather than window/ventilation state. This model uses the base case dynamical equations, but replaces the  $P_V s(t)$  term in equation 1 with a  $\rho c V(t) [T_V(t) - T_I(t)]$  term. This model variant is further referred to as the airflow/supply temperature case.

$$\rho c V(t) [T_V(t) - T_I(t)]$$

Equation 17. Airflow/supply temperature case replacement term

The second model variation tested was a model for two stacked rooms (only applicable to LEES). This model uses the base case dynamical equations for each room, with an additional  $\frac{1}{R_{F2I1}} [T_{F,2}(t) - T_{I,1}(t)]$  term in the first floor equation 1 and an additional  $\frac{1}{R_{F2I1}} [T_{I,1}(t) - T_{F,2}(t)]$  term in the second floor equation C. This model variant is further referred to as the stacked room case.

$$\frac{1}{R_{F2I1}} [T_{F,2}(t) - T_{I,1}(t)], \frac{1}{R_{F2I1}} [T_{I,1}(t) - T_{F,2}(t)]$$

Equation 18. Stacked room case additional terms

The third model variation tested was a model that included solar radiation. This model uses the base case dynamical equations with an additional  $P_{r,I} r(t)$  term in equation A,  $P_{r,W} r(t)$  term in equation B, and  $P_{r,F} r(t)$  term in equation C. This model variant is further referred to as the solar radiation case.

$$P_{r,I} r(t), P_{r,W} r(t), P_{r,F} r(t)$$

Equation 19. Solar radiation case additional terms

The fourth model variation tested was a model that included internal loads. This variation was only tested for IND due to the limited energy data available. This model uses the base case dynamical equations with an additional  $P_{int,I} r(t)$  term in equation A,  $P_{int,W} r(t)$  term in equation B, and  $P_{int,F} r(t)$  term in equation C. This model variant is further referred to as the internal load case.

$$P_{int,I}^{int}(t), P_{int,W}^{int}(t), P_{int,F}^{int}(t)$$

*Equation 20. Internal load case additional terms*

The fifth model variation tested was a model in which all temperature data was normalized by the maximum temperature value. Normalization is done to ensure that all data falls between 0 and 1 to minimize computation time. When simulating the normalized model, the identified parameters must be multiplied by the maximum temperature during simulation. This model variant is further referred to as the normalized case.

The sixth and final model variation tested was a model in which the nonlinear least squares function bounded the parameters in two ways. The first bounded the parameters to adhere to their correct signs (positive or negative). The second bounded the parameters to fall within the order of magnitude of the respective calculated parameter approximations, based on the real thermal and physical properties of each building. This model variant is further referred to as the bounded case.

### *Linearization*

For the model variation using supply temperature and airflow rate, the dynamical equations are non-linear in the inputs and states. To identify the parameters of this model as a linear problem, the dynamical equations must first be linearized around equilibrium. Linearization was done using equation 21. Equilibrium points were chosen to ensure that all terms without inputs or state variables (i.e terms that are constant) disappear. This is done by setting the equilibrium airflow to 0 CFM. See equation 22A, 22B, and 22C for the final linearized dynamical equations.

$$f(x, u) \approx f(x^{eq}, u^{eq}) + \sum_i^N \frac{\partial f}{\partial x_i}(x^{eq}, u^{eq}) * (x_i - x_i^{eq}) + \sum_i^M \frac{\partial f}{\partial u_i}(x^{eq}, u^{eq}) * (u_i - u_i^{eq})$$

*Equation 21. Linearization formula*

$$\begin{aligned} \text{A. } C_I \dot{T}_I(t) &= - \left( \frac{1}{R_{OI}} + \frac{1}{R_{WI}} + \frac{1}{R_{FI}} + \rho c V^{eq} \right) * T_I(t) + \left( \frac{1}{R_{WI}} \right) * T_W(t) + \left( \frac{1}{R_{FI}} \right) * T_F(t) \\ &\quad + \left( \frac{1}{R_{OI}} \right) * T_O(t) + (\rho c [T_v^{eq} - T_I^{eq}]) * V(t) + (\rho c V^{eq}) * T_V(t) \\ \text{B. } C_W \dot{T}_W(t) &= \frac{1}{R_{OW}} [T_O(t) - T_W(t)] + \frac{1}{R_{WI}} [T_I(t) - T_W(t)] \\ \text{C. } C_F \dot{T}_F(t) &= \frac{1}{R_{FI}} [T_I(t) - T_F(t)] \end{aligned}$$

*Equation 22. Linearized dynamical equations with inputs of airflow and supply temperature*

### 4.3.3 Model validation

When the final model variations were selected, each model was validated using real measured data. The following portions of data were selected as validation data for each building:

1. LEES
  - a. Room 110 & 120: 7/25/2015 1:00 PM – 10/7/2015 12:00 AM
  - b. Room 233, 234, 235, 240, 241, & 242: 8/31/2015 10:00 AM - 10/7/2015 12:00 AM
2. IND: 9/30/2015 12:00 PM – 10.31/2015 12:00 AM

### 3. BH: 6/19/2014 12:00 AM – 10/14/2014 9:00 AM

After the validation data set was simulated for each building model, the previously described error parameters were calculated. This process was completed in Matlab.

## 4.4 Comfort and energy analysis

Using the data collected from each building, analysis was conducted to assess the performance of night ventilation with regard to comfort and energy. Four types of analysis were performed in this process. The first was a baseline analysis looking at indoor conditions on specific days and finding daily and seasonal trends across the data set. The second and third analyses were comparisons of comfort and energy metrics across data with and without the use of night ventilation, the first of which using measured data and the second of which using simulated data. The fourth and final analysis was a comparison of indoor conditions to different comfort standards.

### 4.4.1 Baseline data analysis

First, trends of indoor air temperature, mass temperature, and instantaneous damping (see equation 23) were ascertained to determine if any daily or seasonal trends exist. For the US data, seasons were defined as follows: Spring from March to May, Summer from June to August, Fall from September to November, and Winter from December to February. For the India data, seasons were defined as follows: Pre-Monsoon from March to May, Monsoon from June to September, Post-Monsoon from October to November, and Winter from December to February.

Next, numerous comfort and energy metrics were calculated for individual days including daily indoor maximum air temperature ( $T_{I,max}$ ), daily maximum damping (see equation 24), daily indoor temperature range (see equation 25), decrement factor (see equation 26), daily time lag (see equation 27), daily energy removed (see equation 28a), area normalized daily energy removed (see equation 28b), and potential energy efficiency (see equation 29). These metrics are visualized in figure 12. Fan energy was estimated based on the fan motor power curve provided in the product specifications, while the COP was estimated as 4, based on the average COP for “best practice” heat pumps. Each of these metrics was then assessed across time.

$$Damp_{inst} = T_o - T_i$$

*Equation 23. Instantaneous Damping*

$$Damp_{max} = T_{O,max} - T_{I,max}$$

*Equation 24. Daily maximum damping*

$$T_{I,range} = T_{O,max} - T_{I,min}$$

*Equation 25. Daily indoor temperature range*

$$f = \frac{T_{I,max} - T_{I,min}}{T_{O,max} - T_{O,min}}$$

*Equation 26. Decrement factor*

$$\varphi = t(T_{O,max}) - t(T_{I,max})$$

Equation 27. Time lag

$$Q = \int_{t_1}^{t_N} V \rho_{air} c_{air} (T_I(t) - T_O(t)) dt, \quad Q_{norm} = \frac{\int_{t_1}^{t_N} V \rho_{air} c_{air} (T_I(t) - T_O(t)) dt}{Area}$$

Equation 28. A) Daily energy removed, B) Area normalized daily energy removed

$$PEE = (\frac{Q}{COP}) / Q_{fan}$$

Equation 29. Potential energy efficiency

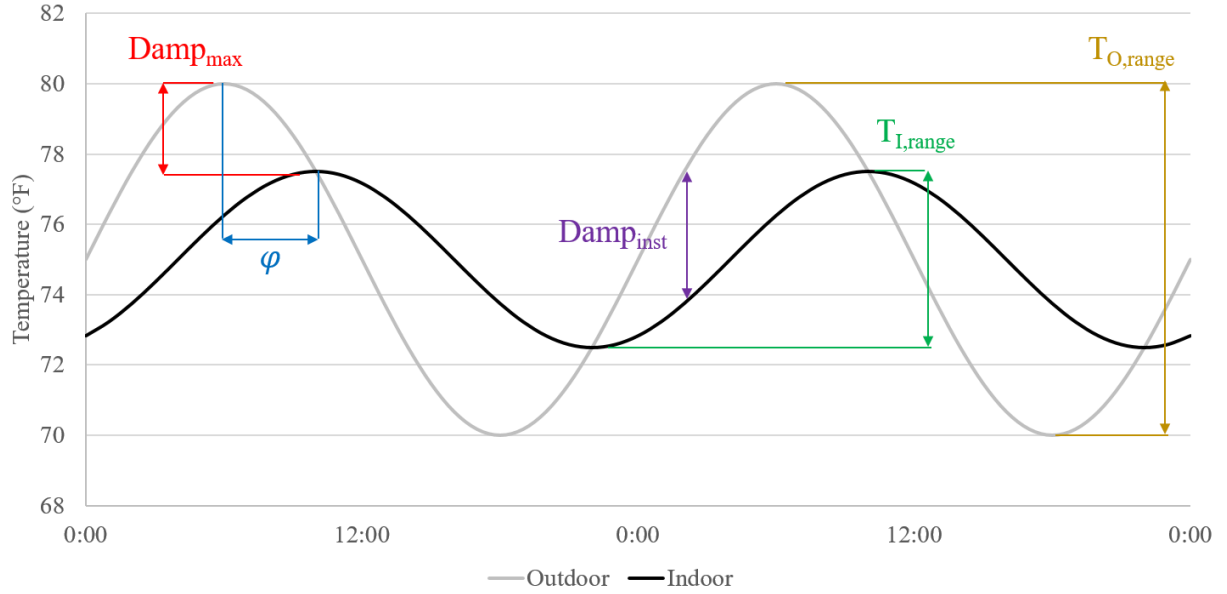


Figure 12. Performance metric visualization

#### 4.4.2 Comparison of night ventilation vs non-night ventilation using real data

Analysis was done to see how the buildings were behaving on days with and without night ventilation. For this comparison, the performance metrics discussed in section 4.4.1 were assessed for both cases. A  $p$ -value  $< .05$  was considered satisfactory for all t-tests.

Remembering that the goal of night ventilation with thermal mass is to reduce the indoor temperature peak and decrement, while maximizing the thermal dampening and lag effects, one strategy was considered to perform better than another if:

- Average  $T_{I,max}$  was lower
- Average  $T_{I,range}$  was lower
- Average  $f$  was lower
- Average  $Damp_{max}$  was higher
- Average  $\varphi$  was higher
- Average  $Q$  was higher
- Average PEE was higher

The night ventilation effect is defined in terms of the day after night ventilation (as described in the building description section) is executed. For the purpose of this analysis, night

ventilation in LEES occurs whenever the airflow rate goes above 700 CFM during unoccupied hours and night ventilation occurs in IND and BH whenever the window is opened for any duration during unoccupied hours. For IND and BH, the non-night ventilation case is defined as days in which the window is closed for the entire day and night. For LEES, there are two forms of the non-night ventilation case. The first is termed regular airflow mode, in which the airflow is at its minimum code-required value and there is no daytime or nighttime cooling. The second is termed daytime cooling mode, in which the airflow is ramped up during occupied daytime hours.

#### 4.4.3 Comparison to comfort standards

After comparing night ventilation and non-night ventilation conditions using measured data, each data set was compared to the ACS for naturally ventilated buildings in ASHRAE Std 55 (2013). The ACS was deemed applicable for each case study due to their use of natural conditioning, lack of mechanical cooling, and prevailing mean outdoor temperature greater than 10 °C (50 °F) and less than 33.5 °C (92.3 °F), which represent the limits of applicability described in the standard. For the purposes of this analysis, a homogenous mean radiant temperature has been estimated based on the area weighted surface temperature (see equation 30). BH data was additionally compared to the newly created India Model for Adaptive Comfort (IMAC), developed at the Centre for Advanced Research in Building Science & Energy (CARBSE) (Manu et al. 2016). For these comparisons, discomfort degree hours (DDH) were calculated for each case (see equation 31). For the critical temperature for the DDH calculation, the ACS or IMAC upper and lower 80% acceptability limit were used for occupied hours. The acceptability limits for ACS and IMAC are generated using equations 33 and 34, where  $\overline{t_{pma(out)}}$  is the prevailing mean outdoor air temperature, calculated by taking the unweighted 7-day moving average of the mean daily outdoor air temperature (see equation 32). For unoccupied hours in LEES and IND, the values of 10 °C (50 °F) and 32 °C (90 °F) were used as temperature thresholds for DDH. For unoccupied hours in BH, the values of 20 °C and 35 °C were used as temperature thresholds for DDH.

$$T_{mr} = \frac{\sum T_{s,i} A_i}{\sum A_i}$$

Equation 30. Area weighted surface temperature

$$DDH_+ = \sum_{t=1}^N h_t (T_{op,t} - T_{crit,t}) \begin{cases} h_t = 1 \text{ h if } T_{op,t} \geq T_{crit,t} \\ h_t = 0 \text{ if } T_{op,t} < T_{crit,t} \end{cases}$$

$$DDH_- = \sum_{t=1}^N h_t (T_{crit,t} - T_{opt,t}) \begin{cases} h_t = 1 \text{ h if } T_{op,t} \leq T_{crit,t} \\ h_t = 0 \text{ if } T_{op,t} > T_{crit,t} \end{cases}$$

Equation 31. Discomfort degree hours

$$\overline{t_{pma(out)}} = \frac{\left( \sum_d^{d+6} \left( \frac{\sum_h^{h+23} T_{O,h,d}}{24} \right) \right)}{7}$$

Equation 32. Prevailing mean outdoor air temperature

$$Limit_{upper} = 0.31 * \overline{t_{pma(out)}} + 21.3(^{\circ}C)/60.5(^{\circ}F)$$

$$Limit_{lower} = 0.31 * \overline{t_{pma(out)}} + 14.3(^{\circ}C)/47.9(^{\circ}F)$$

Equation 33. ACS 80% acceptability limits

$$Limit_{upper} = 0.56 * \overline{t_{pma(out)}} + 17.06$$

$$Limit_{lower} = 0.56 * \overline{t_{pma(out)}} + 8.96$$

Equation 34. IMAC 80% acceptability limits

#### 4.4.4 Comparison of night ventilation vs non-night ventilation using model

Finally, a comparison was done using the previously generated model. To understand how each building would have performed without night ventilation, a simulation was run for each building without the presence of night ventilation. For LEES, this meant running a model in regular airflow mode and daytime cooling mode. For IND and BH, this meant running a model with windows closed all day and night. A simulation was also run for LEES using its control sequence, as per design, and its control sequence only with night ventilation. To assess performance in each ventilation mode, the performance metrics discussed in section 4.4.1 were calculated for the simulations with real inputs, and for simulations with no night ventilation, and later compared. A p-value < .05 was considered satisfactory for all t-tests conducted.

### 4.5 Optimization

Using the model generated for each building, an optimization was run to determine a control strategy that would minimize energy usage, limit changing window state, and maintain comfort. The following describes the methodology used for system optimization of each building.

#### 4.5.1 LEES optimization

LEES optimization was conducted in two ways. The first method minimizes airflow rate, as a proxy for fan energy, while maintaining comfort as a constraint. This optimization uses equation 35 as the objective function and equations 36A-36F as the constraints, in which constraints 1 through 3 utilize Euler's method and the dynamics captured by the model parameters, constraint 4 calculates operative temperature, constraint 5 sets minimum and maximum airflow based on system capacity and code requirements, and constraint 6 sets minimum and maximum operative temperature based on the ACS 80% acceptability limits. This process was completed in Matlab (see appendix 1.8).

$$\min_V \sum_{k=1}^N V(k)$$

Equation 35. LEES objective function with comfort as constraint

- A.  $T_I(k+1) = T_I(k) + \Delta k * \frac{dT_I}{dk}, T_I(1) = T_{I,1}$
- B.  $T_W(k+1) = T_W(k) + \Delta k * \frac{dT_W}{dk}, T_W(1) = T_{W,1}$
- C.  $T_F(k+1) = T_F(k) + \Delta k * \frac{dT_F}{dk}, T_F(1) = T_{F,1}$
- D.  $T_{OP}(k) = (T_I(k) + T_{mr}(k))/2$
- E.  $V_{min}(k) \leq V(k) \leq V_{max}(k)$
- F.  $T_{Op,min}(k) \leq T_{Op}(k) \leq T_{Op,max}(k)$

The second method minimizes airflow rate and temperature deviation from the ACS acceptability limits, rather than constraining the temperature, which allows for flexibility in the system. This optimization uses equation 37 as the objective function and the same constraints as the previous method with the exception of constraint 6, in which  $\alpha_1$  and  $\alpha_2$  are factors used to weigh the importance of energy and comfort. This process was completed in Matlab (see appendix 1.9). After the model was optimized, DDH was calculated with a temperature threshold of ACS upper 80% acceptability limit, and compared to the DDH of measured data.

$$\min_{(T_{op}, V)} \sum_{k=1}^N \alpha_1 \max(T_{op}(k) - T_{\max}(k), T_{\min}(k) - T_{op}(k), 0) + \alpha_2 V(k)$$

Equation 37. LEES objective function with comfort as objective

#### 4.5.2 BH & IND optimization

Because BH and IND do not consume energy with their night ventilation scheme, the BH and IND optimization were conducted by minimizing only the temperature deviation from the ACS acceptability limits. This optimization uses equation 38 as the objective function and the same constraints as the previous method with the exception of constraints 5 and 6. This optimization also uses one additional constraint that limits the number of window state changes in a 24 hour period (see equation 39), in which  $\mu$  is a change of window state. This process was completed in Matlab (see appendix 1.10). After the model was optimized, DDH was calculated with a temperature threshold of ACS upper 80% acceptability limit, and compared to the DDH of measured data.

$$\min_{T_{op}} \sum_{k=1}^N \max(T_{op}(k) - T_{\max}(k), T_{\min}(k) - T_{op}(k), 0)$$

Equation 38. BH & IND objective function

$$\sum_k^{k+24} \mu(s(k)) \leq 2$$

Equation 39. BH & IND additional constraint



## 5. Results

### 5.1 Baseline data analysis

The following shows results of the analysis conducted as described in section 4.4.1. Baseline data analysis.

#### 5.1.1 La Escuelita Elementary School

The hottest week of the data set took place from September 5<sup>th</sup> to September 11<sup>th</sup>, 2015. Indoor conditions were examined from one day of the hottest week in which night ventilation was successfully executed. In classroom 233 on September 10<sup>th</sup>, 2015, the airflow was ramped up between 2 AM and 8 AM to 1100-1500 CFM, as seen in figure 13. After 8 AM, the airflow rate fluctuated between 0 and 300 CFM until 11 PM when it was ramped up again for night ventilation. Throughout the day, the outdoor air temperature had a diurnal swing of 14.4 °C (26 °F), peaking at 30 °C (86 °F) at 1 PM. The indoor air temperature ranged from 21.1 °C (70 °F) to 24.7 °C (76.5 °F) throughout the day, peaking at 3 PM, 2 h after the outdoor air temperature peak. During the night ventilation period, the indoor air temperature decreased by 3.6 °C (6.5 °F). The mass floor temperature ranged from 22.7 °C (73 °F) to 24.7 °C (76.5 °F) throughout the day and decreased by 1.9 °C (3.5 °F) during the night ventilation period. The strategy seems to have been effective at reducing the indoor temperatures during the day.

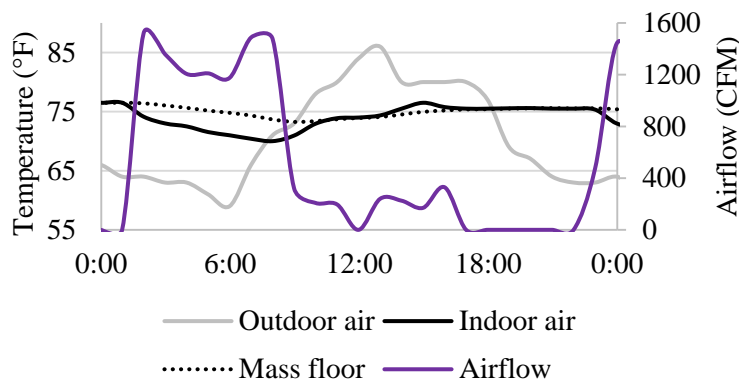


Figure 13. LEES room 233 temperature and airflow profile during and after night ventilation

Throughout the entire week, night ventilation was executed on Saturday, Tuesday, Wednesday, Thursday, and Friday in classroom 233 during unoccupied hours when the mass temperature was above 70 °F, as seen in figure 14. During night ventilation periods, airflow ranged from 800 to 1500 CFM. The outdoor air temperature had a 23.3 °C (42 °F) range across the week, spanning from 11.1 °C (52 °F) to 34.4 °C (94 °F). The daily outdoor air temperature peaks ranged from 25 °C (77 °F) to 33.9 °C (93 °F), taking place between 1 PM and 4 PM. The indoor air temperature and mass temperature both had only a 6.7 °C (12 °F) range across the week, spanning from about 18.3 °C (65 °F) to 25 °C (77 °F), peaking at 20 °C (68 °F) to 25 °C (77 °F) from 6 PM to 11 PM. The indoor air temperature and mass temperature tracked each other very closely, with the exceptions being the two nights (Thursday and Friday) when night ventilation airflow rates

extended for longer periods, resulting in indoor air dropping lower than mass temperature compared to the other days. The hourly instantaneous damping fluctuated between  $-7.8^{\circ}\text{C}$  ( $-14^{\circ}\text{F}$ ) and  $11.1^{\circ}\text{C}$  ( $20^{\circ}\text{F}$ ), peaking anywhere from  $1.1^{\circ}\text{C}$  ( $2^{\circ}\text{F}$ ) to  $11.1^{\circ}\text{C}$  ( $20^{\circ}\text{F}$ ) around 1 PM each day, as seen in figure 15. The strategy was successful in keeping the range of indoor air temperature and mass temperature fairly narrow and consistently delaying the peak daily temperatures. That being said, it seems as though the strategy is not exactly following the design control sequence because night ventilation ran on Saturday.

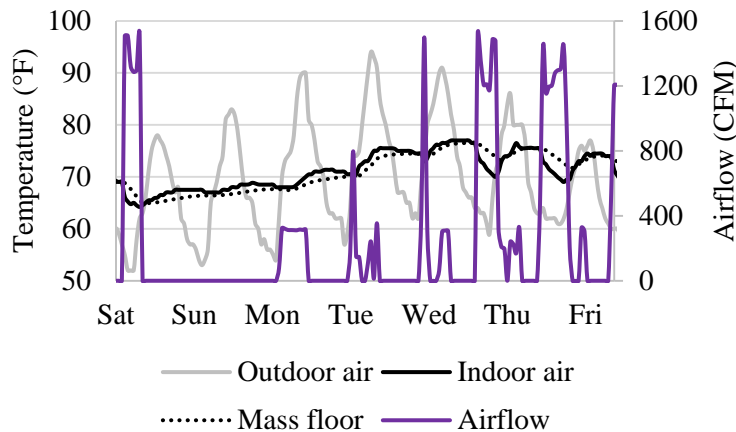


Figure 14. LEES room 233 temperature and airflow profile over one week

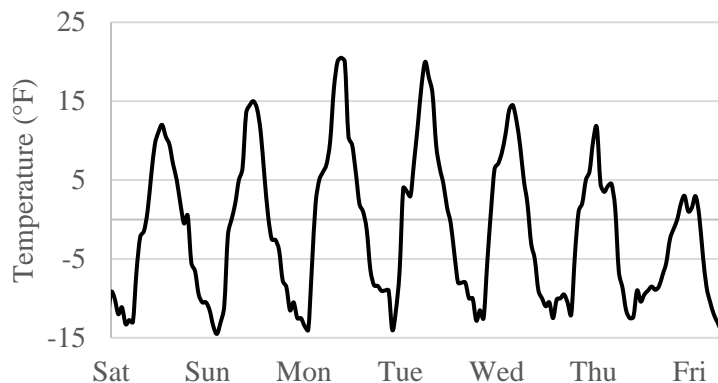


Figure 15. LEES room 233 instantaneous damping over one week

Each of the performance metrics was calculated over the course of the entire data set for all 8 classrooms, with a sample size of 842 d (19,962 h), with 133 d in each of the first floor classrooms and 96 d in each of the second floor classrooms. The daily maximum indoor air temperature ranged from  $18.9^{\circ}\text{C}$  ( $66^{\circ}\text{F}$ ) –  $28.3^{\circ}\text{C}$  ( $83^{\circ}\text{F}$ ), with median values between  $21.7^{\circ}\text{C}$  ( $71^{\circ}\text{F}$ ) and  $23.9^{\circ}\text{C}$  ( $75^{\circ}\text{F}$ ) for each room (figure 16). These low temperature peaks would indicate that the strategy is successfully lowering the indoor temperature. The daily maximum damping ranged from  $-5.6^{\circ}\text{C}$  ( $-10^{\circ}\text{F}$ ) to  $11.1^{\circ}\text{C}$  ( $20^{\circ}\text{F}$ ), with median values between  $-0.6^{\circ}\text{C}$  ( $-1^{\circ}\text{F}$ ) and  $1.7^{\circ}\text{C}$  ( $3^{\circ}\text{F}$ ) for each room (figure 17). The median maximum damping values are fairly low, but this could be explained by the mild climate and fairly low outdoor temperatures. When comparing these parameters across classrooms, the maximum temperature seemed to be higher and maximum damping seemed to be lower in rooms on the southern side of the building

(240-242). This is probably the case because these rooms have solar exposure for a greater amount of time and stronger intensity.

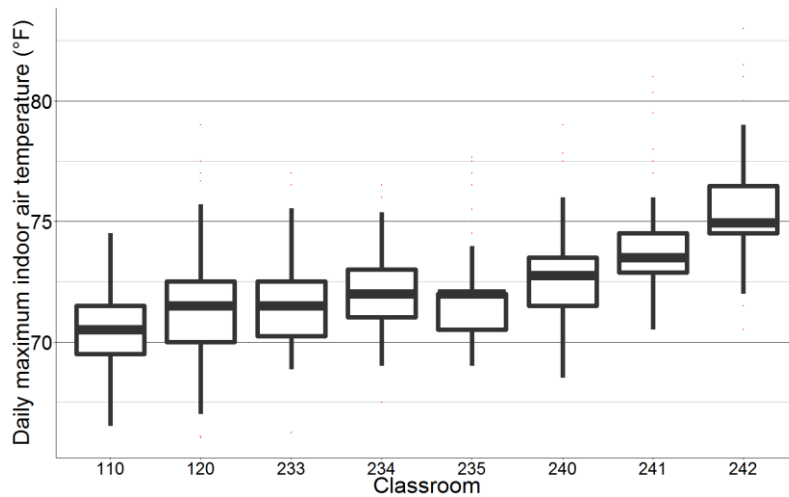


Figure 16. LEES daily maximum indoor air temperature

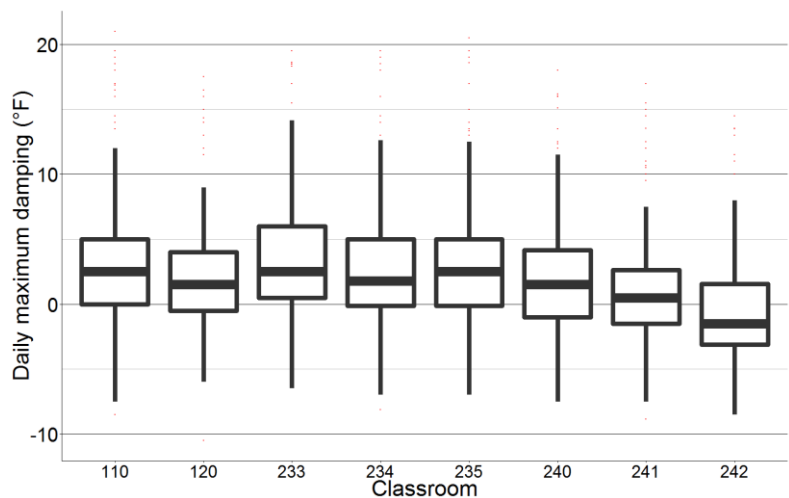


Figure 17. LEES daily maximum damping

The daily indoor air temperature range spanned from 0 to 5.6 °C (10 °F), with median values between 0.3 °C (0.5 °F) and 3.3 °C (6 °F) for each room (figure 18), while the daily decrement factor ranged from 0 to 1.2, with median values of 0.05 to 0.3 for each room (figure 19).

Comparing across classrooms, the daily temperature range and daily decrement factor were noticeably larger for rooms on the second floor, especially those with south facing walls. One of the south facing second story rooms even had a day in which the daily decrement factor above 1, indicating that the indoor temperature range was wider than the outdoor temperature range. The second story rooms probably have higher values for these parameters due to the fact that they are not ground-coupled and that the first story rooms have higher night ventilation airflow setpoints.

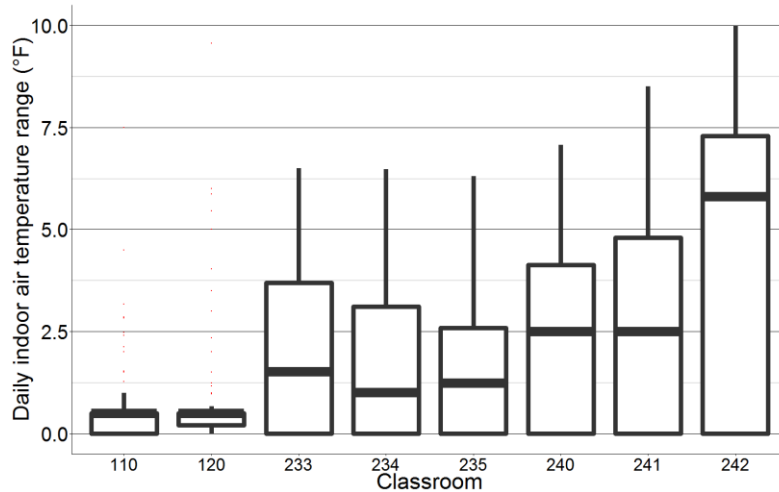


Figure 18. LEES daily indoor air temperature range

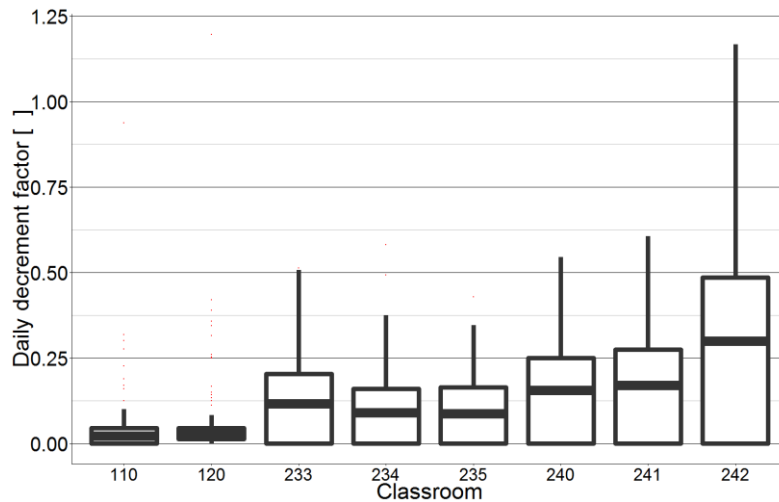


Figure 19. LEES daily decrement factor

Finally, the area normalized daily energy removed from the building during night ventilation ranged from 0 to 300 BTU/ft<sup>2</sup> with median values between 0 and 50 BTU/ft<sup>2</sup> for each classroom (figure 20), while the daily potential energy efficiency ranged from 0 to 22, with median values between 2.5 and 6 for each room (figure 21). Potential energy efficiency above 1 indicates that the strategy is removing more energy than is being consumed. Therefore, the strategy is definitely effective with respect to energy. Comparing across classrooms, rooms 240, 241, and 242 removed significantly more energy than any other room, probably because these rooms were running with increased airflow rates for a larger portion of time. That being said, all of the rooms had similar potential energy efficiency, with the exception of room 241, which had a much higher potential energy efficiency than any of the other rooms. This is probably the case because room 241 is ventilating the space at a lower airflow rate setpoint than other rooms, while simultaneously maintaining a large difference in indoor and outdoor temperature due to the higher indoor air temperatures on the second floor.

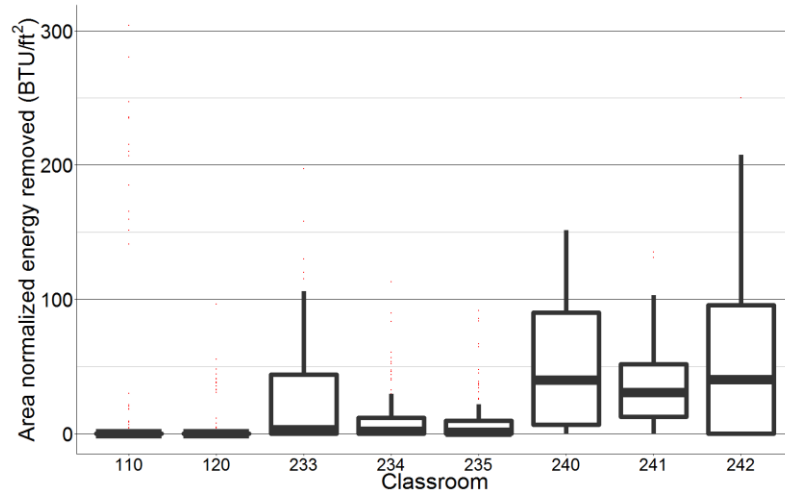


Figure 20. LEES area normalized daily energy removed

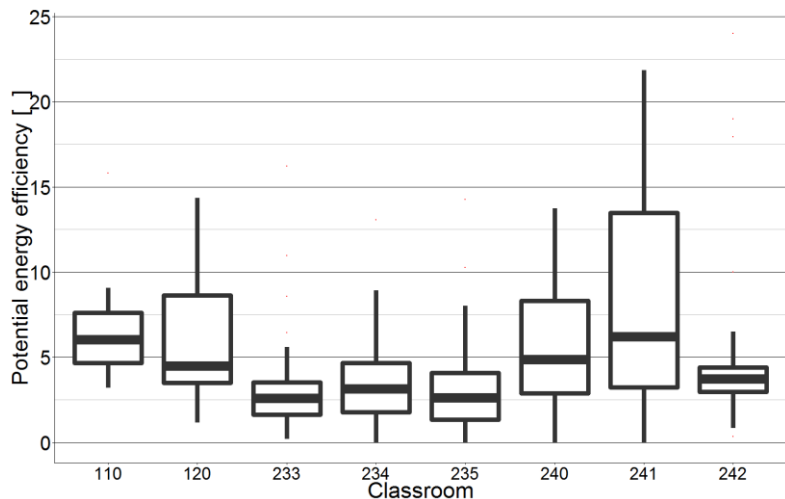


Figure 21. LEES daily potential energy efficiency

### 5.1.2 Indio Building

The hottest week of the data set took place from September 17<sup>th</sup> to September 23<sup>th</sup>, 2015. Indoor conditions were examined from one day of the hottest week in which night ventilation was successfully executed. On September 18<sup>th</sup>, 2015, the windows and skylights were opened between 10 PM and 7:30 AM, as seen in figure 22. After 7:30 AM, the windows stayed closed for the remainder of the day. Throughout the day, the outdoor air temperature had a diurnal swing of 15 °C (27 °F), peaking at 27.8 °C (82 °F) at 2 PM. The indoor air temperature ranged from 20.6 °C (69 °F) to 23.3 °C (74 °F) throughout the day, peaking 6 h after outdoor air temperature at 8 PM. During the night ventilation period, the indoor air temperature decreased by 2.8 °C (5 °F). The mass floor temperature stayed at 20.6 °C (69 °F) throughout the entire night and day. The strategy seems to have been effective at reducing the indoor air temperature and maintaining a constant mass temperature.

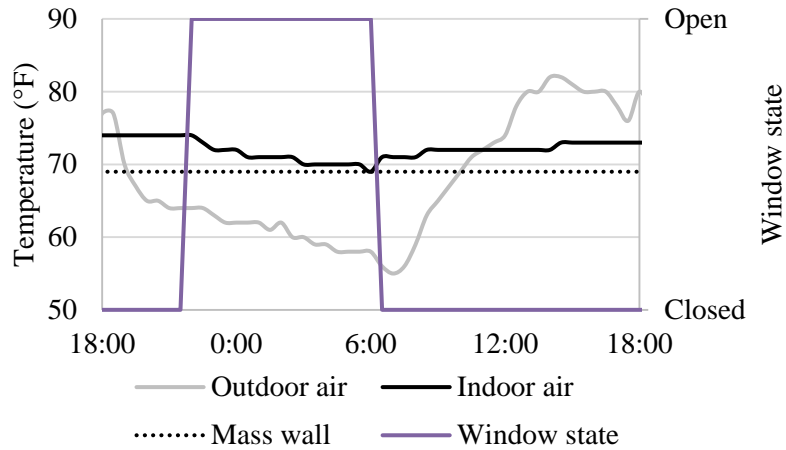


Figure 22. IND temperature and window state profile during and after night ventilation

Throughout the entire week, night ventilation was executed on Friday, Monday, and Wednesday, as seen in figure 23. The night ventilation execution was consistent with the design criteria of indoor air temperature above 21.1 °C (70 °F) and outdoor air temperature below 20 °C (68 °F). During night ventilation periods, windows were open for timespans of 3.5 to 8.5 h. The outdoor air temperature had a 28.3 °C (51 °F) range across the week, spanning from 11.7 °C (53 °F) to 40 °C (104 °F). The daily outdoor air temperature peaks ranged from 23.9 °C (75 °F) to 40 °C (104 °F), taking place between 12 PM and 6:30 PM. The indoor air temperature had only a 2.2 °C (4 °F) range across the week, spanning from about 21.1 °C (70 °F) to 23.3 °C (74 °F), staying between 22.8 °C (73 °F) and 23.3 °C (74 °F) for most of the daytime hours. The mass temperature remained at a constant value of 20.6 °C (69 °F) for the entire week. The hourly instantaneous damping fluctuated between -10 °C (-18 °F) and 16.7 °C (30 °F), peaking at varying times of the day between 12 PM and 6 PM, as seen in figure 24. The strategy was successful in keeping the range of indoor air temperature extremely narrow, which is probably the reason why instantaneous damping has such a large range of values. That being said, the strategy did not seem to impact the mass temperature or delay the peak indoor air temperatures. It is possible that the indoor air temperature and mass temperature have little fluctuation due to the fact that the mass is so heavy that it is effectively maintaining constant indoor temperatures without the need for additional passive cooling.

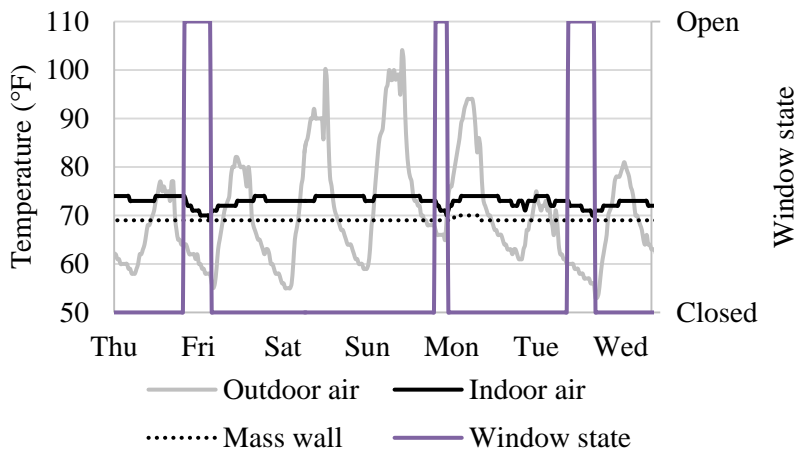


Figure 23. IND temperature and window state profile over one week

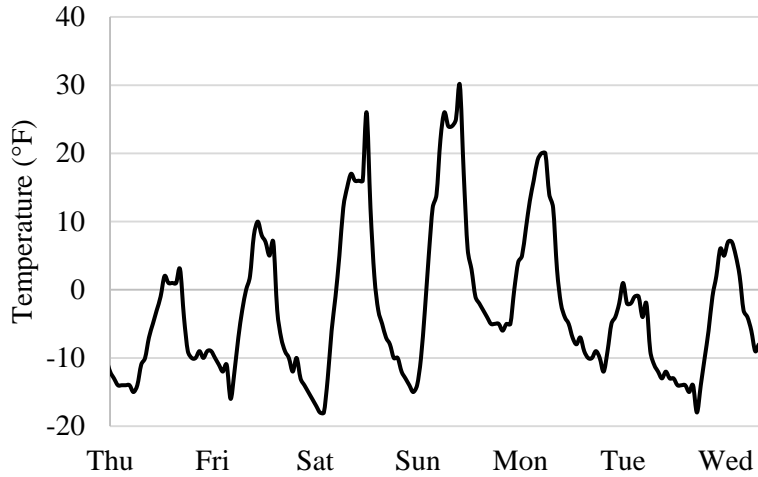


Figure 24. IND instantaneous damping over one week

Each of the performance metrics was calculated over the course of the entire data set, with a sample size of 60 d (1440 h). The daily maximum indoor air temperature ranged from 22.2 °C (72 °F) – 23.9 °C (75 °F), with a median value of 23.1 °C (73.5 °F) (figure 25A). These low temperature peaks would indicate that the strategy is successfully lowering the indoor temperature. The daily maximum damping ranged from -1.1 °C (-2 °F) to 11.7 °C (21 °F), with a median value of 3.9 °C (7 °F) (figure 25B). The large range in maximum damping values and very narrow range of indoor temperature peaks suggests that damping is fairly independent of the indoor temperature and depends almost entirely on the outdoor temperature. The daily time lag ranged from -10 to 8 h, with a median value of 0 h (figure 25C). This suggest that the time of indoor air temperature peak is independent of the outdoor temperature, and probably dominated by the internal load.

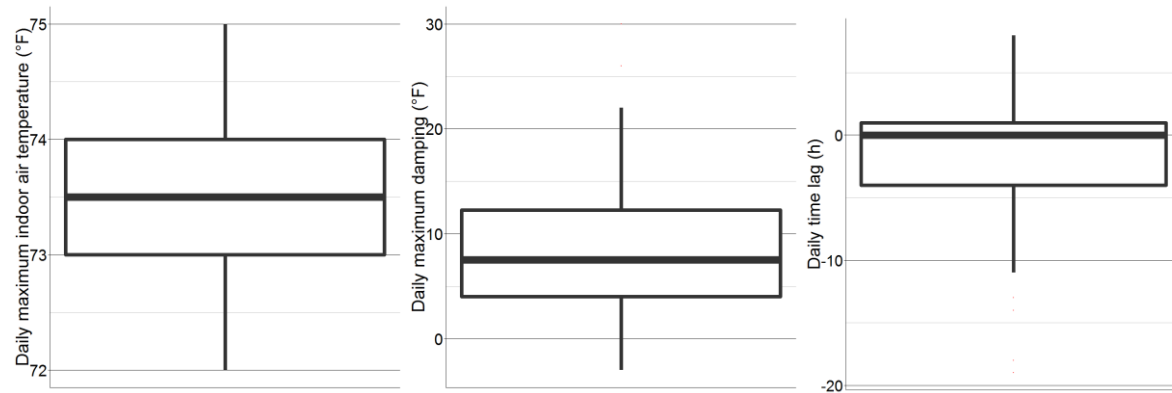


Figure 25. A) IND daily maximum indoor air temperature; B) IND daily maximum damping; C) IND time lag

The daily indoor air temperature range spanned from 0 to 3.9 °C (5 °F), with a median value of 1.1 °C (2 °F) (figure 26A), while the daily decrement factor ranged from 0 to 0.22, with median value of .1 (figure 26B). It should be noted that the median range of indoor air temperature is very small, further suggesting that the indoor air temperature is not reliant on the outdoor air temperature.

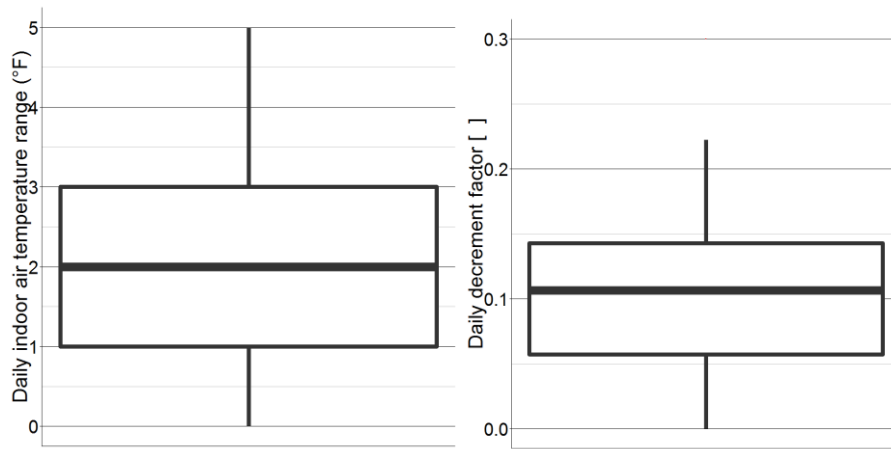


Figure 26. A) IND daily indoor air temperature range; B) IND daily decrement factor

### 5.1.3 Blessing House

One of the hottest weeks of the data set with consistent night ventilation took place from May 17<sup>th</sup> to May 23<sup>rd</sup>, 2014. Indoor conditions were first examined from one day of this week. On May 23<sup>rd</sup>, 2014, the window was open from 5 PM to 7 AM, and closed for the remainder of the day until 6 PM, as seen in figure 27. Throughout the day, the outdoor air temperature had a diurnal swing of 13 °C, peaking at 39 °C at 2 PM. The indoor air temperature ranged from 29 to 31 °C throughout the day, peaking 5 h after outdoor air temperature at 7 PM. During the night ventilation period, the indoor air temperature decreased by 2 °C. The mass wall temperature ranged from 30 to 33 °C throughout the day and decreased by 2 °C during the night ventilation period. The strategy seems to have been effective at reducing the indoor air and mass temperatures for the beginning of the daytime period.

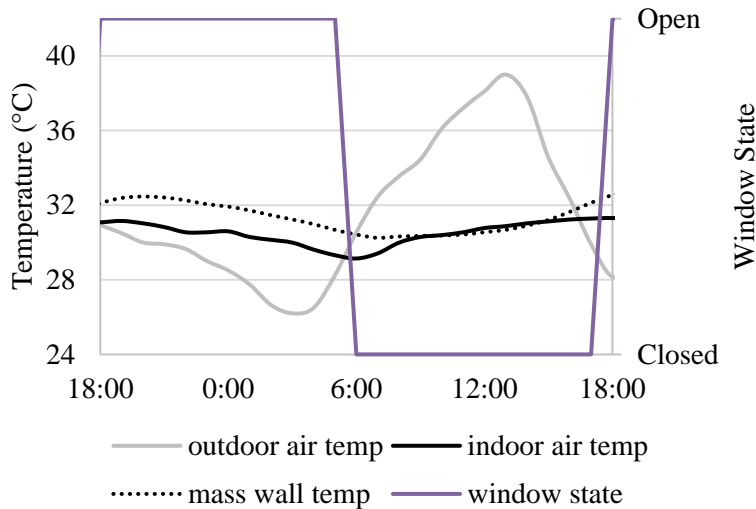


Figure 27. BH temperature and window state profile during and after night ventilation



Night ventilation was executed every night of this week, keeping the windows open between 11 and 14 h, as seen in figure 28. (Since this is a residential building, rather than a commercial building like the other two, it's not surprising that weekend and weekday operation is similar). The outdoor air temperature had a 13.5 °C range across the week, spanning from 25.5 to 39 °C. The daily outdoor air temperature peaks ranged from 34.5 to 39 °C, taking place between 10 AM and 1 PM. The indoor air temperature had only a 3 °C range across the week, spanning from about 28.5 to 31.5 °C, peaking at 30.5 to 31.5 °C from 4 PM to 7 PM. The mass temperature also had a 3 °C range across the week, but spanned from about 30 to 33 °C, peaking at 31.5 to 33 °C from 5 PM to 10 PM, always a few hours after indoor air temperature. The hourly instantaneous damping fluctuated between -4.5 and 8.5 °C, peaking anywhere from 4 to 8.5 °C between 10 AM and 1 PM each day, as seen in figure 29. The strategy was successful in keeping the range of indoor air temperature and mass temperature fairly narrow and consistently delaying the peak daily temperatures.

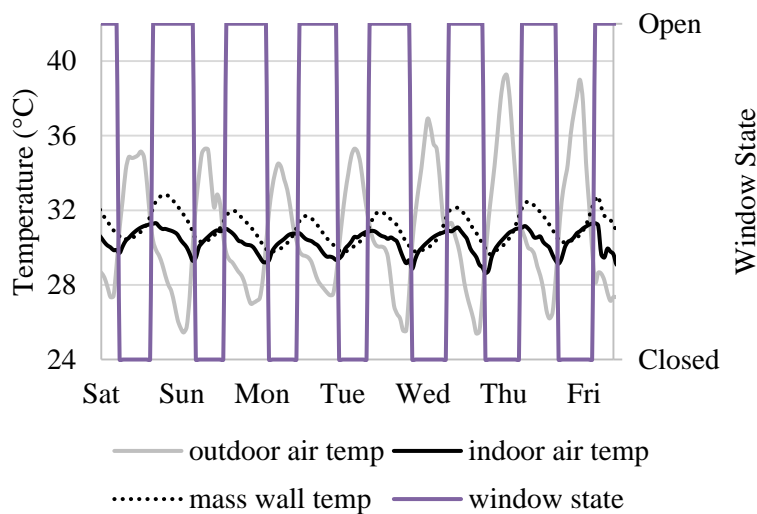


Figure 28. BH temperature and window state over one week

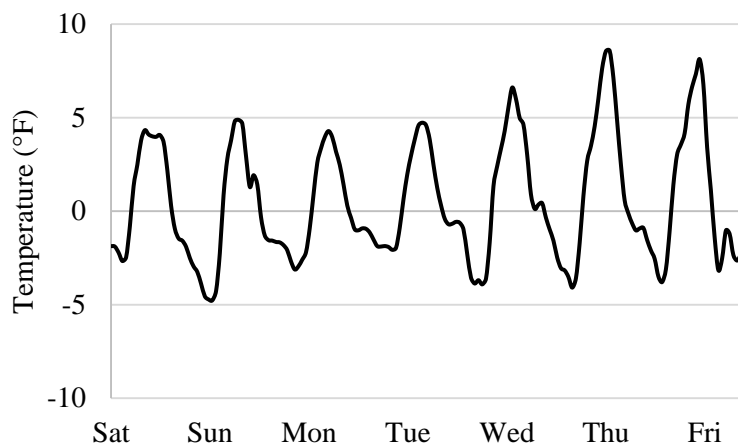


Figure 29. BH instantaneous damping over one week

Each of the performance metrics was calculated over the course of the entire data, with a sample size of 357 d (8577 h), with 92 days in Pre-Monsoon, 122 days in Monsoon, 53 days in Post-Monsoon, and 90 days in Winter. The daily maximum indoor air temperature ranged from 22.5 – 32.5 °C, with median values between 25 and 30 °C for each season (figure 30). When comparing daily peak temperature across seasons, the parameter is highest during the Pre-Monsoon and Monsoon seasons, probably because these are the seasons with the highest outdoor temperatures. The daily maximum damping ranged from 0 to 8.5 °C, with median values between 3.5 and 5 °C for each season (figure 31). Unlike peak temperature, this parameter was lowest during the Pre-Monsoon and Monsoon seasons, indicating that even though the outdoor temperatures are higher, the indoor temperatures are maintaining consistent values. The daily time lag ranged from 1 to 11 h, with median values between 6 and 7 h for each season (figure 32). Time lag stayed fairly consistent across seasons.

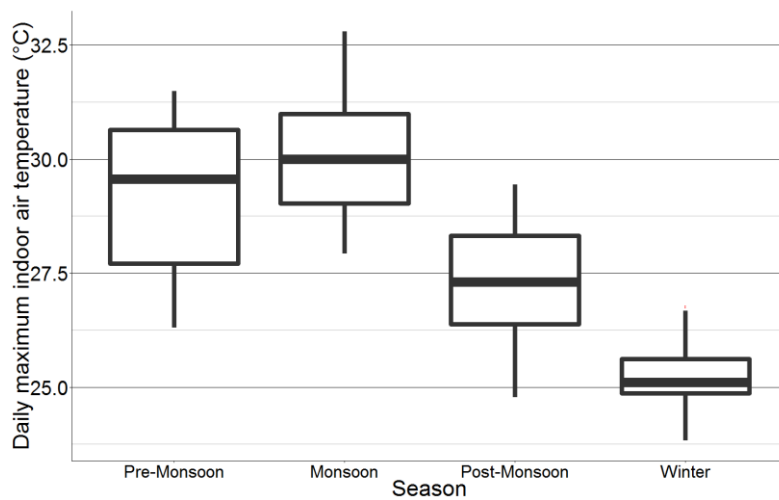


Figure 30. BH daily maximum indoor air temperature by season

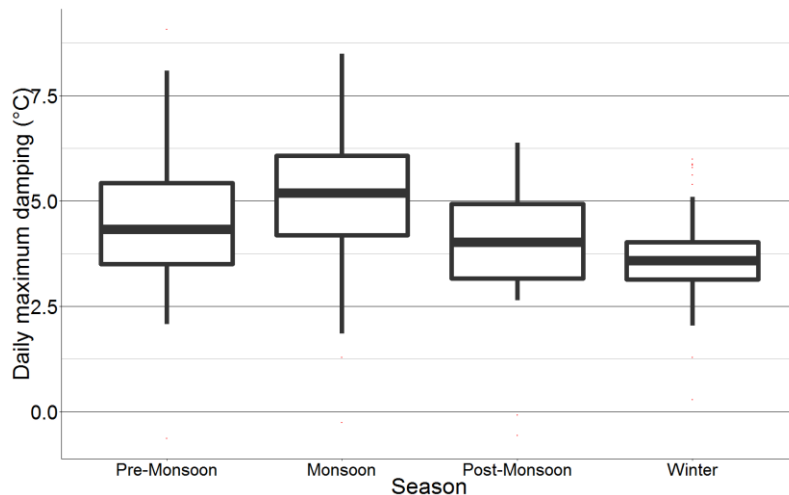


Figure 31. BH daily maximum damping by season

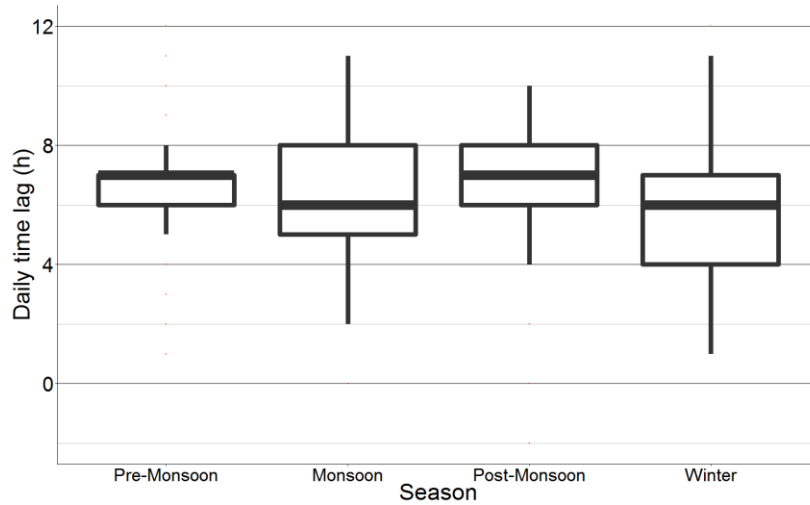


Figure 32. BH daily time lag by season

The daily indoor air temperature range spanned from 0.2 to 3 °C, with median values between 1.3 and 1.9 °C for each season (figure 33), while the daily decrement factor ranged from 0.05 to 0.3, with median values of 0.15 to 0.2 for each season (figure 34). Comparing across seasons, like peak temperature, the daily temperature range and decrement factor were larger for the Pre-Monsoon and Monsoon seasons, but by less than 1 °C. Finally, the daily energy removed ranged from 0 to 300,000 kJ, with median values between 0 and 100,000 kJ for each season (figure 35). The daily energy removed is significantly higher for the Monsoon season than any other season, probably because this season has the strongest winds.

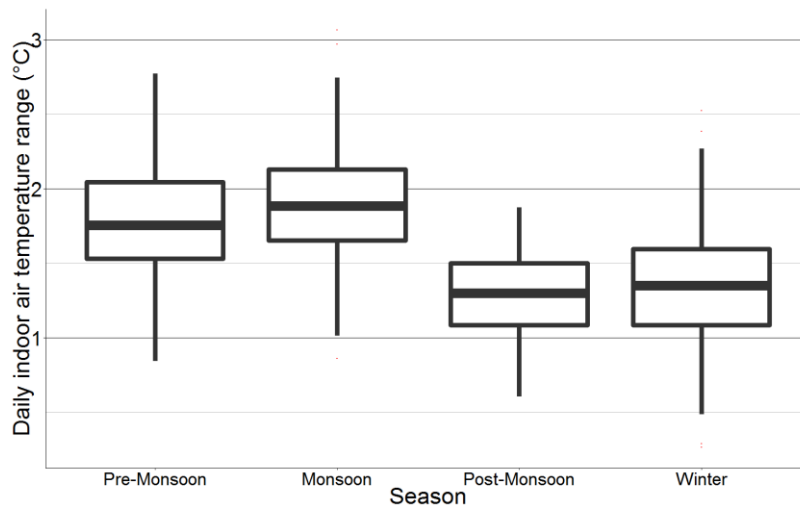


Figure 33. BH indoor air temperature range by season

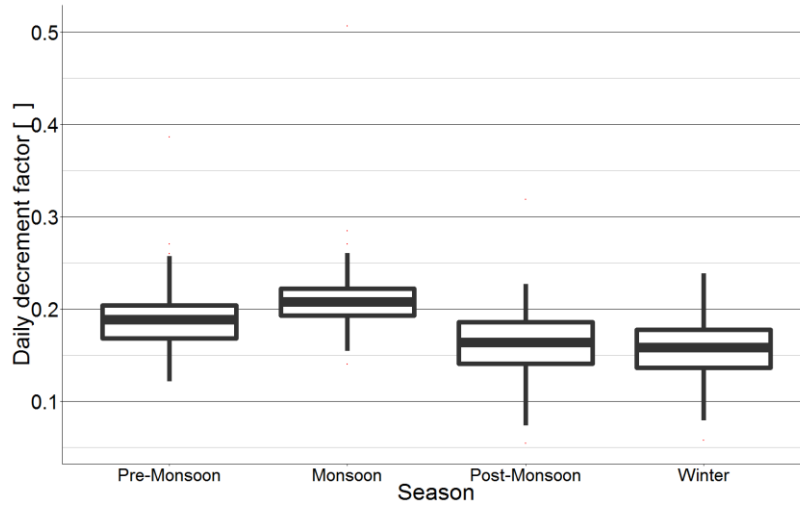


Figure 34. BH decrement factor by season

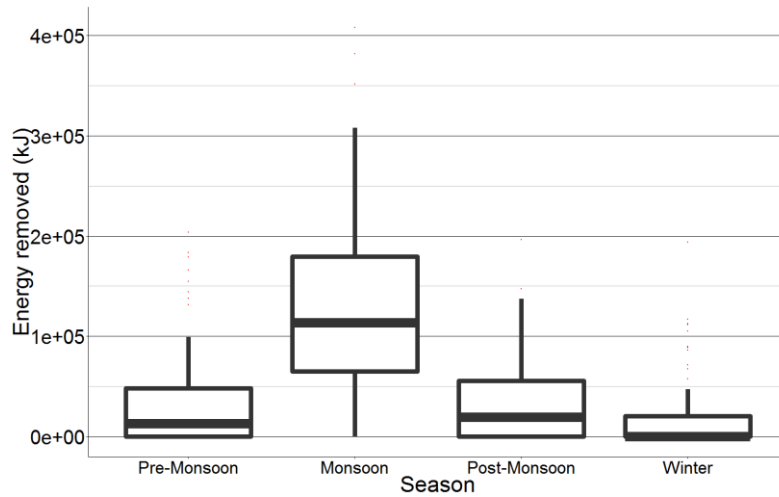


Figure 35. BH energy removed by season

## 5.2 Comparison to comfort standards

Using the methodology discussed in section 4.4.3, the data was analyzed with respect to the existing comfort standards. The following shows the results of that analysis.

### 5.2.1 La Escuelita Elementary School

In analyzing the 2-3 months of data from each classroom, it was discovered that the operative temperature never exceeded the upper ACS comfort limit. However, the operative temperature tended to hover around the lower ACS comfort limit for almost the entire data set, as seen in figure 36, and in some instances even go below the limit, indicating that the space is being overcooled. Each classroom has at least a few days in which the daily DDH (with respect to the lower comfort limit) exceeds 0 (approximately 19% of data). The average daily DDH across all 8 classrooms is 0.46 °C-h (0.82 °F-h). In some instances, the daily DDH reached as high as 13.3 °C-h (24 °F-h).

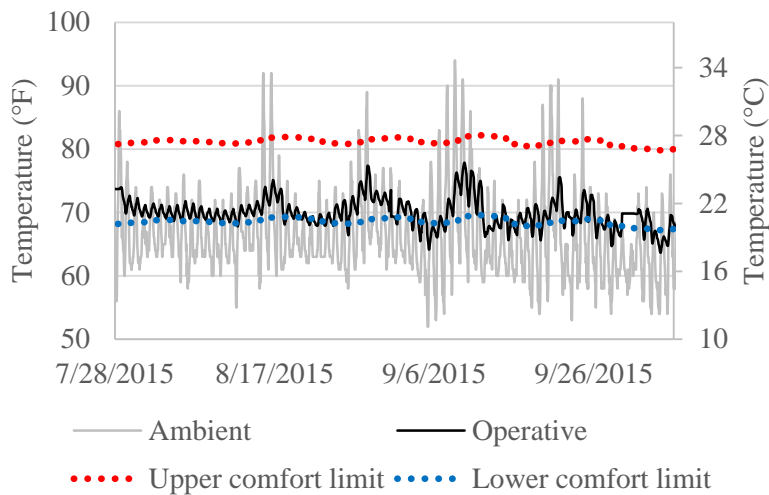


Figure 36. LEES room 233 operative temperature with ACS limits

### 5.2.2 Indio Building

In analyzing the two months of data from IND, it was discovered that the operative temperature never exceeded the upper ACS comfort limit or dropped below the lower ACS comfort limit, as shown in figure 37, and therefore the daily DDH never exceeds 0. That being said, the operative temperature seemed to stay very close to the lower ACS comfort limit, indicating that there is little need for additional cooling.

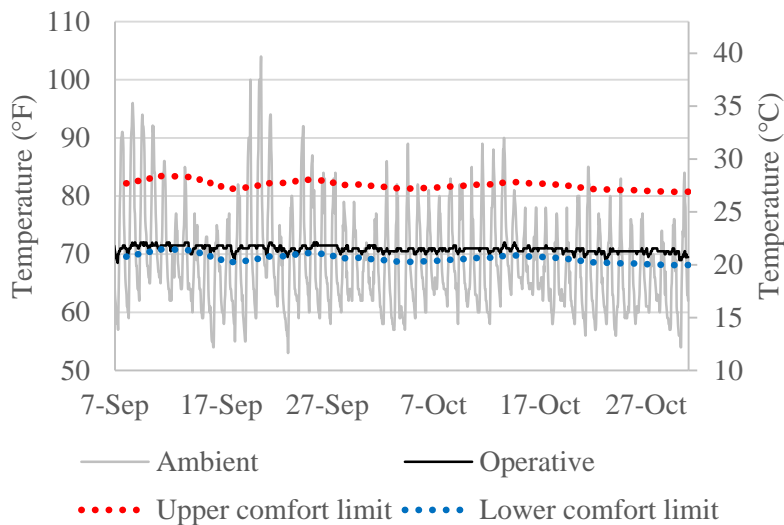


Figure 37. IND operative temperature with ACS limits

### 5.2.3 Blessing House

In analyzing the full year of data from BH with respect to IMAC, it was discovered that the operative temperature never exceeded the upper IMAC comfort limit or fell below the lower

IMAC limit, as shown in figure 38. However, when comparing the data to the ACS comfort limits, it was found that the operative temperature exceeded the upper ACS comfort limit for approximately 12% of the year, during the Pre-Monsoon and Monsoon seasons,. There is a wide spread of operative temperature across the year, but the operative temperature remains closer to the upper comfort limits for a higher proportion of the year. The average daily DDH across the year is approximately 0.38 °C-h. The daily DDH (with respect to the upper ACS comfort limit) exceeds 0 for 42% of the Pre-Monsoon season and 37% of the Monsoon season. During the Pre-Monsoon season, the average daily DDH is 0.58 °C-h and goes as high as 6 °C-h. During the Monsoon season, the average daily DDH is 0.68 °C-h and goes as high as 9.5 °C-h. The total DDH for the entire year is 131.7 °C-h.

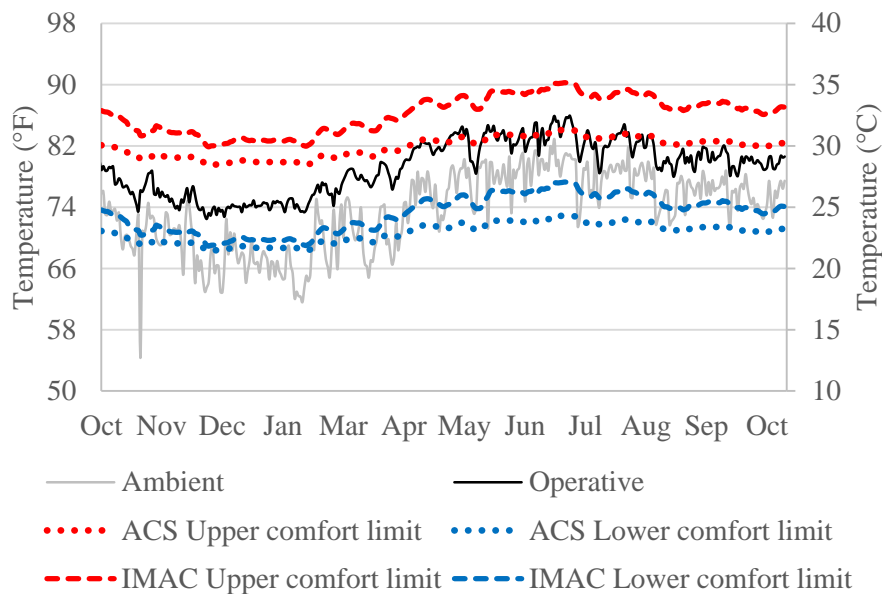


Figure 38. BH operative temperature with ACS & IMAC comfort limits

## 5.3 Comparison of night ventilation vs non-night ventilation using real data

Using the methodology discussed in section 4.4.1, the building conditions were assessed during periods with and without night ventilation. This, in turn, showed the magnitude of effect that the night ventilation strategy had on the building conditions. The following shows the results of that analysis.

### 5.3.1 La Escuelita Elementary School

For this analysis, parameters were compared for the following ventilation modes: regular airflow – only minimum allowable ventilation during occupied hours (RA), regular airflow with night ventilation (NV), regular airflow with daytime cooling – ramped up airflow rates during the day (DC), regular airflow with night ventilation and daytime cooling (NV+DC). Additionally, these results were calculated from the combination of data from all 8 classrooms, with a total sample size of 842 d (591 d with RA, 111 d with NV, 32 d with DC, and 108 d with NV+DC). Time lag

was not compared due to the fact that indoor temperature typically peaked before outdoor temperature, probably because of the mild climate. The  $p$ -values and differences in averages between each ventilation mode can be seen in table 3.

Metric	NV-RA		DC-RA		NV+DC-RA		DC-NV		NV+DC-NV		NV+DC-DC	
	Diff	P	Diff	P	Diff	P	Diff	P	Diff	P	Diff	P
$T_{i,max}$	0.33	0.53	2.61	1.1E-08	0.79	0.0085	2.28	1.1E-05	0.45	0.49	-1.83	7.9E-04
$Damp_{max}$	-0.43	0.89	3.52	0.0042	0.40	0.91	3.95	0.0036	0.82	0.71	-3.13	0.035
$T_{i,range}$	2.55	0	2.17	1.1E-08	2.94	0.00	-0.38	0.77	0.38	0.48	0.76	0.22
$f$	0.18	0	0.089	0.0029	0.20	0.00	-0.088	0.010	0.023	0.61	0.11	5.2E-04
$Q$	33980	0	5415	0.89	64031	0.00	-28566	0.0042	30051	9.7E-07	58616	5.4E-11
PEE	-1.95	7.9E-04	-3.60	6.8E-04	-2.46	1.2E-05	-1.65	0.34	-0.51	0.84	1.15	0.65
DDH	1.80	0	-0.16	0.99	1.98	0.00	-1.96	0.0011	0.17	0.96	2.13	3.7E-04

Table 3. Differences and  $p$ -values for LEES real data performance metrics

Statistically significant differences were seen between daytime cooling and the other three ventilation modes with regard to daily maximum temperature and daily maximum damping. On average, daily maximum indoor air temperature was about 1.1 °C (2 °F) higher for daytime cooling (figure 39) and daily maximum damping was about 1.7 °C (3 °F) – 2.2 °C (4 °F) higher for daytime cooling (figure 40). This would suggest that although the indoor peak temperature is higher with daytime cooling, the strategy was more effective at reducing the peak indoor temperature compared to peak outdoor temperature than night ventilation or regular airflow. This is probably the case because daytime cooling is taking place on days with the highest outdoor air temperature.

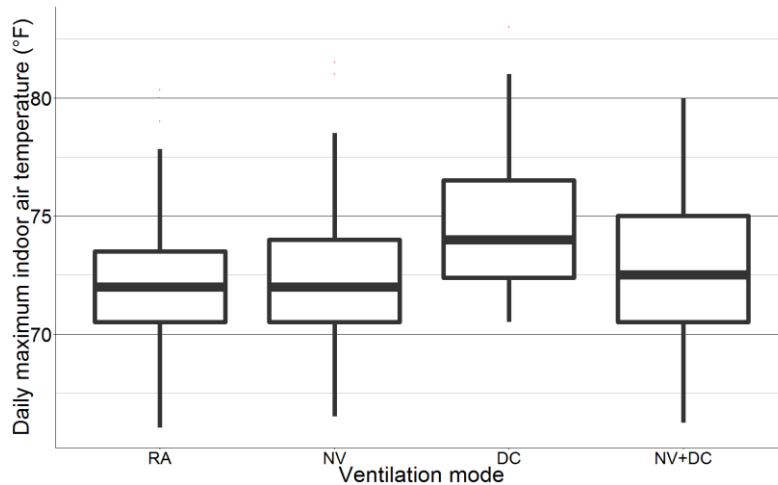


Figure 39. LEES daily maximum indoor air temperature with & without night ventilation

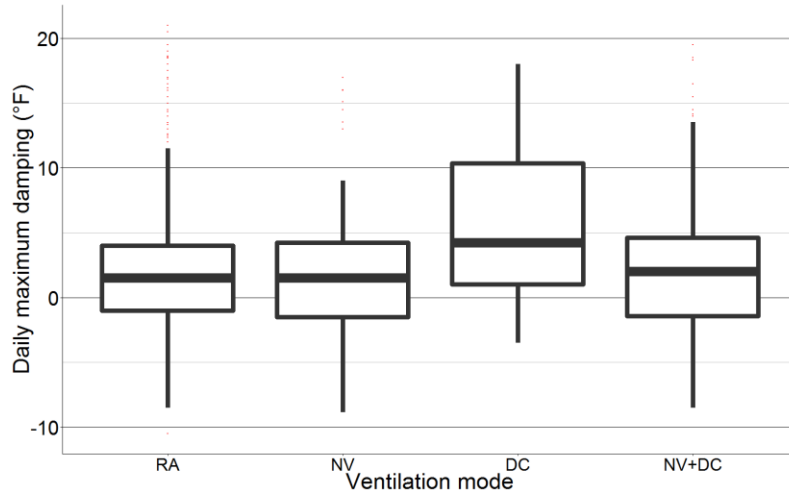


Figure 40. LEES daily maximum damping with & without night ventilation

Statistically significant differences were seen between regular airflow and the other three ventilation modes with regard to indoor air temperature range and decrement factor. On average, indoor air temperature range was 1.1 °C (2 °F) – 1.7 °C (3 °F) lower for regular airflow (figure 41) and decrement factor was 0.1-0.2 lower for regular airflow (figure 42). Although we would expect the daytime cooling and night ventilation strategies to decrease the indoor temperature range and decrement factor, the strategies are probably decreasing the minimum temperature as opposed to the maximum temperature, thus increasing the temperature range.

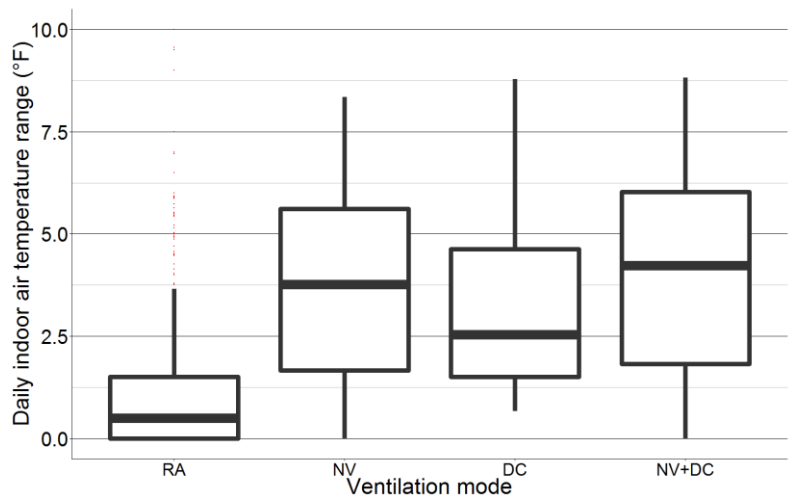


Figure 41. LEES daily indoor air temperature range with & without night ventilation



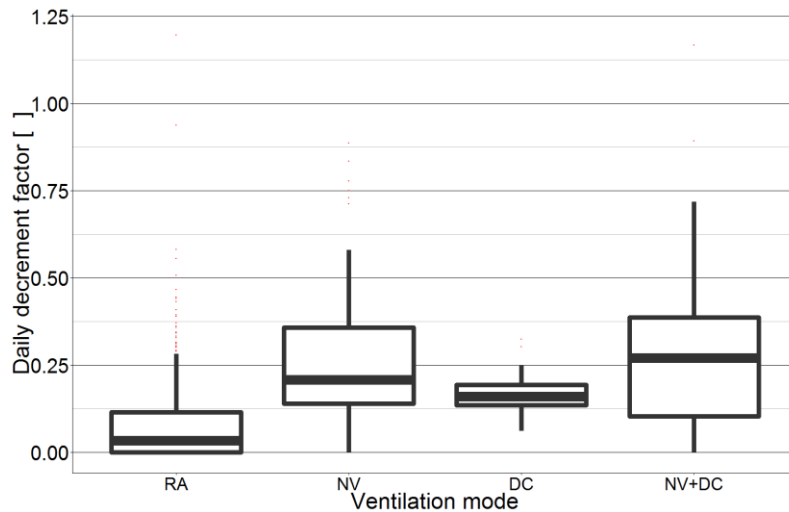


Figure 42. LEES daily decrement factor with & without night ventilation

Statistically significant differences were seen between each ventilation mode with regard to daily energy removed (figure 43). As expected, combined night ventilation and daytime cooling flushed the most heat from the building, followed by night ventilation, then daytime cooling, then regular airflow. This suggests that night ventilation is more effective than daytime cooling and regular airflow at removing heat. However, no statistically significant differences were seen between night ventilation and daytime cooling with regards to potential energy efficiency. Rather, potential energy efficiency was seen to be higher for regular airflow than the other three ventilation modes by about 2-4 (figure 44). This suggests that even without the increased airflow, heat is still being removed from the space.

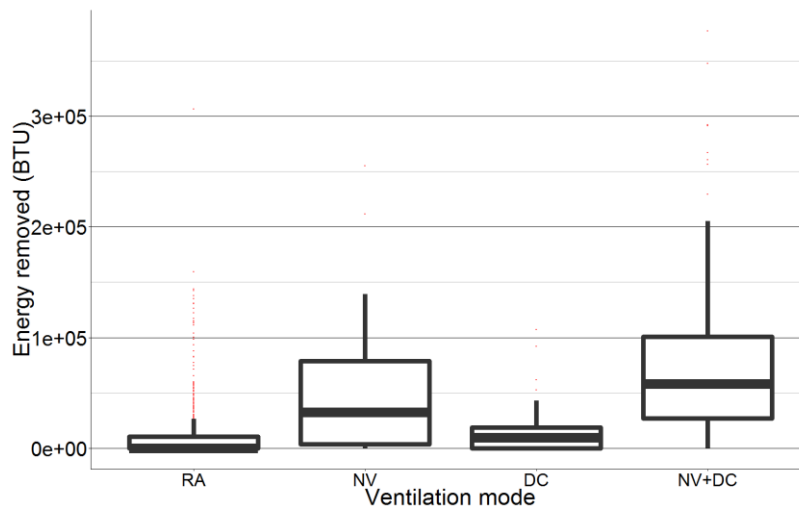


Figure 43. LEES daily energy removed with & without night ventilation

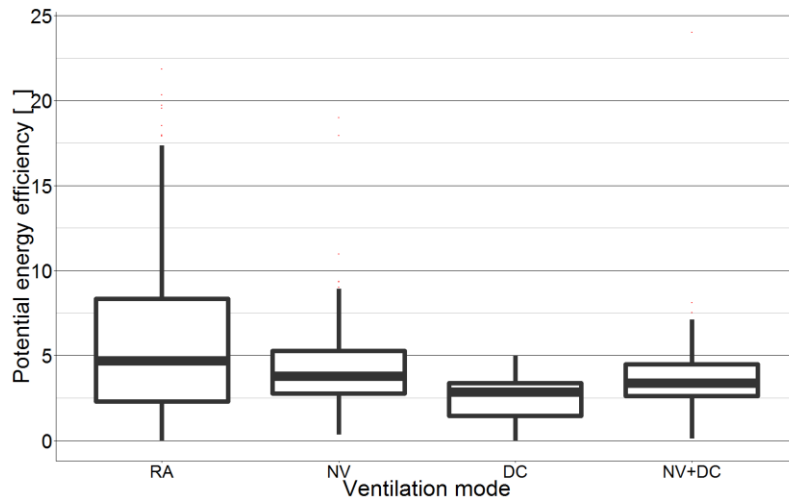


Figure 44. LEES daily potential energy efficiency with & without night ventilation

Finally, statistically significant differences were seen between each of the ventilation modes with regard to daily discomfort degree hours below the minimum comfort limit. Discomfort degree hours was highest for night ventilation and combined night ventilation and daytime cooling, and lowest for regular airflow and daytime cooling (figure 45). This suggests that night ventilation is overcooling the building. In other climates or buildings, it would be important to also look at discomfort degree hours that might occur above the maximum comfort limit.

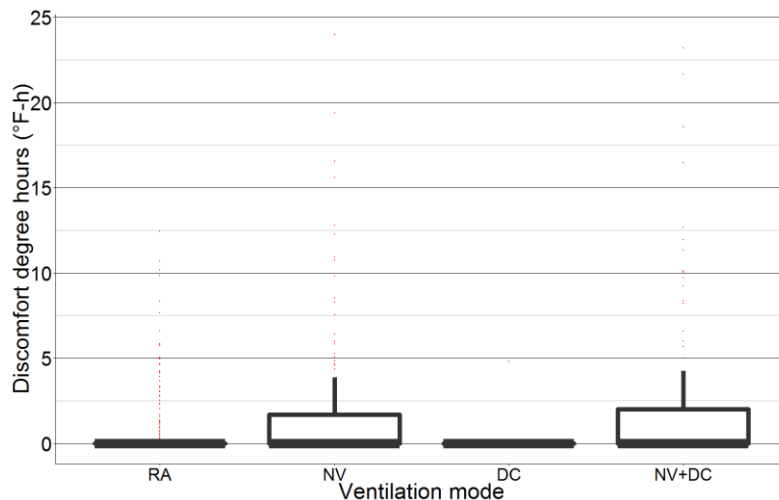


Figure 45. LEES daily discomfort degree hours below minimum ACS limit with & without night ventilation

### 5.3.2 Indio Building

For this analysis, parameters were compared with night ventilation (NV) and without night ventilation (no NV), with a total sample size of 60 d (18 d with NV and 42 without NV). The  $p$ -values and differences in averages between each ventilation mode can be seen in table 4.

Metric	NV – No NV	
	Diff	P
<b>T<sub>i,max</sub></b>	0.11	0.57
<b>Damp<sub>max</sub></b>	-0.024	0.99
<b>T<sub>i,range</sub></b>	1.71	1.1E-08
<b>F</b>	0.067	1.1E-04
<b>TL</b>	5.52	5.1E-05
<b>DDH</b>	0.12	0.070

Table 4. Differences and *p*-values for IND real data performance metrics

No statistically significant differences were seen between days with and without night ventilation with regard to daily maximum indoor air temperature and daily maximum damping. This suggests that the night ventilation strategy is not reducing the indoor temperatures. However, statistically significant differences were seen between days with and without night ventilation with regard to daily time lag. On average, daily time lag was about 5 hours larger for days with night ventilation than days without night ventilation (figure 46). This suggests that even though the night ventilation strategy is not impacting the magnitude of the indoor temperature, it is still delaying the peak temperature inside.

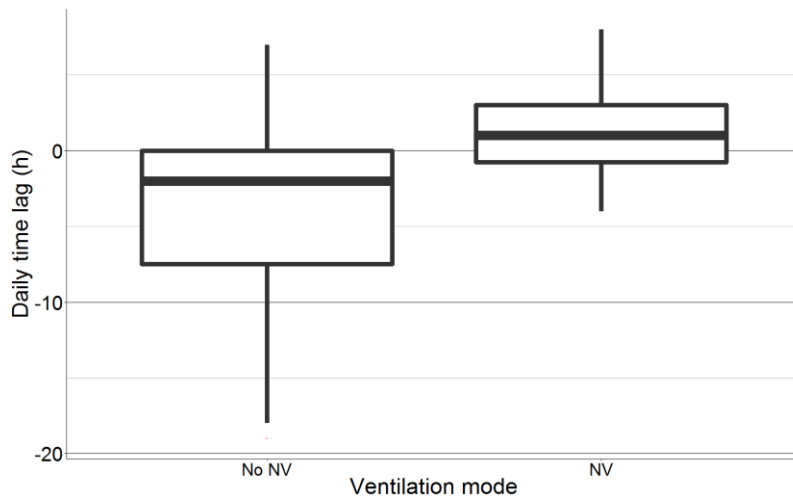


Figure 46. IND daily time lag with & without night ventilation

Statistically significant differences were also seen between days with and without night ventilation with regard to daily indoor air temperature range, daily decrement factor, and daily discomfort degree hours below the minimum comfort limit. However, the effect size of these differences, which is the magnitude of the effect that difference has on the performance metric, is not significant. This suggests that the night ventilation did not have an impact on the temperature range or time outside of comfort.

### 5.3.3 Blessing House

For this analysis, parameters were compared with night ventilation (NV) and without night ventilation (no NV), with a total sample size of 357 d (300 d with NV and 57 d without NV). The *p*-values and differences in averages between each ventilation mode can be seen in table 5.

Metric	NV – No NV	
	Diff	P
<b>T<sub>i,max</sub></b>	3.04	2.2E-16
<b>Damp<sub>max</sub></b>	0.77	1.6E-04
<b>T<sub>i,range</sub></b>	0.35	1.3E-06
<b>F</b>	0.044	1.4E-11
<b>TL</b>	0.34	0.36
<b>Q</b>	67187	2.2E-16
<b>DDH</b>	0.42	2.3E-08

Table 5. Differences and p-values for BH real data performance metrics

Statistically significant differences were seen between days with and without night ventilation with regard to daily maximum indoor air temperature. However, on average, maximum indoor temperature was about 3 °C higher for days with night ventilation than days without night ventilation (figure 47). This is probably the case because there are so many more days of the data set that use night ventilation than do not use night ventilation, therefore skewing the sample size for each case.

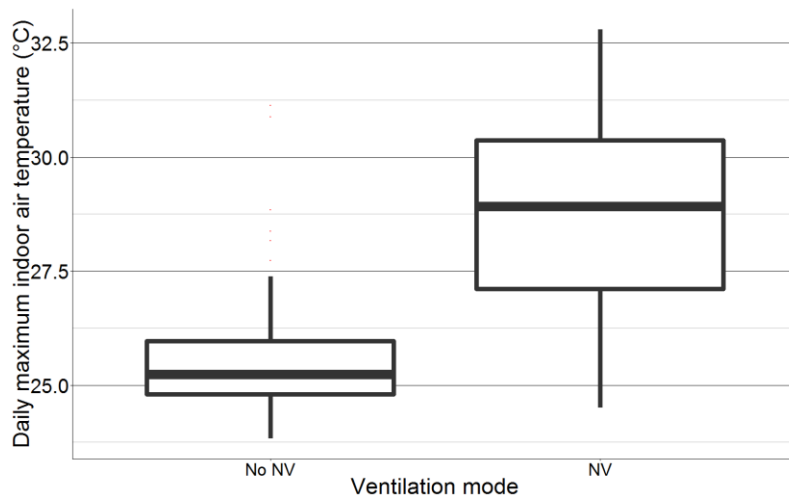


Figure 47. BH daily maximum indoor air temperature with & without night ventilation

Statistically significant differences were seen between days with and without night ventilation with regard to daily maximum damping. That being said, on average, maximum damping was less than 1 °C higher for days with night ventilation than days without night ventilation, which is probably not enough to feel a difference. No statistically significant differences were seen between days with and without night ventilation with regard to daily time lag. This suggests that the night ventilation strategy is not delaying the peak temperatures.

Statistically significant differences were also seen between days with and without night ventilation with regard to daily maximum damping, daily indoor air temperature range, daily decrement factor, and daily discomfort degree hours above the maximum comfort limit. However, the effect size of these differences is not significant. This suggests that the night ventilation did not have an impact on the temperature range, damping or time outside of comfort.

The one parameter to have a statistically significant difference between cases and a large effect size is daily energy removed. However, this result is expected due to the fact no heat is removed by ventilation in the case with closed windows.

## 5.4 Model selection

Using the methodology laid out in section 4.3, temperature prediction models were generated for each of the case studies in order to simulate the buildings with and without night ventilation. The following presents the final models selected for each of the buildings and the respective model errors.

### 5.4.1 La Escuelita Elementary School

The model selected for LEES uses controllable inputs of supply temperature and ventilation rate, uncontrollable inputs of outdoor air temperature and solar radiation, and outputs of indoor air temperature, mass wall temperature, and mass floor temperature. Because the model was nonlinear in the inputs and states, it was linearized. The selected model was not normalized. The dynamical equations for this model can be seen in equation 40. The upper bounds and lower bounds for parameter identification, along with the identified parameter values can be seen in table 6. The model error parameters for the training data and validation data are found in tables 7 and 8, respectively. Figure 48 visualizes the real and simulated training data.

$$\begin{aligned}
1. \quad C_I \dot{T}_I(t) &= -\left(\frac{1}{R_{OI}} + \frac{1}{R_{WI}} + \frac{1}{R_{FI}} + \rho c V^{eq}\right) * T_I(t) + \left(\frac{1}{R_{WI}}\right) * T_W(t) + \left(\frac{1}{R_{FI}}\right) * T_F(t) + \\
&\quad \left(\frac{1}{R_{OI}}\right) * T_O(t) + \left(\rho c [T_v^{eq} - T_I^{eq}]\right) * V(t) + (\rho c V^{eq}) * T_V(t) + P_{r,I} r(t) \\
2. \quad C_W \dot{T}_W(t) &= \frac{1}{R_{WI}} * T_I(t) - \left(\frac{1}{R_{OW}} + \frac{1}{R_{WI}}\right) * T_W(t) + \frac{1}{R_{OW}} * T_O(t) + P_{r,W} r(t) \\
3. \quad C_F \dot{T}_F(t) &= \frac{1}{R_{FI}} * T_I(t) - \frac{1}{R_{FI}} * T_F(t) + P_{r,F} r(t)
\end{aligned}$$

*Equation 40. Final dynamical equations for LEES model*

Parameter	LB	UB	Room 110	Room 120	Room 233	Room 234	Room 235	Room 240	Room 241	Room 242
$-1/C_i*(1/R_{OI} + 1/R_{WI} + 1/R_{FI} + \rho C V^{eq})$	-30	0	-17.8	-22.2	-1.4	-20.9	-30.0	-19.3	-17.1	-19.4
$1/(C_i*R_{WI})$	0	30	2.1	6.3	0.29	3.3	0.47	7.9	2.5	4.8
$1/(C_i*R_{FI})$	0	30	16.2	4.8	0.92	14.9	22.7	9.0	11.8	10.6
$1/(C_i*R_{OI})$	0	30	2.3E-06	0.10	3.7E-14	1.8E-06	1.2	4.4E-07	0.32	4.7E-06
$1/C_i*\rho C*(T_v^{eq}-T_i^{eq})$	-30	0	-2.8E-14	-3.8E-14	-1.8E-08	-1.1E-03	-4.3E-03	-2.5E-03	-1.8E-06	-1.8E-09
$1/C_i*\rho C V^{eq}$	0	30	0.18	10.6	0.20	3.1	5.7	2.9	2.9	3.9
$P_{r,I}$	0	30	2.5E-10	3.8E-14	2.4E-14	2.6E-14	3.0E-14	0.0	3.3E-03	4.9E-08
$1/(C_w*R_{WI})$	0	30	20.9	29.7	24.6	19.8	0.12	1.5	14.2	14.1
$-1/C_w*(1/R_{OW} + 1/R_{WI})$	-30	0	-21.7	-30.0	-29.9	-24.3	-0.20	-2.0	-17.7	-17.5
$1/(C_w*R_{OW})$	0	30	0.73	1.2	5.8	4.7	0.090	0.39	3.5	3.7
$P_{r,W}$	0	30	4.4E-10	3.8E-14	2.4E-14	0.0	1.7E-03	2.3E-06	1.0E-06	9.0E-07
$1/(C_F*R_{FI})$	0	30	0.84	0.020	0.19	1.5E-01	0.22	0.11	0.21	0.14
$-1/(C_F*R_{FI})$	-30	0	-0.87	-0.020	-0.19	-1.5E-01	-0.22	-0.12	-0.21	-0.14
$P_{r,F}$	0	30	1.5E-11	3.8E-14	2.1E-04	1.1E-04	3.0E-14	4.2E-04	1.7E-04	1.7E-04

Table 6. Final parameters for LEES model

Classroom	110	120	233	234	235	240	241	242
RMSE	1.54	0.71	0.75	0.91	0.91	1.24	1.22	1.4
CVRMSE	0.012	0.010	0.013	0.013	0.011	0.020	0.017	0.017
MAPE (%)	1.5%	0.65%	0.80%	0.89%	0.91%	1.2%	1.3%	1.5%
SDAPE (%)	1.6%	0.72%	0.70%	0.90%	0.88%	1.3%	1.1%	1.3%
MAE (°F)	1.06	0.47	0.56	0.64	0.65	0.83	0.90	1.07
SDAE (°F)	1.12	0.53	0.49	0.65	0.64	0.93	0.82	0.94

Table 7. LEES model error for training data

Classroom	110	120	233	234	235	240	241	242
RMSE	1.5	1.6	1.4	1.4	1.6	2.2	2.2	3.0
CVRMSE	0.012	0.023	0.023	0.021	0.020	0.041	0.030	0.030
MAPE (%)	1.5%	1.6%	1.6%	1.6%	1.9%	2.1%	2.3%	3.1%
SDAPE (%)	1.6%	1.7%	1.3%	1.2%	1.3%	2.0%	1.8%	2.4%
MAE (°F)	1.06	1.1	1.1	1.1	1.3	1.5	1.7	2.3
SDAE (°F)	1.12	1.2	0.89	0.87	0.93	1.6	1.4	1.9

Table 8. LEES model error for validation data

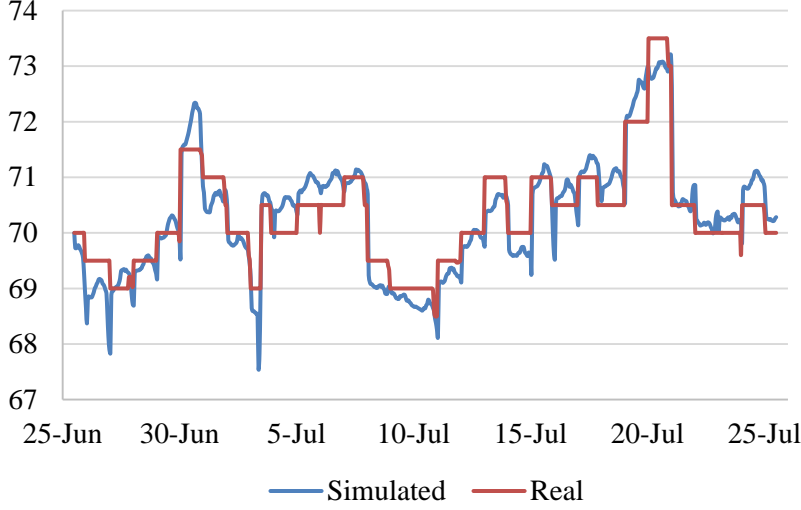


Figure 48. Real and simulated data in LEES room 110

## 5.4.2 Indio Building

The model selected for IND uses a controllable input of window state, uncontrollable inputs of outdoor air temperature and internal load, and outputs of indoor air temperature, mass wall temperature, and mass floor temperature. The selected model was not normalized. The dynamical equations for this model can be seen in equation 41. The upper bounds and lower bounds for parameter identification, along with the identified parameter values can be seen in table 9. The model error parameters for the training data and validation data are found in table 10.

1.  $C_I \dot{T}_I(t) = \frac{1}{R_{OI}} [T_O(t) - T_I(t)] + \frac{1}{R_{WI}} [T_W(t) - T_I(t)] + \frac{1}{R_{FI}} [T_F(t) - T_I(t)] + P_V s(t) + P_{int,I} int(t)$
2.  $C_W \dot{T}_W(t) = \frac{1}{R_{OW}} [T_O(t) - T_W(t)] + \frac{1}{R_{WI}} [T_I(t) - T_W(t)] + P_{int,W} int(t)$
3.  $C_F \dot{T}_F(t) = \frac{1}{R_{FI}} [T_I(t) - T_F(t)] + P_{int,F} int(t)$

Equation 41. Final dynamical equations for IND model

Parameter	LB	UB	Value
$1/(C_I \cdot R_{OI})$	0	10	0.52
$1/(C_I \cdot R_{WI})$	0	1	1.0
$1/(C_I \cdot R_{FI})$	0	10	9.3
$P_V$	-30	0	-9.1E-04
$P_{int,I}$	0	10	3.0E-04
$1/(C_W \cdot R_{OW})$	0	0.1	0.0019
$1/(C_W \cdot R_{WI})$	0	0.01	6.3E-05
$P_{int,W}$	0	10	7.5E-12
$1/(C_F \cdot R_{FI})$	0	0.1	0.0057
$P_{int,F}$	0	10	3.3E-09

Table 9. Final parameters for IND model

	RMSE	CVRMSE	MAPE (%)	SDAPE (%)	MAE (°F)	SDAE (°F)
Training data	1.7	0.026	1.9%	1.4%	1.4	1.0
Validation data	1.6	0.024	1.6%	1.4%	1.2	1.0

Table 10. IND model error

### 5.4.3 Blessing House

The model selected for BH uses a controllable input of window state, uncontrollable inputs of outdoor air temperature and solar radiation, and outputs of indoor air temperature, mass wall temperature, and mass floor temperature. The selected model was not normalized. The dynamical equations for this model can be seen in equation 42. The upper bounds and lower bounds for parameter identification, along with the identified parameter values can be seen in table 11. The model error parameters for the training data and validation data are found in table 12.

$$\begin{aligned}
1. \quad C_I \dot{T}_I(t) &= \frac{1}{R_{OI}} [T_O(t) - T_I(t)] + \frac{1}{R_{WI}} [T_W(t) - T_I(t)] + \frac{1}{R_{FI}} [T_F(t) - T_I(t)] + P_V s(t) + P_{r,I} r(t) \\
2. \quad C_W \dot{T}_W(t) &= \frac{1}{R_{OW}} [T_O(t) - T_W(t)] + \frac{1}{R_{WI}} [T_I(t) - T_W(t)] + P_{r,W} r(t) \\
3. \quad C_F \dot{T}_F(t) &= \frac{1}{R_{FI}} [T_I(t) - T_F(t)] + P_{r,F} r(t)
\end{aligned}$$

Equation 42. Final dynamical equations for BH model



Parameter	LB	UB	Value
$1/(C_i \cdot R_{oi})$	0	30	1.5
$1/(C_i \cdot R_{wi})$	0	30	29.8
$1/(C_i \cdot R_{fi})$	0	30	3.1
$P_v$	-100	0	-22.9
$P_{r,z}$	0	10	1.1E-11
$1/(C_w \cdot R_{ow})$	0	0.1	0.024
$1/(C_w \cdot R_{wi})$	0	0.1	0.044
$P_{r,w}$	0	10	1.1E-06
$1/(C_f \cdot R_{fi})$	0	0.1	0.10
$P_{r,f}$	0	10	1.9E-06

Table 11. Final parameters for BH model

	RMSE	CVRMSE	MAPE (%)	SDAPE (%)	MAE (°C)	SDAE (°C)
Training data	0.79	0.029	2.3%	1.8%	0.62	0.49
Validation data	1.1	0.036	2.1%	1.5%	0.60	0.43

Table 12. BH model error

## 5.5 Comparison of night ventilation vs non-night ventilation using model data

Although measured indoor conditions were compared in section 5.3, this could not truly capture how the buildings would have performed with and without night ventilation across the entire data set. For this reason, the models explained in section 5.4 along with the methodology discussed in section 4.4.2, were used to assess the building conditions if the night ventilation had been implemented for the entire duration of data collection, and if no night ventilation was implemented for the entire data set. The following shows the results of that analysis.

### 5.5.1 La Escuelita Elementary School

For this analysis, parameters were compared for the model runs with the following ventilation inputs: measured airflow inputs (Real), regular airflow – minimum allowable ventilation during occupied hours (RA), night ventilation according to the control sequence (NV), daytime cooling – ramped up airflow rates during the day according to the control sequence (DC), night ventilation and daytime cooling according to the control sequence (NV+DC). Additionally, these results were calculated from the combination of data from all 8 classrooms. No statistically significant differences were seen between model simulations with different ventilation inputs with regard to daily maximum indoor temperature, daily maximum damping, daily temperature range, decrement factor, or daily discomfort degree hours. This indicates that, in the context of these buildings and climates, the airflow rate has a very small influence on the indoor conditions, which are much more closely correlated to the supply temperature. The only metrics to have a statistically significant difference between models with different ventilation inputs were energy removed and potential energy efficiency. All of the models with simulated ventilation inputs

removed less energy than the model with real inputs. The simulated ventilation models are probably removing less heat because the real building is going into night ventilation or daytime cooling more often than the design control sequence calls for, which calls into question how the control sequence has changed since operation began. In addition, the simulated ventilation models have lower potential energy efficiency than the model with real ventilation inputs, probably because the real building is often not ventilating the building during occupied hours, whereas the models with simulated ventilation inputs are forced to have a code required minimum airflow rate during occupied hours, causing them to consume more fan energy.

## 5.5.2 Indio Building

For this analysis, performance metrics were compared using model simulations with night ventilation (NV) and without night ventilation (no NV). No statistically significant differences were seen between model simulations with and without night ventilation. This indicates that the strategy was not impacting the internal conditions.

## 5.5.3 Blessing House

For this analysis, performance metrics were compared using model simulations with night ventilation (NV) and without night ventilation (no NV), with a total sample size of 712 d (356 with NV and 356 without NV). The *p*-values and differences in averages between each ventilation mode can be seen in table 13.

Metrics	NV – No NV					
	All seasons		Pre-Monsoon		Monsoon	
	<i>Diff</i>	<i>P</i>	<i>Diff</i>	<i>P</i>	<i>Diff</i>	<i>P</i>
<b>T<sub>i,max</sub></b>	-0.57	3.9E-03	-0.71	8.9E-03	-0.65	4.9E-04
<b>Damp<sub>max</sub></b>	0.57	3.5E-09	0.71	8.1E-04	0.66	6.8E-05
<b>T<sub>i,range</sub></b>	0.63	2.2E-16	0.69	0.0	0.73	0.0
<b>f</b>	0.072	2.2E-16	0.075	0.0	0.083	0.0
<b>TL</b>	0.22	0.14	0.10	0.69	0.28	0.15
<b>Qday</b>	71503	2.2E-16	41805	0.0	152743	0.0
<b>DDH<sub>p,day</sub></b>	-2.1	1.3E-07	-3.6	2.5E-05	-3.5	4.7E-05

Table 13. Differences and *p*-values for BH simulated data performance metrics

Statistically significant differences were seen between model runs with and without night ventilation with regard to daily maximum indoor air temperature and daily maximum damping. However, on average, maximum indoor temperature and maximum damping were less than 1 °C different for model runs with and without night ventilation, even during the warmest seasons of the year (figure 49 and 50). The daily maximum indoor air temperature seen in this comparison confirms that the values seen in section 5.3.3 were higher for night ventilation periods only because of uneven sample sizes, and not because the strategy was unsuccessful. The maximum damping seen in this comparison matches the values seen in section 5.3.3. Although the indoor temperature peaks are only lower by 0.6-0.7 °C and the maximum damping is only higher by 0.6-0.7 °C for the night ventilation simulation, this is still improving the indoor conditions and can help improve comfort when paired with other strategies. No statistically significant

differences were seen between model runs with and without night ventilation with regard to time lag, which matches the results from section 5.3.3.

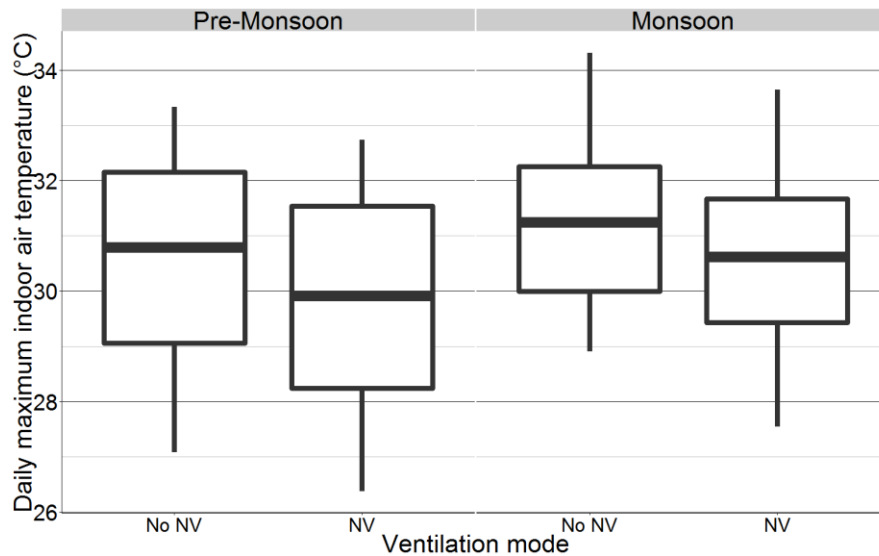


Figure 49. BH simulation daily maximum indoor air temperature with & without night ventilation

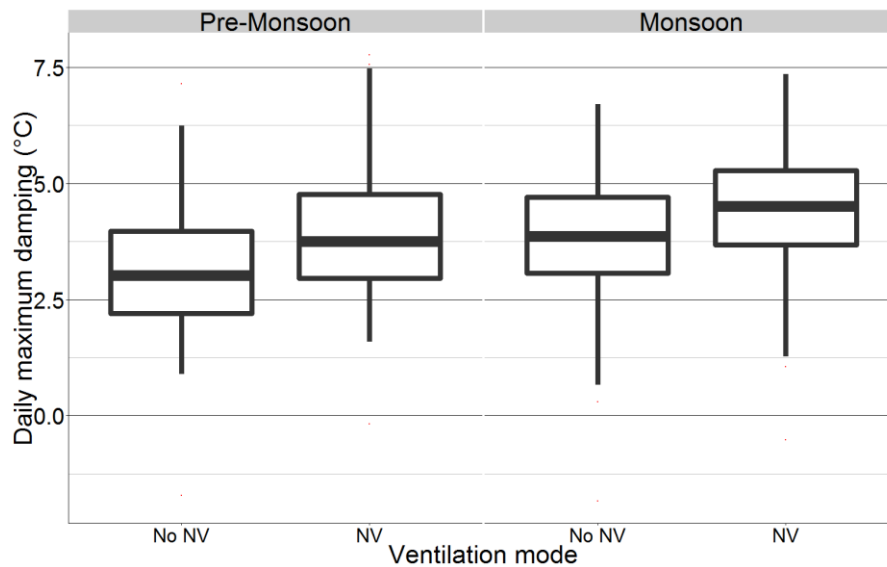


Figure 50. BH simulation daily maximum damping with & without night ventilation

Statistically significant differences were also seen between model runs with and without night ventilation with regard to daily indoor air temperature range and daily decrement factor. However, the effect size of these differences is not significant. This matches the results from section 5.3.3. As expected, statistically significant differences were seen between model runs with and without night ventilation with regard to daily energy removed, especially in the Monsoon season. Once again, this is expected because the model run with windows closed cannot remove any heat by ventilation.

Finally, statistically significant differences were seen between model runs with and without night ventilation with regard to daily discomfort degree hours above the maximum comfort limit. On average, the model run with night ventilation had 3.5 °C-h less than the model run without night ventilation in the Pre-Monsoon and Monsoon seasons (figure 51). This difference could have a large impact on the comfort of the occupants inside the space.

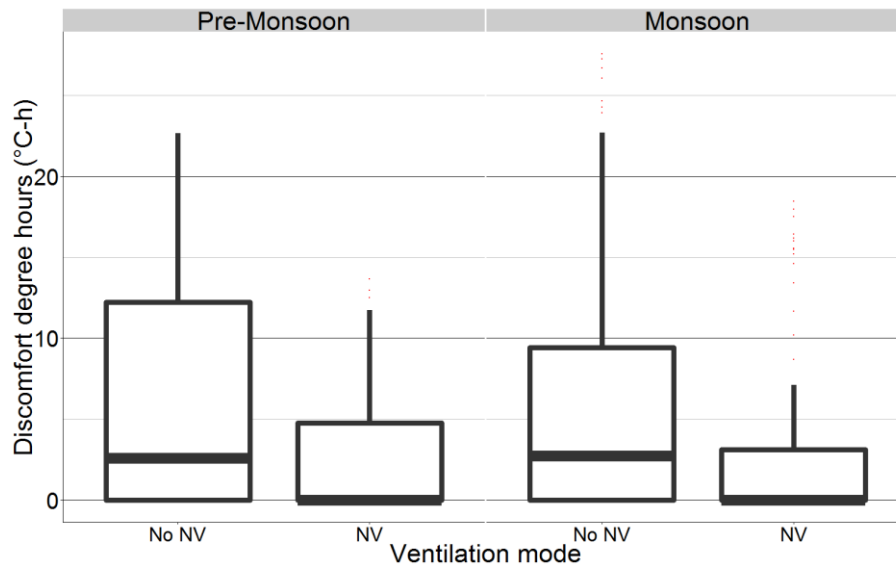


Figure 51. BH simulation daily discomfort degree hours above maximum ACS limit with & without night ventilation

## 5.6 Optimization

Using the methodology described in section 4.5 and the selected models from section 5.5, the controls for each building were optimized to minimize energy and maximize comfort. The results of this analysis are seen below.

### 5.6.1 La Escuelita Elementary School

The optimization with comfort limits as a constraint unfortunately could not be solved, due to the fact that even without night ventilation, the operative temperature still falls below the lower comfort limit. After running the optimization which minimizes the time outside of the comfort limits on all classrooms, the system operated with only minimum allowable airflow. This suggests that these classrooms need no night ventilation to satisfy comfort requirements.

### 5.6.2 Indio Building

Because the identified parameter associated with window state was so small, there was minimal impact on the indoor conditions from night ventilation. Therefore, the controls for night ventilation in IND were not optimized.

### 5.6.3 Blessing House

The window state of the BH was optimized for one week in April in which the operative temperature went above the upper ACS comfort limit (see figure 52). Surprisingly, the optimization resulted in keeping the window open for the entire duration of the week. A comparison was done between the models with optimized window state, real window state, and closed windows, with a total sample size of 21 d (7 d with real inputs, 7 d with closed windows, and 7 d with optimized inputs). The  $p$ -values and differences in averages between the models can be seen in table 14.

Metric	Optimized – Real		Optimized – No NV	
	<i>Diff</i>	<i>P</i>	<i>Diff</i>	<i>P</i>
$T_{i,max}$	-0.8359	0.004384	-1.62082	3.14E-06
$Damp_{max}$	0.835902	0.308303	1.620821	0.022933
$T_{i,range}$	-0.93602	1.14E-06	-0.07166	0.825989
$f$	-0.10849	3.64E-13	-0.00749	0.380734
TL	-1	0.403914	0	1
Q	-3526.46	0.982782	33154.08	0.243722
DDH	-12.6385	0.035525	-33.4952	2.98E-06

Table 14. Differences and  $p$ -values for BH optimized data performance metrics

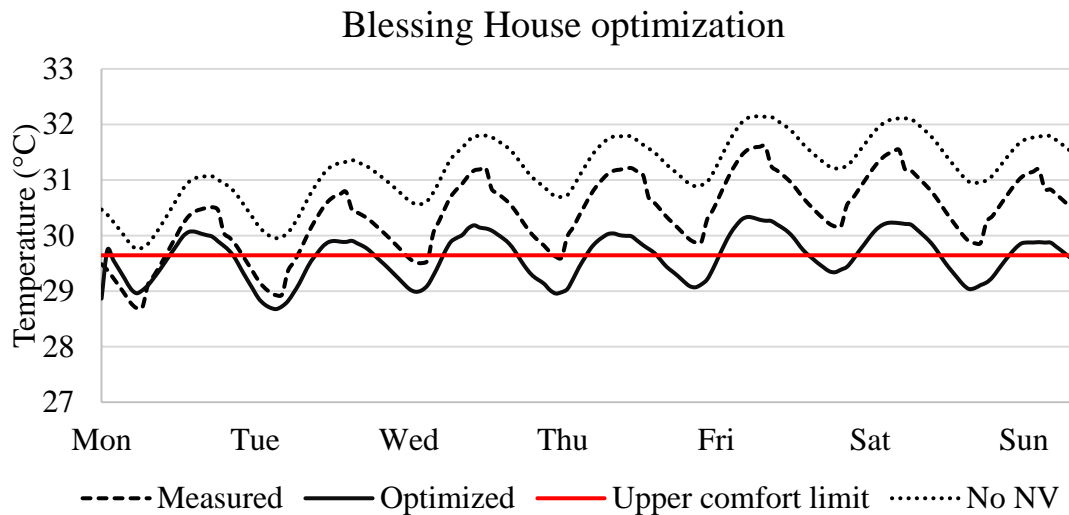


Figure 52. BH measured, optimized, & no NV operative temperature

A statistically significant difference was seen between the optimized model and the other two models with regard to daily maximum indoor air temperature, daily maximum damping, and daily discomfort degree hours above the ACS limit. Although the optimized model only performed 0.8 °C better than the model with real window state, it nearly doubled the reduction in temperature compared to the case with no night ventilation (figures 53 & 54). With regard to the discomfort degree hours, the optimized model outperformed both other models to an extremely large degree, which was the objective of the optimization (figure 55). The discomfort degree hours were reduced by approximately 56% after incorporating night ventilation, and a further 34% by optimizing the controls. This suggests that if the building were to use model predictive control in determining when to open the windows, they could significantly improve the comfort inside the space.

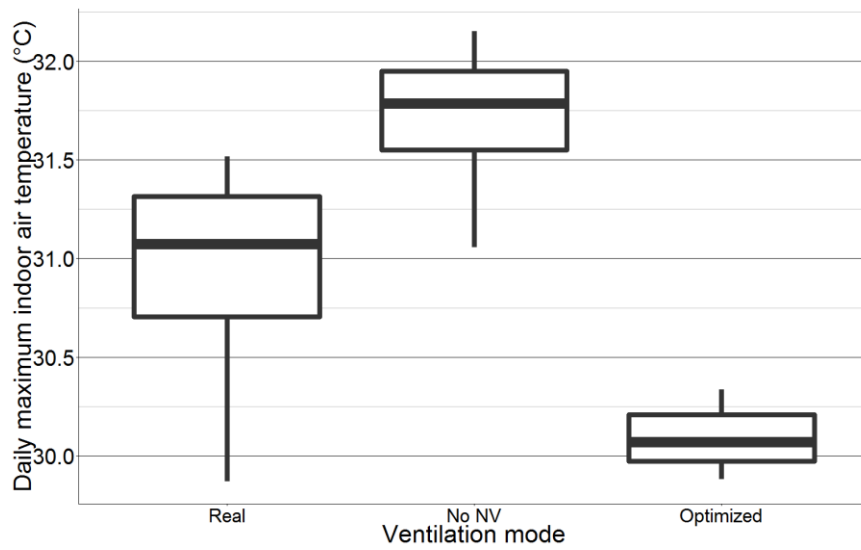


Figure 53. BH daily maximum indoor air temperature, measured, optimized, & no NV

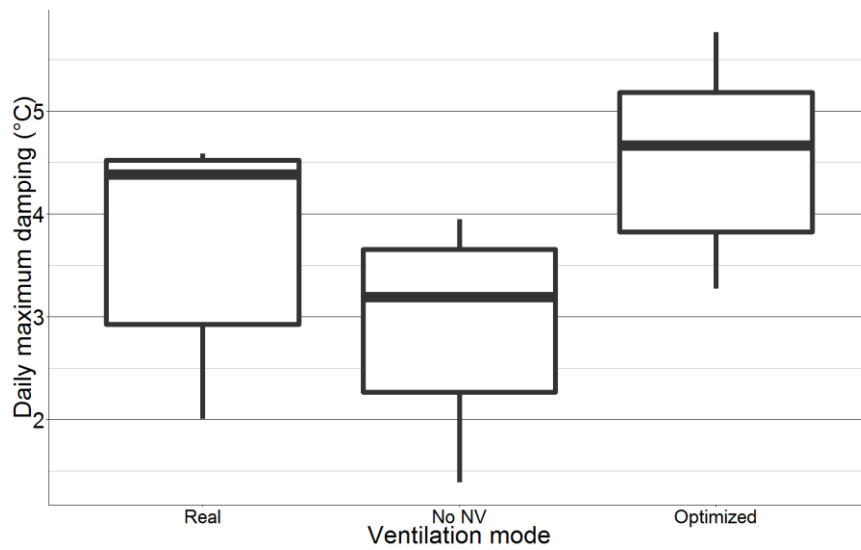


Figure 54. BH daily maximum damping, measured, optimized, & no NV

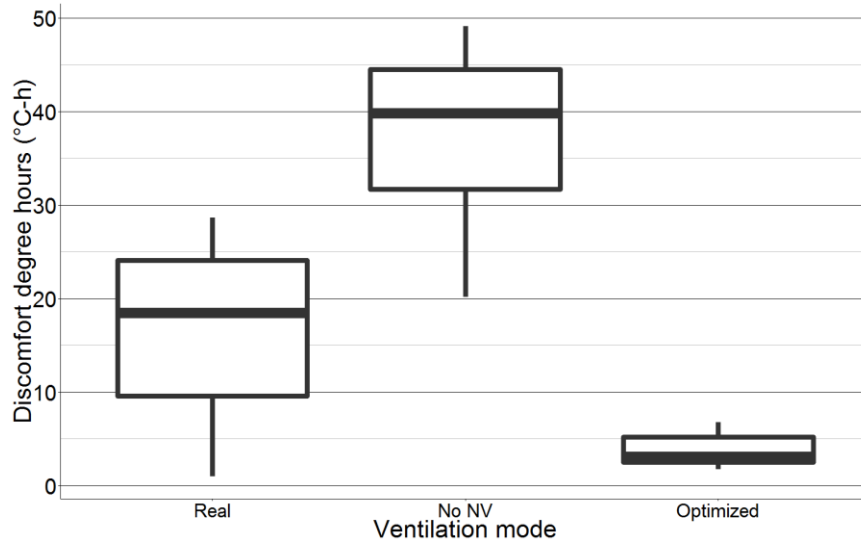


Figure 55. BH daily discomfort degree hours above maximum ACS limit, measured, optimized, & no NV

One notable result of the optimization was that the daily indoor air temperature range daily decrement factor were much lower than the model with real inputs, but approximately equal to the model with closed windows (figures 56 & 57). It is expected that these metrics would decrease after optimization, but is surprising that they would have no significant difference from the case with closed windows.

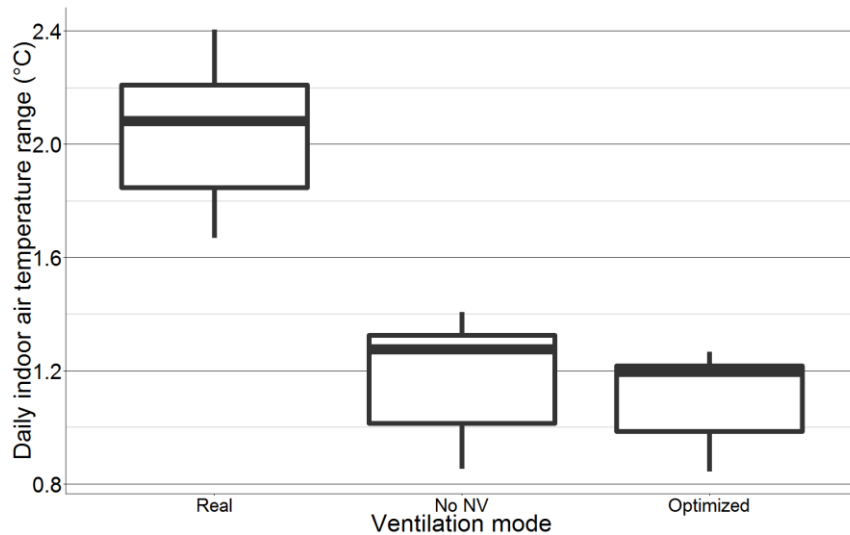


Figure 56. BH daily indoor air temperature range, measured, optimized, & no NV

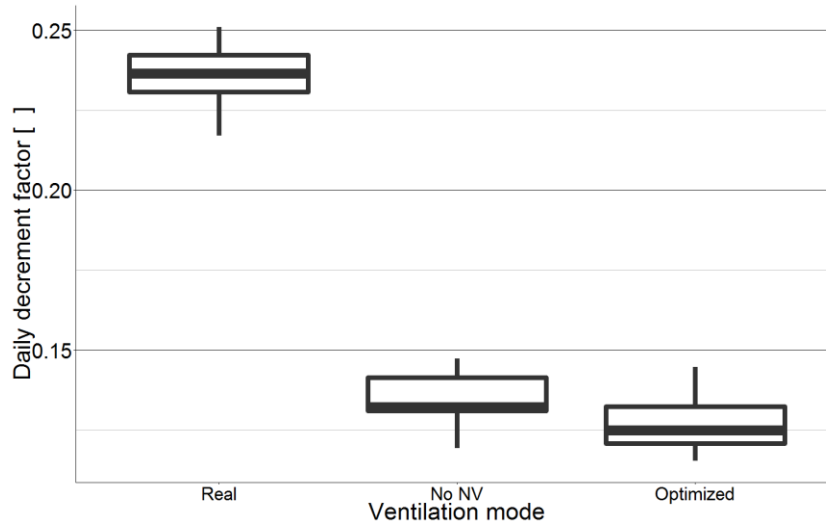


Figure 57. BH daily decrement factor, measured, optimized, & no NV

## 5.7 Designer & operator interviews

### 5.7.1 La Escuelita Elementary School

Interviews were conducted on several dates during the Spring of 2016 with the LEES controls design team, led by Glenn Friedman (principal at Taylor Engineering), and Brent Eubanks (currently an engineer at Integral Group, but who was with Taylor Engineering during the design of LEES). These interviews resulted in learning the details of how the LEES controls setpoints, as described in section 4.1.1, were selected, and helped understand the patterns in the measured data.

The mass temperature setpoint was chosen in order to avoid morning warmup and the outdoor air temperature setpoint was chosen based on professional experience and intuition. A difference of 5.6 °C (10 °F) between the outdoor air temperature and mass temperature was believed to be the minimum difference necessary to achieve a driving force in night flushing. Mass temperature was chosen as a setpoint as opposed to indoor air temperature because it was assumed that the indoor air temperature would not reflect the necessity of night ventilation due to the fact that the air temperature was so dependent on occupancy loads. That being said, the designers acknowledge that the mass temperature is not an ideal setpoint because it is the embedded temperature as opposed to surface temperature. It was chosen to use embedded sensors rather than surface sensors to make sure they did not get damaged or tampered with. Mechanical night ventilation was chosen over natural night ventilation to ensure better security of the building and control over the indoor conditions.

During design, the thermal comfort studies suggested that the strategy would maintain a mass temperature below 23.9 °C (75 °F). The measured performance of the night ventilation strategy shown here matched the designers' expectations on an individual day-by-day basis in that the mass temperature consistently decreased during night ventilation periods. The fact that the second-story rooms were seeing a larger impact from the night ventilation than the first-story rooms also matched the designers' expectations because the second-story rooms are not ground



coupled. That being said, the designers were surprised by the degree to which the strategy was overcooling the space. It was hypothesized that the strategy might be overcooling because the ventilation system is not always following the designed control sequence due to the fact that six individual coders independently programmed the controls and therefore, they might not have been programmed correctly.

### 5.7.2 Indio Building

Interviews were conducted in the Spring of 2016 with the IND building operator, Eric Sande, owner of Intertie Automation, and the IND controls design team, led by Neil Bulger and Shannon Allison, associate principals at Integral Group, along with Alex Krickx and Stefan Gracik, engineers at Integral Group. These interviews resulted in learning the details of how the IND controls setpoints, as described in section 4.1.2, were selected, and again helped understand the patterns in the measured data. The setpoints were chosen as the lowest temperatures needed to keep the next day's indoor temperature below the upper comfort limit in the design team's model. The setpoints were then optimized by the building operator through trial and error. Indoor air temperature was chosen as a setpoint over mass temperature because there were no mass temperature sensors in the original design. However, mass temperature sensors were embedded 1 inch into the mass during construction.

A few potential problems with the strategy were brought up over the course of these interviews. The windows set to open for night ventilation are inset and the actuators allow the windows to open up only 8 inches for security purposes, which limits the free open area below the values tested during modeling. Another potential problem is that two closed pavilions containing conference rooms were added to the center of the open office, which were not part of the original design.

The performance of the strategy did not meet the designers' expectations in that they were surprised to see the lack of fluctuation in mass temperature. It was hypothesized that the impact of night ventilation on indoor conditions was minimal compared to the impact of heavy mass. In addition, the design team suggested that because the building is only 2/3 occupied and therefore has low internal loads, the night ventilation strategy might not be necessary. The question arose of what the critical value for internal loads is at which the night ventilation strategy starts to have noticeable impact on indoor conditions.

The building operator indicated that although the building was achieving its temperature setpoints, the occupants were not satisfied with the internal conditions of the office. In addition to the passive cooling strategy, the building has two rooftop air conditioning units that are almost never used. The mechanical cooling setpoint is 25 °C (77 °F), which the occupants felt was too high, according to feedback given to the building operator. It is unusual that this complaint was raised because according to the data, the temperature never went above 23.9 °C (75 °F).

### 5.7.3 Blessing House

An interview with the designer/owner/resident of BH was conducted the summer of 2015. This resident indicated that he is very satisfied with the conditions inside his home and has no

problem manually operating the windows each day. He also explained that although he does not follow a specific control sequence in the BH night ventilation strategy, he tends to open the windows as soon as he notices that the outdoor air temperature has fallen below the indoor air temperature.

# Discussion

## 6.1 Performance of night ventilation in LEES

The results of this study clearly suggest that the night ventilation strategy, in combination with the physical construction of the building, is successfully keeping LEES below the maximum comfort limit during hot periods. According to the measured data, the night ventilation strategy is more successful than any other ventilation mode at lowering the indoor temperatures, implying there is no need for mechanical cooling in this buildings. This being said, results of the predictive modeling showed that the mode parameter identified for airflow rate is very small compared to the parameters identified for all other inputs, which suggests that the airflow rate has very little impact on the indoor conditions. One possible explanation for this disagreement between model results and measured results is the fact that the airflow rate might have more impact on the indoor conditions during warmer days and the data used for parameter identification might not have included the hottest days of the data set. Regardless of the impact of airflow rate, the indoor temperature is still significantly damped compared to the outdoor air temperature.

Although the space is being successfully cooled, the strategy is sometimes overcooling the classrooms, which suggests that there may be a mismatch between the design intent and patterns of operation in the building. Because night ventilation is reducing the indoor temperature too low during nighttime periods, the system is actually using more energy in the morning to warm up the space before occupancy. There are a few explanations for this overcooling, one being that the mass temperature setpoint for entering night ventilation is simply too low. Another potential explanation is that the specification of a difference of 5.6 °C (10 °F) between mass temperature and outdoor air temperature for entering night ventilation is too high, especially because this occurs so often in the mild climate. It is very telling that when the controls were optimized to minimize time outside of the comfort bounds, the system never entered night ventilation mode. It is recommended that the building operator increase the mass temperature setpoint or reduce the necessary difference between outdoor and mass temperature for entering night ventilation.

The system might also be overcooling the space because the current controls do not match the designed control sequence. It was seen that the system was entering and leaving night ventilation at different times than the control sequence calls for. In addition, the first floor classrooms had periods of no ventilation during occupied hours, even though the designed control sequence calls for minimum allowable airflow. For this study, the operating control sequence was not obtained and the building operator was not available for interview. A thorough investigation is still needed to fully understand why the current system is behaving this way.

LEES is the only one of the three case studies that required the consumption of energy to run the night ventilation strategy. Although the system consistently had very high energy efficiency, the fact that the space was being overcooled suggests that there is still energy being wasted by running the fans too often. As seen in the measured data, some of the classrooms achieved similar indoor temperatures with and without night ventilation, probably due to the very mild climate. If the increased airflow is not necessary to achieve the same condition, this fan energy

could be saved and a similar amount of heat could still be dissipated through the mass. In addition, the energy consumed to reheat the space in the morning was not taken into consideration in this calculation, as the energy efficiency was only examined for heat removed.

While the study suggests that the strategy is overcooling, the applicability of the adaptive comfort model to LEES is still in question. Firstly, the standard requires that the space be occupant-controlled and naturally conditioned. The LEES ventilation system is not controlled by its occupants and its use of fan assisted ventilation is still technically a form of mechanical conditioning. In addition, the use of the adaptive comfort model is not thoroughly tested in schools with young children. One study that took place in a naturally ventilated elementary school found that the observed lower 80% acceptability limit was 1.7 °C below the value listed in the ASHRAE standard (Hwang et al. 2009). Another study that took place in a naturally ventilated elementary school saw that the predicted thermal acceptability according to the adaptive comfort model did not match the surveyed acceptability values (Kwok and Chun 2003).

## 6.2 Performance of night ventilation in IND

The results of this study suggest that the night ventilation strategy, in combination with the physical construction of the building, has no discernable impact on the internal conditions of the space. The model results and measured results were in agreement on this matter. The most likely reason for the low impact of night ventilation is the extremely high level of thermal mass and low internal loads. This goes against the designers' expectation that higher mass allows for better night ventilation performance. The very thick concrete walls and floor are likely able to take care of the load all on their own. In addition, the mass is so heavy that it is probably reducing the range of indoor temperature, which in turn prevents a noticeable effect from night ventilation. It is entirely possible that the night ventilation strategy would have a larger impact if the mass was less heavy or if the internal loads were higher.

In the modeling work, although the identified model parameter for internal loads was extremely small, the parameter identification was done using data measured at 2/3 occupancy. If the building were fully occupied, this parameter likely would have been more significant. There is probably a critical value of internal load that varies from building to building, at which the night ventilation strategy is worth using. Additionally, the strategy never ran for more than a few days at a time. Because the mass is so heavy, the strategy might have shown a higher effect on internal conditions if run for many days in a row. Finally, it is possible that the strategy was not showing a serious effect due to the fact that the free open area for night ventilation calculated during design is larger than the actual free open area, thus overestimating the modeled airflow.

Like LEES, the applicability of the adaptive comfort model to IND is also in question because of the lack of occupant control. Although the operative temperature remained within the adaptive comfort model 80% acceptability limits for the entire data set, the occupants were not satisfied with the indoor temperatures according to the building operator. This is especially surprising because the operative temperature hovered right above the lower comfort limit. This might suggest that the adaptive comfort model is not accurately predicting satisfaction for this type of space, emphasizing the importance for occupants having personal control of the windows during the daytime.

## 6.3 Performance of night ventilation in BH

The results of this study suggest that the night ventilation strategy, in combination with the physical construction of the building, successfully lowers the indoor temperature, removes heat from the space, and reduces discomfort degree hours, especially during the hottest seasons of the year. This is very significant because the strategy implemented in BH is very simple and the night ventilation is not always believed to work successfully in hot and humid climates. This being said, the effect size of damping the indoor temperature due to night ventilation is fairly small. Although small differences in temperature can make a larger difference in climates with high humidity, the strategy probably cannot achieve enough on its own to take care of the entire load. Night ventilation, paired with other low energy strategies, such as ceiling fans, has the potential to maintain comfort in this climate. In analyzing comfort with measured data, the annual discomfort degree hours was approximately 131.7 °C-h. If the air speed were increased to 0.6 m/s through the use of ceiling fans, the annual discomfort degree hours drops to 2.6 °C-h, and 0 °C-h at air speeds above 0.6 m/s. This was calculated using the adjusted adaptive comfort model limits for increased air speeds.

The optimization of BH window opening controls resulted in further improved comfort and temperature reduction. This suggests that the use of model predictive control could show great benefit for BH. It was very surprising to see that the optimization kept the windows open for all daytime and nighttime hours of the week, indicating that daytime natural ventilation can also improve the indoor conditions. Although the outdoor air temperature is higher during the day, the increased airflow from natural ventilation could be helping flush heat out of the space. Alternatively, it is possible that the model is overestimating the impact of daytime ventilation due to the simplicity of the model. The impact of ventilation is captured just by the state of window. The identified model parameter for window state is negative, probably because the windows are typically only open when the outdoor air temperature is below the indoor air temperature, and therefore the model interprets open windows as removing heat. This may not be the case when outdoor air temperature is higher than indoor air temperature.

Finally, there is a question of which comfort model is more appropriate for BH. While the adaptive comfort model has already been accepted in the ASHRAE standard, the India model for adaptive comfort is specifically relevant for cases in India. The fact that India's model for adaptive comfort produces no discomfort degree hours suggests that people acclimated to the climate of India might have a higher temperature threshold and therefore the night ventilation strategy would suffice for keeping people comfortable in BH.

## 6.4 Comparison of case studies

Although each of the case studies is very different and no specific attribute can by itself account for the overall performance of night ventilation in each building, the performance metrics of each case study were compared, with a sample size of 1259 d (842 d in LEES, 60 d in IND, and 357 d in BH). The *p*-values and differences in averages between each case study can be seen in table 15.

Metric	IND - LEES		BH - LEES		BH - IND	
	Diff	P	Diff	P	Diff	P
$T_{i,max}$	1.2	0.0052	10.5	4.8E-14	9.3	4.8E-14
$Damp_{max}$	6.5	7.6E-14	5.4	4.8E-14	-1.1	0.27
$T_{i,range}$	0.27	0.56	0.99	9.5E-14	0.72	0.024
$f$	-0.024	0.40	0.053	3.9E-09	0.076	1.9E-04
TL	2.1	0.092	10.7	4.8E-14	8.6	8.8E-14
Q	N/A	N/A	31604	0.00	N/A	N/A
$Q_{norm}$	N/A	N/A	201	0.00	N/A	N/A

Table 15. Differences and p-values across case study measured data performance metrics

With regard to daily maximum indoor air temperature, BH had a much higher average than the other two buildings, but this can simply be attributed to the fact that BH is in a much hotter climate. On the other hand, there was only a 0.56 °C (1 °F) difference between LEES and IND average values, which suggests that different levels of mass and types of night ventilation were resulting in approximately the same daily temperature peaks. With regard to daily maximum damping, BH and IND had a much higher effect size than LEES (figure 58). The only obvious similarity between BH and IND is the use of natural night ventilation. It is possible that natural night ventilations lends itself to higher values of maximum damping due to the fact that the open windows allow the space to more closely follow nighttime temperatures, whereas air must travel through ducts for mechanical night ventilation, possibly gaining some heat along the way.

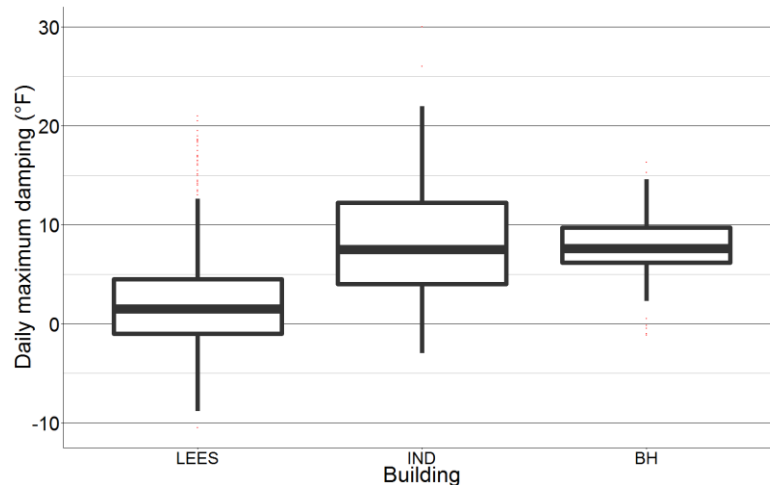


Figure 58. Daily maximum damping for each case study

With regard to daily time lag and temperature range, BH had a much higher effect size than LEES and IND (figures 59). These two metrics are probably closely related. Due to the fact that the mild climates in LEES and IND kept their temperature range so low, the indoor air temperature did not require much time to peak. In BH, the temperature range was wider and thus required more time to hit that peak.

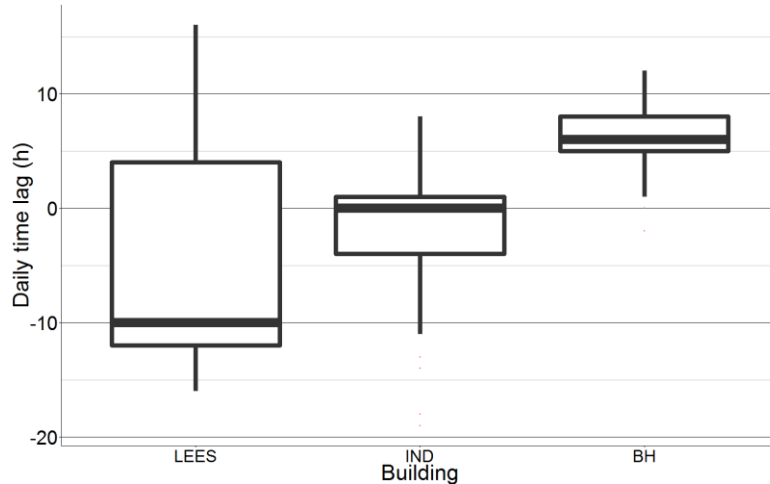


Figure 59. Daily time lag for each case study

On the whole, no generalizable conclusions can be made about the effect of each night ventilation parameter based on just three case studies, each in a different climate with very different controls. That being said, the fact that both LEES and IND had indoor conditions near the bottom or below the ACS lower comfort limit indicates that night ventilation could have the tendency to overcool when used in mild climates, and that cooling by night ventilation may not even be needed. In addition, the similar performance in IND and LEES shows that the type of ventilation system and control sequence are probably less significant to the performance of the strategy than the climate it is used in. Finally, the overall performance of night ventilation seemed to be better in BH than LEES or IND, possibly suggesting that the strategy might be better suited to hotter climate.

## 6.5 Limitations to study

There are numerous limitations to this study, most of which are attributed to the limited availability of data. Firstly, many parameters critical to the model calculations conducted in this study were not available and therefore had to be estimated. This includes the use of floor temperature as a substitute for wall temperature, embedded mass temperature as a substitute for surface temperature, and mean radiant temperature estimated using area-weighted mass temperature. In some cases, the depth of the embedded mass temperature sensor was not known. Other data that was unavailable had to be estimated using TMY3 climate data, including solar radiation and for BH, outdoor air velocity. Although these estimates were considered acceptable for the study, the results would have been more accurate had these values actually been measured. Additionally, the timespan in which data was available limited the potential outcomes of the study. While we were able to obtain an entire year of data for BH, the other two case studies only had a few months of data, which prevented the analysis of monthly and seasonal trends.

Another major limitation to the study is the simplicity of the model generated for comparison. Although this model achieved very small errors compared to measured data, the model still utilizes very simplified dynamical equations, and therefore cannot truly capture the dynamics of the heat in the space. For example, the model does not take infiltration into consideration.

The final limitation to this study is the lack of a control case. In terms of the performance within each individual buildings, there was no control period in which night ventilation was not used. We were simply given data during a real operation period of the building, which often skewed the amount of data we had under a specific ventilation mode. In terms of the performance across case studies, there was no control building to which the case studies could be compared. Each case study has extremely different physical and systems characteristics, and one had a very different climate than the other two, which makes it difficult to make any generalizable conclusions about the performance of night ventilation.



## 7. Conclusions

Data was obtained from three different buildings, each using night ventilation for cooling, with varying control strategies (both mechanical and natural), climates (mild and hot/humid), and levels of thermal mass (medium and heavy). The design and configuration of each building's control strategy was then investigated and laid out in detail.

Subsequently, the performance of night ventilation in each building with regard to indoor thermal conditions was assessed using measured data and comparing it to the adaptive comfort model. The results of this analysis indicate that the buildings using the night ventilation strategy in a mild climate are successfully keeping the indoor operative temperature below the upper 80% acceptability comfort limit. However, the case studies in the mild climate are also cooling more than necessary at times, sometimes bringing the operative temperature at or below the lower 80% comfort limit. The building in the hot and humid climate is going above the upper 80% comfort limit on the hottest days of the year, but still keeping the operative temperature within the 80% comfort bounds for 88% of the year.

Next, a hybrid model was developed for each case study, based on simplified resistance/capacitance equations, to predict the indoor conditions of the building with inputs including outdoor air temperature, solar radiation, internal loads, ventilation rate, and window state. These models were then fit to a training data set and validated against measured data, each providing temperature predictions with acceptable error.

Then, an assessment was done of the effect of the night ventilation strategy on indoor conditions and heat removal within each building, using both measured data and the temperature prediction model. For the building with medium mass using mechanical night ventilation in a mild climate, there were no significant differences in internal conditions between the different ventilation modes. Additionally, it was seen that the system had higher energy efficiency, the ratio of heat removed to fan energy consumed, when night ventilation was not running due to the influence of the mild climate and low internal loads. For the building with heavy mass, using automated natural night ventilation in a mild climate, the indoor temperature had very little fluctuation and there were no significant differences between cases with and without night ventilation, most likely due to the impact of the heavy mass and mild climate. For the building with medium mass using manual natural night ventilation in a hot and humid climate, the night ventilation strategy successfully lowered indoor temperatures and helped remove heat, but could not remove enough on its own to satisfy comfort requirements.

Finally, using the predictive model, the control strategy for each building was optimized to minimize the amount of time outside of the comfort bounds. In the two buildings in the mild climate, because the night ventilation strategy had such a small impact on the internal conditions of the buildings, the optimized controls did not demand any night ventilation. On the other hand, the building in the hot and humid climate saw an even further reduction in discomfort degree hours after the controls were optimized.

## 8. Future work

### 8.1 Daytime ventilation

After optimization of the BH mode, it was seen that the model achieved the least discomfort degree hours when the windows were open during both the day and night. This suggests that daytime ventilation through operable windows might help improve the comfort inside the building. This goes against the idea that the cool nighttime temperatures are what is driving the success of night ventilation. The performance of daytime natural ventilation for cooling should be further investigated.

### 8.2 Ceiling fans

In addition to the use of night ventilation for cooling, LEES and IND also make use of ceiling fans to increase air speeds during occupied hours and help improve the comfort inside the space. Further investigation is required to understand how the night ventilation strategy might be impacted by the use of ceiling fans, and vice versa.

### 8.3 Morning warmup

Because LEES tends to be overcooling the classrooms, morning warmup is often needed prior to occupancy, which consumes energy for heating. This, in turn, might be counterproductive to running night ventilation in the first place. More research should be done to understand exactly when and why the classrooms enter morning warmup, how much energy the morning warmup is consuming, and whether changes in the operation of night ventilation can reduce the need for morning warmup and hence save energy.

### 8.4 Impact of high humidity

In analyzing the performance of night ventilation in BH, air temperature and mean radiant temperature were the only parameters of thermal comfort that were taken into account. However, BH is located in an extremely humid climate, which can have a strong impact on thermal comfort. Additional analysis is necessary to determine exactly how high humidity affects the performance of night ventilation.

### 8.5 Applicability of ACS

As discussed in section 6, there is a question of whether or not the adaptive comfort model is applicable to these case studies, due to the the lack of occupant control over daytime ventilation in LEES and IND, and the program of LEES (schools instead of office buildings). The adaptive comfort model should specifically be tested in other buildings with these conditions by implementing occupant comfort surveys and comparing the results to the predicted ACS values.

## 8.6 Critical internal loads

As per the discussion with the Integral Group design team, it was hypothesized that there exists a critical value of internal loads at which the cooling effect of the night ventilation strategy will begin to become perceptible. This hypothesis should be tested, probably using an energy simulation.

## 8.6 Implement new control strategy

Although controls were optimized within the model, the optimized controls have not been configured at the actual buildings. If model predictive control were to be implemented at each of these buildings, or if the temperature setpoints were to simply be adjusted based on the analysis conducted in this study, another round of data collection and analysis could take place in order to compare the performance of night ventilation before and after a controls intervention.

## 9. References

- Artmann, N., H. Manz, and P. Heiselberg. 2007. "Climatic Potential for Passive Cooling of Buildings by Night-Time Ventilation in Europe." *Applied Energy* 84 (2): 187–201. doi:10.1016/j.apenergy.2006.05.004.
- . 2008. "Parameter Study on Performance of Building Cooling by Night-Time Ventilation." *Renewable Energy* 33 (12): 2589–98. doi:10.1016/j.renene.2008.02.025.
- Blondeau, Patrice, Maurice Spérandio, and Francis Allard. 1997. "Night Ventilation for Building Cooling in Summer." *Solar Energy* 61 (5): 327–35.
- Da Graça, G. Carrilho, Q. Chen, L. R. Glicksman, and L. K. Norford. 2002. "Simulation of Wind-Driven Ventilative Cooling Systems for an Apartment Building in Beijing and Shanghai." *Energy and Buildings* 34 (1): 1–11.
- Davis, Lucas W., and Paul J. Gertler. 2015. "Contribution of Air Conditioning Adoption to Future Energy Use under Global Warming." *Proceedings of the National Academy of Sciences* 112 (19): 5962–67. doi:10.1073/pnas.1423558112.
- de Dear, Richard J., and Gail Schiller Brager. 1998. "Developing an Adaptive Model of Thermal Comfort and preference/Discussion." *ASHRAE Transactions* 104: 145.
- Eubanks, Brent. 2014. "Climate-Adapted Design." <http://search.proquest.com/openview/0ebe3c4b23b272c0b4feab2a97b585b1/1?pq-origsite=gscholar>.
- Fanger, Poul O., and others. 1970. "Thermal Comfort. Analysis and Applications in Environmental Engineering." *Thermal Comfort. Analysis and Applications in Environmental Engineering*. <http://www.cabdirect.org/abstracts/19722700268.html>.
- Finn, Donal P., Darragh Connolly, and Paul Kenny. 2007. "Sensitivity Analysis of a Maritime Located Night Ventilated Library Building." *Solar Energy* 81 (6): 697–710. doi:10.1016/j.solener.2006.10.008.
- Gagge, A. Pharo, A. P. Fobelets, and LoG Berglund. 1986. "A Standard Predictive Index of Human Response to the Thermal Environment." *ASHRAE Trans.:(United States)* 92 (CONF-8606125-). <http://www.osti.gov/scitech/biblio/6494216>.
- Gagliano, A., F. Patania, F. Nocera, and C. Signorello. 2014. "Assessment of the Dynamic Thermal Performance of Massive Buildings." *Energy and Buildings* 72 (April): 361–70. doi:10.1016/j.enbuild.2013.12.060.
- García, Carlos E., David M. Prett, and Manfred Morari. 1989. "Model Predictive Control: Theory and practice—A Survey." *Automatica* 25 (3): 335–48. doi:10.1016/0005-1098(89)90002-2.
- Geros, V., M. Santamouris, A. Tsangrasoulis, and G. Guarracino. 1999. "Experimental Evaluation of Night Ventilation Phenomena." *Energy and Buildings* 29 (2): 141–54.
- Givoni, Baruch. 1992a. "Comfort, Climate Analysis and Building Design Guidelines." *Energy and Buildings* 18 (1): 11–23.
- . 1992b. "Comfort, Climate Analysis and Building Design Guidelines." *Energy and Buildings* 18 (1): 11–23.
- . 1998. "Effectiveness of Mass and Night Ventilation in Lowering the Indoor Daytime Temperatures. Part I: 1993 Experimental Periods." *Energy and Buildings* 28 (1): 25–32.
- Hwang, Ruey-Lung, Tzu-Ping Lin, Chen-Peng Chen, and Nai-Jung Kuo. 2009. "Investigating the Adaptive Model of Thermal Comfort for Naturally Ventilated School Buildings in Taiwan." *International Journal of Biometeorology* 53 (2): 189–200. doi:10.1007/s00484-008-0203-2.

- Kolokotroni, M., and Aj Aronis. 1999a. "Cooling-Energy Reduction in Air-Conditioned Offices by Using Night Ventilation." *Applied Energy* 63 (4): 241–53.
- . 1999b. "Cooling-Energy Reduction in Air-Conditioned Offices by Using Night Ventilation." *Applied Energy* 63 (4): 241–53.
- Kolokotroni, M., B. C. Webb, and S. D. Hayes. 1998. "Summer Cooling with Night Ventilation for Office Buildings in Moderate Climates." *Energy and Buildings* 27 (3): 231–37.
- Kubota, Tetsu, Doris Toe Hooi Chyee, and Supian Ahmad. 2009. "The Effects of Night Ventilation Technique on Indoor Thermal Environment for Residential Buildings in Hot-Humid Climate of Malaysia." *Energy and Buildings* 41 (8): 829–39. doi:10.1016/j.enbuild.2009.03.008.
- Kwok, Alison G, and Chungyoon Chun. 2003. "Thermal Comfort in Japanese Schools." *Solar Energy* 74 (3): 245–52. doi:10.1016/S0038-092X(03)00147-6.
- Liping, Wang, and Wong Nyuk Hien. 2007. "The Impacts of Ventilation Strategies and Facade on Indoor Thermal Environment for Naturally Ventilated Residential Buildings in Singapore." *Building and Environment* 42 (12): 4006–15.
- Manu, Sanyogita, Yash Shukla, Rajan Rawal, Leena E. Thomas, and Richard de Dear. 2016. "Field Studies of Thermal Comfort across Multiple Climate Zones for the Subcontinent: India Model for Adaptive Comfort (IMAC)." *Building and Environment* 98 (March): 55–70. doi:10.1016/j.buildenv.2015.12.019.
- McNeil, Michael A., and Virginie E. Letschert. 2008. "Future Air Conditioning Energy Consumption in Developing Countries and What Can Be Done about It: The Potential of Efficiency in the Residential Sector." *Lawrence Berkeley National Laboratory*. <http://eprints.cdlib.org/uc/item/64f9r6wr.pdf>.
- Medved, Sašo, Miha Babnik, Boris Vidrih, and Ciril Arkar. 2014. "Parametric Study on the Advantages of Weather-Predicted Control Algorithm of Free Cooling Ventilation System." *Energy* 73 (August): 80–87. doi:10.1016/j.energy.2014.05.080.
- Pfafferott, Jens, Sebastian Herkel, and Martina Jäschke. 2003. "Design of Passive Cooling by Night Ventilation: Evaluation of a Parametric Model and Building Simulation with Measurements." *Energy and Buildings* 35 (11): 1129–43. doi:10.1016/j.enbuild.2003.09.005.
- Pfafferott, Jens, Sebastian Herkel, and Matthias Wambsganß. 2004. "Design, Monitoring and Evaluation of a Low Energy Office Building with Passive Cooling by Night Ventilation." *Energy and Buildings* 36 (5): 455–65. doi:10.1016/j.enbuild.2004.01.041.
- Santamouris, Matheos, and Demosthenes Asimakopoulos. 1996. *Passive Cooling of Buildings*. Earthscan. <https://books.google.com/books?hl=en&lr=&id=tLHsJ0-vEkYC&oi=fnd&pg=PR9&dq=Passive+Cooling+of+Buildings&ots=MX1G-stuHi&sig=V03LDkXeMj3KLGzHfJa-bbw-aLs>.
- Santamouris, M., G. Mihalakakou, A. Argiriou, and D. Asimakopoulos. 1996. "On the Efficiency of Night Ventilation Techniques for Thermostatically Controlled Buildings." *Solar Energy* 56 (6): 479–83.
- Santamouris, M., A. Sfakianaki, and K. Pavlou. 2010. "On the Efficiency of Night Ventilation Techniques Applied to Residential Buildings." *Energy and Buildings* 42 (8): 1309–13. doi:10.1016/j.enbuild.2010.02.024.
- Shaviv, Edna, Abraham Yezioro, and Isaac G. Capeluto. 2001. "Thermal Mass and Night Ventilation as Passive Cooling Design Strategy." *Renewable Energy* 24 (3): 445–52.

- Vidrih, Boris, Ciril Arkar, and Sašo Medved. 2016. “Generalized Model-Based Predictive Weather Control for the Control of Free Cooling by Enhanced Night-Time Ventilation.” *Applied Energy* 168: 482–92.
- Zhang, Rongpeng, Yisu Nie, Khee Poh Lam, and Lorenz T. Biegler. 2014. “Dynamic Optimization Based Integrated Operation Strategy Design for Passive Cooling Ventilation and Active Building Air Conditioning.” *Energy and Buildings* 85 (December): 126–35. doi:10.1016/j.enbuild.2014.09.032.

# 10. Appendices

## 10.1 Matlab code

### 10.1.1 Window state data conversion

```
%% Load Data
data_full = xlsread('Danya_Room.xlsx');
window = xlsread('Window_State.xlsx');

%Calculate airflow and window state
d_year = data_full(:,1);
d_month = data_full(:,2);
d_day = data_full(:,3);
d_hour = data_full(:,4);
airflow = data_full(:,10);

w_year = window(:,3);
w_month = window(:,4);
w_day = window(:,5);
w_hour = window(:,6);
w_state = window(:,8);

airflow_new(1) = airflow(1);
s(1) = 1;

for i = 2:length(airflow)
    k = 0;
    for j = 1:length(w_state)
        if d_year(i) == w_year(j)
            if d_month(i) == w_month(j)
                if d_day(i) == w_day(j)
                    if d_hour(i) == w_hour(j)
                        if w_state(j) == 1
                            airflow_new(i) = 0;
                            s(i) = 0;
                            k = 1;
                        else
                            airflow_new(i) = airflow(i);
                            s(i) = 1;
                            k = 1;
                        end
                    end
                end
            end
        end
    end
end
if k == 0
    if s(i-1) == 1
        airflow_new(i) = airflow(i);
        s(i) = 1;
    else
        airflow_new(i) = 0;
    end
end
```

```

        s(i) = 0;
    end
end
end

data_full = [data_full,airflow_new',s'];

```

## 10.1.2 Persistence of excitation

### **Dynamical equations with airflow and supply temperature**

```

%% Persistence of excitation

%%% PE of phi 1
phi = [air_in, mass_wall, mass_floor, air_out, air_flow, air_supply]'; % <--
---- enter signals for 3D parametric model
t_end = t(end);
PE_mat = zeros(6);

phi_sq = zeros(6,6,length(t));
for k = 1:length(t)
    phi_sq(:, :, k) = phi(:, k) * phi(:, k)';
end
PE_mat(1,1) = 1/t_end * trapz(t, phi_sq(1,1,:));
PE_mat(2,1) = 1/t_end * trapz(t, phi_sq(2,1,:));
PE_mat(3,1) = 1/t_end * trapz(t, phi_sq(3,1,:));
PE_mat(4,1) = 1/t_end * trapz(t, phi_sq(4,1,:));
PE_mat(5,1) = 1/t_end * trapz(t, phi_sq(5,1,:));
PE_mat(6,1) = 1/t_end * trapz(t, phi_sq(6,1,:));
PE_mat(1,2) = 1/t_end * trapz(t, phi_sq(1,2,:));
PE_mat(2,2) = 1/t_end * trapz(t, phi_sq(2,2,:));
PE_mat(3,2) = 1/t_end * trapz(t, phi_sq(3,2,:));
PE_mat(4,2) = 1/t_end * trapz(t, phi_sq(4,2,:));
PE_mat(5,2) = 1/t_end * trapz(t, phi_sq(5,2,:));
PE_mat(6,2) = 1/t_end * trapz(t, phi_sq(6,2,:));
PE_mat(1,3) = 1/t_end * trapz(t, phi_sq(1,3,:));
PE_mat(2,3) = 1/t_end * trapz(t, phi_sq(2,3,:));
PE_mat(3,3) = 1/t_end * trapz(t, phi_sq(3,3,:));
PE_mat(4,3) = 1/t_end * trapz(t, phi_sq(4,3,:));
PE_mat(5,3) = 1/t_end * trapz(t, phi_sq(5,3,:));
PE_mat(6,3) = 1/t_end * trapz(t, phi_sq(6,3,:));
PE_mat(1,4) = 1/t_end * trapz(t, phi_sq(1,4,:));
PE_mat(2,4) = 1/t_end * trapz(t, phi_sq(2,4,:));
PE_mat(3,4) = 1/t_end * trapz(t, phi_sq(3,4,:));
PE_mat(4,4) = 1/t_end * trapz(t, phi_sq(4,4,:));
PE_mat(5,4) = 1/t_end * trapz(t, phi_sq(5,4,:));
PE_mat(6,4) = 1/t_end * trapz(t, phi_sq(6,4,:));
PE_mat(1,5) = 1/t_end * trapz(t, phi_sq(1,5,:));
PE_mat(2,5) = 1/t_end * trapz(t, phi_sq(2,5,:));
PE_mat(3,5) = 1/t_end * trapz(t, phi_sq(3,5,:));
PE_mat(4,5) = 1/t_end * trapz(t, phi_sq(4,5,:));
PE_mat(5,5) = 1/t_end * trapz(t, phi_sq(5,5,:));
PE_mat(6,5) = 1/t_end * trapz(t, phi_sq(6,5,:));
PE_mat(1,6) = 1/t_end * trapz(t, phi_sq(1,6,:));
PE_mat(2,6) = 1/t_end * trapz(t, phi_sq(2,6,:));
PE_mat(3,6) = 1/t_end * trapz(t, phi_sq(3,6,:));

```



```

PE_mat(4,6) = 1/t_end * trapz(t, phi_sq(4,6,:));
PE_mat(5,6) = 1/t_end * trapz(t, phi_sq(5,6,:));
PE_mat(6,6) = 1/t_end * trapz(t, phi_sq(6,6,:));

PE_lam_min = min(eig(PE_mat));
fprintf(1,'PE Level for Phi_1: %1.4f\n',PE_lam_min);

%%% PE of phi 2
phi = [air_in, mass_wall, air_out]'; % <----- enter signals for 3D
parametric model
t_end = t(end);
PE_mat = zeros(3);

phi_sq = zeros(3,3,length(t));
for k = 1:length(t)
    phi_sq(:, :, k) = phi(:,k) * phi(:,k)';
end
PE_mat(1,1) = 1/t_end * trapz(t, phi_sq(1,1,:));
PE_mat(2,1) = 1/t_end * trapz(t, phi_sq(2,1,:));
PE_mat(3,1) = 1/t_end * trapz(t, phi_sq(3,1,:));
PE_mat(1,2) = 1/t_end * trapz(t, phi_sq(1,2,:));
PE_mat(2,2) = 1/t_end * trapz(t, phi_sq(2,2,:));
PE_mat(3,2) = 1/t_end * trapz(t, phi_sq(3,2,:));
PE_mat(1,3) = 1/t_end * trapz(t, phi_sq(1,3,:));
PE_mat(2,3) = 1/t_end * trapz(t, phi_sq(2,3,:));
PE_mat(3,3) = 1/t_end * trapz(t, phi_sq(3,3,:));

PE_lam_min = min(eig(PE_mat));
fprintf(1,'PE Level for Phi_2: %1.4f\n',PE_lam_min);

%%% PE of phi 3
phi = [air_in, mass_floor]'; % <----- enter signals for 3D parametric model
t_end = t(end);
PE_mat = zeros(2);

phi_sq = zeros(2,2,length(t));
for k = 1:length(t)
    phi_sq(:, :, k) = phi(:,k) * phi(:,k)';
end
PE_mat(1,1) = 1/t_end * trapz(t, phi_sq(1,1,:));
PE_mat(2,1) = 1/t_end * trapz(t, phi_sq(2,1,:));
PE_mat(1,2) = 1/t_end * trapz(t, phi_sq(1,2,:));
PE_mat(2,2) = 1/t_end * trapz(t, phi_sq(2,2,:));

PE_lam_min = min(eig(PE_mat));
fprintf(1,'PE Level for Phi_3: %1.4f\n',PE_lam_min);

```

### **Dynamical equations with window state**

```

%% Persistence of excitation

%%% PE of phi 1
phi = [(air_out-air_in), (mass_wall-air_in), (mass_floor-air_in), s, rad]';
% <----- enter signals for 3D parametric model
t_end = t(end);
PE_mat = zeros(5);

```

```

phi_sq = zeros(5,5,length(t));
for k = 1:length(t)
    phi_sq(:, :, k) = phi(:, k) * phi(:, k)';
end
PE_mat(1,1) = 1/t_end * trapz(t, phi_sq(1,1,:));
PE_mat(2,1) = 1/t_end * trapz(t, phi_sq(2,1,:));
PE_mat(3,1) = 1/t_end * trapz(t, phi_sq(3,1,:));
PE_mat(4,1) = 1/t_end * trapz(t, phi_sq(4,1,:));
PE_mat(5,1) = 1/t_end * trapz(t, phi_sq(5,1,:));
PE_mat(1,2) = 1/t_end * trapz(t, phi_sq(1,2,:));
PE_mat(2,2) = 1/t_end * trapz(t, phi_sq(2,2,:));
PE_mat(3,2) = 1/t_end * trapz(t, phi_sq(3,2,:));
PE_mat(4,2) = 1/t_end * trapz(t, phi_sq(4,2,:));
PE_mat(5,2) = 1/t_end * trapz(t, phi_sq(5,2,:));
PE_mat(1,3) = 1/t_end * trapz(t, phi_sq(1,3,:));
PE_mat(2,3) = 1/t_end * trapz(t, phi_sq(2,3,:));
PE_mat(3,3) = 1/t_end * trapz(t, phi_sq(3,3,:));
PE_mat(4,3) = 1/t_end * trapz(t, phi_sq(4,3,:));
PE_mat(5,3) = 1/t_end * trapz(t, phi_sq(5,3,:));
PE_mat(1,4) = 1/t_end * trapz(t, phi_sq(1,4,:));
PE_mat(2,4) = 1/t_end * trapz(t, phi_sq(2,4,:));
PE_mat(3,4) = 1/t_end * trapz(t, phi_sq(3,4,:));
PE_mat(4,4) = 1/t_end * trapz(t, phi_sq(4,4,:));
PE_mat(5,4) = 1/t_end * trapz(t, phi_sq(5,4,:));
PE_mat(1,5) = 1/t_end * trapz(t, phi_sq(1,5,:));
PE_mat(2,5) = 1/t_end * trapz(t, phi_sq(2,5,:));
PE_mat(3,5) = 1/t_end * trapz(t, phi_sq(3,5,:));
PE_mat(4,5) = 1/t_end * trapz(t, phi_sq(4,5,:));
PE_mat(5,5) = 1/t_end * trapz(t, phi_sq(5,5,:));

PE_lam_min = min(eig(PE_mat));
fprintf(1, 'PE Level for Phi_1: %1.4f\n', PE_lam_min);

%%% PE of phi 2
phi = [(air_out-mass_wall), (air_in-mass_wall), rad]'; % <----- enter
signals for 3D parametric model
t_end = t(end);
PE_mat = zeros(3);

phi_sq = zeros(3,3,length(t));
for k = 1:length(t)
    phi_sq(:, :, k) = phi(:, k) * phi(:, k)';
end
PE_mat(1,1) = 1/t_end * trapz(t, phi_sq(1,1,:));
PE_mat(2,1) = 1/t_end * trapz(t, phi_sq(2,1,:));
PE_mat(3,1) = 1/t_end * trapz(t, phi_sq(3,1,:));
PE_mat(1,2) = 1/t_end * trapz(t, phi_sq(1,2,:));
PE_mat(2,2) = 1/t_end * trapz(t, phi_sq(2,2,:));
PE_mat(3,2) = 1/t_end * trapz(t, phi_sq(3,2,:));
PE_mat(1,3) = 1/t_end * trapz(t, phi_sq(1,3,:));
PE_mat(2,3) = 1/t_end * trapz(t, phi_sq(2,3,:));
PE_mat(3,3) = 1/t_end * trapz(t, phi_sq(3,3,:));

PE_lam_min = min(eig(PE_mat));
fprintf(1, 'PE Level for Phi_2: %1.4f\n', PE_lam_min);

```

```

%%% PE of phi 3
phi = [(air_in-mass_floor)]'; % <----- enter signals for 3D parametric
model
t_end = t(end);
PE_mat = zeros(2);

phi_sq = zeros(2,2,length(t));
for k = 1:length(t)
    phi_sq(:, :, k) = phi(:, k) * phi(:, k)';
end
PE_mat(1,1) = 1/t_end * trapz(t, phi_sq(1,1,:));
PE_mat(2,1) = 1/t_end * trapz(t, phi_sq(2,1,:));
PE_mat(1,2) = 1/t_end * trapz(t, phi_sq(1,2,:));
PE_mat(2,2) = 1/t_end * trapz(t, phi_sq(2,2,:));

PE_lam_min = min(eig(PE_mat));
fprintf(1, 'PE Level for Phi 3: %1.4f\n', PE_lam_min);

```

### 10.1.3 Gradient descent method

#### LEES gradient descent

```

%% Gradient Descent parameter identification

% Assemble Data
data = [t, air_in, mass_wall, mass_floor, air_out, air_flow, air_supply];

% Initial conditions
multiplier = 1;
theta_hat0_1 = multiplier*[-16, 4.2, 4.6, 3.9, -.00031, 3.9];
theta_hat0_2 = multiplier* [.13, -.14, .0027];
theta_hat0_3 = multiplier* [.094, -.094];

% Update Law Gain
eta = .01;
Gam1 = eta*eye(6);
Gam2 = eta*eye(3);
Gam3 = eta*eye(2);

% Integrate ODEs
[~, y1] = ode23s(@ (t,y) ode_gradient1(t,y,data,Gam1), t, theta_hat0_1);
[~, y2] = ode23s(@ (t,y) ode_gradient2(t,y,data,Gam2), t, theta_hat0_2);
[~, y3] = ode23s(@ (t,y) ode_gradient3(t,y,data,Gam3), t, theta_hat0_3);

% Parse output
theta_hat_1 = y1;
theta_hat_2 = y2;
theta_hat_3 = y3;

```

#### BH gradient descent

```

%% Gradient Descent parameter identification
% Assemble Data
data = [t, air_in, mass_wall, mass_floor, air_out, s, rad];

```

```

% Initial conditions
multiplier = 1;
theta_hat0_1 = multiplier* [.2, .4, .2, -100, 1];
theta_hat0_2 = multiplier* [.001, .001, 1];
theta_hat0_3 = multiplier* [.003, 1];

% Update Law Gain
eta = .01;
Gam1 = eta*eye(5);
Gam2 = eta*eye(3);
Gam3 = eta*eye(2);

% Integrate ODEs
[~,y1] = ode23s(@(t,y) ode_gradient1_sol(t,y,data,Gam1), t, theta_hat0_1);
[~,y2] = ode23s(@(t,y) ode_gradient2_sol(t,y,data,Gam2), t, theta_hat0_2);
[~,y3] = ode23s(@(t,y) ode_gradient3_sol(t,y,data,Gam3), t, theta_hat0_3);

% Parse output
theta_hat_1 = y1;
theta_hat_2 = y2;
theta_hat_3 = y3;

```

### IND gradient descent

```

%% Gradient Descent parameter identification
% Assemble Data
data = [t, air_in, mass_wall, mass_floor, air_out, s, rad];

% Initial conditions
multiplier = 1;
theta_hat0_1 = multiplier* [3, .04, 3, -1, 1];
theta_hat0_2 = multiplier* [.001, .0001, 1];
theta_hat0_3 = multiplier* [.01, 1];

% Update Law Gain
eta = .01;
Gam1 = eta*eye(5);
Gam2 = eta*eye(3);
Gam3 = eta*eye(2);

% Integrate ODEs
[~,y1] = ode23s(@(t,y) ode_gradient1(t,y,data,Gam1), t, theta_hat0_1);
[~,y2] = ode23s(@(t,y) ode_gradient2(t,y,data,Gam2), t, theta_hat0_2);
[~,y3] = ode23s(@(t,y) ode_gradient3(t,y,data,Gam3), t, theta_hat0_3);

% Parse output
theta_hat_1 = y1;
theta_hat_2 = y2;
theta_hat_3 = y3;

```

### LEES ode\_gradient1.m

```

% ode_gradient1.m
% ODEs for the gradient parameter identification algorithm
% t          : time
% theta_h    : parameter estimate
% data       : input-output data used to feed algorithm

```

```

% Gam          : Update law gain

function [theta_h_dot1] = ode_gradient1(t,theta_h,data,Gam)

%% Parse Input Data
it = data(:,1);           %time vector [hr]
iair_in = data(:,2);      %outdoor air temperature [deg F]
imass_wall = data(:,3);   %supply temperature [deg F]
imass_floor = data(:,4);  %indoor air temperature [deg F]
iair_out = data(:,5);     %wall mass temperature [deg F]
iair_flow = data(:,6);    %floor mass temperature [deg F]
iair_supply = data(:,7);  %air flow [CFM]
isol = data(:,8);         %radiation [BTU]

%% Interpolate data
air_in = interp1(it,iair_in,t);
mass_wall = interp1(it,imass_wall,t);
mass_floor = interp1(it,imass_floor,t);
air_out = interp1(it,iair_out,t);
air_flow = interp1(it,iair_flow,t);
air_supply = interp1(it,iair_supply,t);
sol = interp1(it,isol,t);

%% Parametric model notation
% Sampling time step
dt = 1;

% Compute Room temperature at NEXT time step
air_in_plus = interp1(it,iair_in,t+dt);

% Compute \dot{T} using forward difference in time
% z = \dot{T} = (T(t+dt) - T(t))/dt
z = (air_in_plus - air_in)/dt;

% Assemble regressor vector, \phi
phi = [air_in, mass_wall, mass_floor, air_out, air_flow, air_supply, sol]';

%% Gradient Update Law
% Normalization signal
msq = 1 + phi'*phi;

% Estimation error: \epsilon = z - \theta_h^T \phi
epsilon = (z - theta_h'*phi)/msq;

% Update Law
theta_h_dot1 = Gam * epsilon * phi;

```

### LEES ode\_gradient2.m

```

% ode_gradient2.m
% ODEs for the gradient parameter identification algorithm
% t          : time
% theta_h    : parameter estimate
% data       : input-output data used to feed algorithm
% Gam        : Update law gain

```

```

function [theta_h_dot2] = ode_gradient2(t,theta_h,data,Gam)

%% Parse Input Data
it = data(:,1);           %time vector [hr]
iair_in = data(:,2);      %outdoor air temperature [deg F]
imass_wall = data(:,3);   %supply temperature [deg F]
imass_floor = data(:,4);  %indoor air temperature [deg F]
iair_out = data(:,5);     %wall mass temperature [deg F]
iair_flow = data(:,6);    %floor mass temperature [deg F]
iair_supply = data(:,7);  %air flow [CFM]
isol = data(:,8);         %radiation [BTU]

%% Interpolate data
air_in = interp1(it,iair_in,t);
mass_wall = interp1(it,imass_wall,t);
mass_floor = interp1(it,imass_floor,t);
air_out = interp1(it,iair_out,t);
air_flow = interp1(it,iair_flow,t);
air_supply = interp1(it,iair_supply,t);
sol = interp1(it,isol,t);

%% Parametric model notation
% Sampling time step
dt = 1;

% Compute mass wall temperature at NEXT time step
mass_wall_plus = interp1(it,imass_wall,t+dt);

% Compute \dot{T} using forward difference in time
% z = \dot{T} = (T(t+dt) - T(t))/dt
z = (mass_wall_plus - mass_wall)/dt;

% Assemble regressor vector, \phi
phi = [air_in, mass_wall, air_out, sol]';

%% Gradient Update Law
% Normalization signal
msq = 1 + phi'*phi;

% Estimation error: \epsilon = z - \theta_h^T \phi
epsilon = (z - theta_h'*phi)/msq;

% Update Law
theta_h_dot2 = Gam * epsilon * phi;

```

### LEES ode\_gradient3.m

```

% ode_gradient3.m
% ODEs for the gradient parameter identification algorithm
% t           : time
% theta_h     : parameter estimate
% data        : input-output data used to feed algorithm
% Gam         : Update law gain

function [theta_h_dot3] = ode_gradient3(t,theta_h,data,Gam)

```

```

%% Parse Input Data
it = data(:,1);           %time vector [hr]
iair_in = data(:,2);      %outdoor air temperature [deg F]
imass_wall = data(:,3);   %supply temperature [deg F]
imass_floor = data(:,4);  %indoor air temperature [deg F]
iair_out = data(:,5);     %wall mass temperature [deg F]
iair_flow = data(:,6);    %floor mass temperature [deg F]
iair_supply = data(:,7);  %air flow [CFM]
isol = data(:,8);         %radiation [BTU]

%% Interpolate data
air_in = interp1(it,iair_in,t);
mass_wall = interp1(it,imass_wall,t);
mass_floor = interp1(it,imass_floor,t);
air_out = interp1(it,iair_out,t);
air_flow = interp1(it,iair_flow,t);
air_supply = interp1(it,iair_supply,t);
sol = interp1(it,isol,t);

%% Parametric model notation
% Sampling time step
dt = 1;

% Compute floor mass temperature at NEXT time step
mass_floor_plus = interp1(it,imass_floor,t+dt);

% Compute \dot{T} using forward difference in time
% z = \dot{T} = (T(t+dt) - T(t))/dt
z = (mass_floor_plus - mass_floor)/dt;

% Assemble regressor vector, \phi
phi = [air_in, mass_floor, sol]';

%% Gradient Update Law
% Normalization signal
msq = 1 + phi'*phi;

% Estimation error: \epsilon = z - \theta_h^T \phi
epsilon = (z - theta_h'*phi)/msq;

% Update Law
theta_h_dot3 = Gam * epsilon * phi;

```

### BH & IND ode\_gradient1.m

```

% ode_gradient1.m
% ODEs for the gradient parameter identification algorithm
% t          : time
% theta_h    : parameter estimate
% data       : input-output data used to feed algorithm
% Gam        : Update law gain

function [theta_h_dot1] = ode_gradient1(t,theta_h,data,Gam)

%% Parse Input Data
it = data(:,1);           %time vector [hr]

```

```

iair_in = data(:,2);           %outdoor air temperature [deg C]
imass_wall = data(:,3);       %supply temperature [deg C]
imass_floor = data(:,4);      %indoor air temperature [deg C]
iair_out = data(:,5);         %wall mass temperature [deg C]
is = data(:,6);               %state [0/1]
irad = data(:,7);             %radiation [J]

%% Interpolate data
air_in = interp1(it,iair_in,t);
mass_wall = interp1(it,imass_wall,t);
mass_floor = interp1(it,imass_floor,t);
air_out = interp1(it,iair_out,t);
s = interp1(it,is,t);
rad = interp1(it,irad,t);

%% Parametric model notation
% Sampling time step
dt = 1;

% Compute Room temperature at NEXT time step
air_in_plus = interp1(it,iair_in,t+dt);

% Compute \dot{T} using forward difference in time
% z = \dot{T} = (T(t+dt) - T(t))/dt
z = (air_in_plus - air_in)/dt;

% Assemble regressor vector, \phi
phi = [(air_out-air_in), (mass_wall-air_in), (mass_floor-air_in), s, rad]';

%% Gradient Update Law
% Normalization signal
msq = 1 + phi'*phi;

% Estimation error: \epsilon = z - \theta_h^T \phi
epsilon = (z - theta_h'*phi)/msq;

% Update Law
theta_h_dot1 = Gam * epsilon * phi;

```

### BH & IND ode\_gradient2.m

```

% ode_gradient2.m
% ODEs for the gradient parameter identification algorithm
% t           : time
% theta_h     : parameter estimate
% data        : input-output data used to feed algorithm
% Gam         : Update law gain

function [theta_h_dot2] = ode_gradient2(t,theta_h,data,Gam)

%% Parse Input Data
it = data(:,1);           %time vector [hr]
iair_in = data(:,2);      %outdoor air temperature [deg F]
imass_wall = data(:,3);   %supply temperature [deg F]
imass_floor = data(:,4);  %indoor air temperature [deg F]
iair_out = data(:,5);     %wall mass temperature [deg F]

```



```

irad = data(:,7);           %radiation [J]

%% Interpolate data
air_in = interp1(it,iair_in,t);
mass_wall = interp1(it,imass_wall,t);
mass_floor = interp1(it,imass_floor,t);
air_out = interp1(it,iair_out,t);
rad = interp1(it,irad,t);

%% Parametric model notation
% Sampling time step
dt = 1;

% Compute mass wall temperature at NEXT time step
mass_wall_plus = interp1(it,imass_wall,t+dt);

% Compute \dot{T} using forward difference in time
% z = \dot{T} = (T(t+dt) - T(t))/dt
z = (mass_wall_plus - mass_wall)/dt;

% Assemble regressor vector, \phi
phi = [(air_out-mass_wall), (air_in-mass_wall), rad]';

%% Gradient Update Law
% Normalization signal
msq = 1 + phi'*phi;

% Estimation error: \epsilon = z - \theta_h^T \phi
epsilon = (z - theta_h'*phi)/msq;

% Update Law
theta_h_dot2 = Gam * epsilon * phi;

```

### BH & IND ode\_gradient3.m

```

% ode_gradient3.m
% ODEs for the gradient parameter identification algorithm
% t           : time
% theta_h     : parameter estimate
% data        : input-output data used to feed algorithm
% Gam         : Update law gain

function [theta_h_dot3] = ode_gradient3(t,theta_h,data,Gam)

%% Parse Input Data
it = data(:,1);           %time vector [hr]
iair_in = data(:,2);      %outdoor air temperature [deg F]
imass_wall = data(:,3);   %supply temperature [deg F]
imass_floor = data(:,4);  %indoor air temperature [deg F]
iair_out = data(:,5);     %wall mass temperature [deg F]
irad = data(:,7);         %radiation [J]

%% Interpolate data
air_in = interp1(it,iair_in,t);
mass_wall = interp1(it,imass_wall,t);
mass_floor = interp1(it,imass_floor,t);

```

```

air_out = interp1(it,iair_out,t);
rad = interp1(it,irad,t);

%% Parametric model notation
% Sampling time step
dt = 1;

% Compute floor mass temperature at NEXT time step
mass_floor_plus = interp1(it,imass_floor,t+dt);

% Compute \dot{T} using forward difference in time
% z = \dot{T} = (T(t+dt) - T(t))/dt
z = (mass_floor_plus - mass_floor)/dt;

% Assemble regressor vector, \phi
phi = [(air_in-mass_floor), rad]';

%% Gradient Update Law
% Normalization signal
msq = 1 + phi'*phi;

% Estimation error: \epsilon = z - \theta_h^T \phi
epsilon = (z - theta_h'*phi)/msq;

% Update Law
theta_h dot3 = Gam * epsilon * phi;

```

#### 10.1.4 Nonlinear least squares method

##### LEES nonlinear least squares

```

%% Parameter Estimation using lsqnonlin

% Options for the algorithm
optim_options = optimset('Display', 'iter',...
'TolFun', 1e-10,... %default: 1e-4
'TolX', 1e-6... %default: 1e-4
);
%'MaxFunEvals', 700,... % default: 100 * num of variables
%'MaxIter', 100000,... % default: 400
%'Algorithm','levenberg-marquardt'); %default:
%optim_options = [];

%% Run lsqnonlin

% Load initial p-values
load('./gradient_descent_values_1story_vent_1month_A1.mat')

% Nonlinear optimization of parameters
[p,resnorm,residual] = lsqnonlin(@mle_error_vent, Theta_Hat,...
[-30,0,0,0,-30,0,0,0,-30,0,0,0,-30,0],...
[0,30,30,30,1,30,30,30,0,30,30,30,0,30],...
optim_options,t, U_hat, That0, air_in, mass_wall, mass_floor);

Theta_Hat = p;

```

### BH nonlinear least squares

```
%% Parameter Estimation using lsqnonlin

% Options for for the algorithm
optim_options = optimset('Display', 'iter',...
'TolFun', 1e-10,... %default: 1e-4
'TolX', 1e-6... %default: 1e-4
);
%'MaxFunEvals', 700,... % default: 100 * num of variables
%'MaxIter', 100000,... % default: 400
%'Algorithm','levenberg-marquardt'); %default:
%optim_options = [];

%% Run lsqnonlin

% Load initial p-values
load('./gradient_descent_values_sol_-100.mat')

% Nonlinear optimization of parameters
[p,resnorm,residual] = lsqnonlin(@mle_error_novent, Theta_Hat,...
    [0, 0, 0, -100, 0, 0, 0, 0, 0, 0],...
    [30, 30, 30, 0, 10, .1, .1, 10, .1, 10],...
    optim_options,t, U_hat, That0, air_in, mass_wall, mass_floor);

Theta_Hat = p;
```

### IND nonlinear least squares

```
%% Parameter Estimation using lsqnonlin

% Options for for the algorithm
optim_options = optimset('Display', 'iter',...
'TolFun', 1e-10,... %default: 1e-4
'TolX', 1e-6... %default: 1e-4
);
%'MaxFunEvals', 700,... % default: 100 * num of variables
%'MaxIter', 100000,... % default: 400
%'Algorithm','levenberg-marquardt'); %default:
%optim_options = [];

%% Run lsqnonlin

% Load initial p-values
load('./gradient_descent_values.mat')

% Nonlinear optimization of parameters
[p,resnorm,residual] = lsqnonlin(@mle_error_novent, Theta_Hat,...
    [0,0,0,-30,0,0,0,0,0,0],...
    [10,1,10,0,10,.1,.01,10,.1,10],...
    optim_options,t, U_hat, That0, air_in, mass_wall, mass_floor);

Theta_Hat = p;
```

### LEES mle\_error\_vent.m

```

function xi = mle_error_vent(Theta_Hat,t, U_hat, That0,air_in, mass_wall,
mass_floor)
% This function will calculate the error between measured and simulation
% Initially set as maximum likelihood error (hence the name) but changed
% to the square error.

% Simulate building system
[That,t] = build_sim_vent(t, U_hat, Theta_Hat, That0);

% Select parameter to optimize
y_1 = That(:,1);
y_2 = That(:,2);
y_3 = That(:,3);

% Compute the error
%xi = (air_in(:)-y_1(:) + mass_wall(:)-y_2(:) + mass_floor(:)-y_3(:)).^2;
xi = [air_in(:)-y_1(:), mass_wall(:)-y_2(:), mass_floor(:)-y_3(:)];

end

```

#### LEES build\_sim\_vent.m

```

function [That,t] = build_sim_vent(t, U_hat, Theta_Hat, That0)
% This function will simulation the results of the system.
% This function is used in the non-linear optimization script
%
% t = time for the simulation
% U = the state matrix
% Theta_Hat = vector of parameters to define the state space equation
% That0 = vector of initial conditions of indoor air, mass wall, and mass
% floor

% Definitions of the A and B matrix of the dynamical equations
Ahat = [Theta_Hat(1), Theta_Hat(2), Theta_Hat(3);...
        Theta_Hat(8), Theta_Hat(9), 0;...
        Theta_Hat(12), 0, Theta_Hat(13)];

Bhat = [Theta_Hat(4), Theta_Hat(5), Theta_Hat(6), Theta_Hat(7);...
        Theta_Hat(10), 0, 0, Theta_Hat(11);...
        0, 0, 0, Theta_Hat(14)];

% Output states only (dummy variables, not used later)
C_dummy = eye(3);
D_dummy = 0;

sys_hat = ss(Ahat, Bhat, C_dummy, D_dummy);

% Simulate
[That,t] = lsim(sys_hat, U_hat, t, That0);

end

```

#### BH & IND mle\_error\_novent.m

```

function xi = mle_error_novent(Theta_Hat,t, U_hat, That0,air_in, mass_wall,
mass_floor)
% This function will calculate the error between measured and simulation

```

```

% Initially set as maximum likelihood error (hence the name) but changed
% to the square error.

% Simulate building system
[That,t] = build_sim_novent(t, U_hat, Theta_Hat, That0);

% Select parameter to optimize
y_1 = That(:,1);
y_2 = That(:,2);
y_3 = That(:,3);

% Compute the error
xi = [air_in(:)-y_1(:), mass_wall(:)-y_2(:), mass_floor(:)-y_3(:)];

end

```

#### BH & IND build\_sim\_novent.m

```

function [That,t] = build_sim_novent(t, U_hat, Theta_Hat, That0)
% This function will simulation the results of the system.
% This function is used in the non-linear optimization script
%
% t = time for the simulation
% U = the state matrix
% Theta_Hat = vector of parameters to define the state space equation
% That0 = vector of inital conditions of indoor air, mass wall, and mass
% floor

% Definitions of the A and B matrix of the dynamical equations
Ahat = [(-Theta_Hat(1)-Theta_Hat(2)-Theta_Hat(3)), Theta_Hat(2),
Theta_Hat(3);...
        Theta_Hat(7), -Theta_Hat(6)-Theta_Hat(7), 0;...
        Theta_Hat(9), 0, -Theta_Hat(9)];

Bhat = [Theta_Hat(1), Theta_Hat(4), Theta_Hat(5);...
        Theta_Hat(6), 0, Theta_Hat(8);...
        0, 0, Theta_Hat(10)];

% Output states only (dummy variables, not used later)
C_dummy = eye(3);
D_dummy = 0;

sys_hat = ss(Ahat, Bhat, C_dummy, D_dummy);

% Simulate
[That,t] = lsim(sys_hat, U_hat, t, That0);

end

```

### 10.1.5 Model simulation

#### LEES

```

% Simulate final parameters
Ahat = [Theta_Hat(1), Theta_Hat(2), Theta_Hat(3);...

```

```

        Theta_Hat(8), Theta_Hat(9), 0;...
        Theta_Hat(12), 0, Theta_Hat(13)];

Bhat = [Theta_Hat(4), Theta_Hat(5), Theta_Hat(6), Theta_Hat(7);...
        Theta_Hat(10), 0, 0, Theta_Hat(11);...
        0, 0, 0, Theta_Hat(14)];

% Output states only (dummy variables, not used later)
C_dummy = eye(3);
D_dummy = 0;

% State space model
sys_hat = ss(Ahat, Bhat, C_dummy, D_dummy);

% Simulation of initial estimates of parameters

% Input vector from training data set
U_hat = [air_out, air_flow, air_supply, sol];

% Initial conditions
That0 = [air_in(1); mass_wall(1); mass_floor(1)];

% Simulate
[~,~,That] = lsim(sys_hat, U_hat, t, That0);

```

#### **BH & IND**

```

%Simulate initial parameters
Ahat = [(-Theta_Hat(1)-Theta_Hat(2)-Theta_Hat(3)), Theta_Hat(2),
        Theta_Hat(3);...
        Theta_Hat(7), -Theta_Hat(6)-Theta_Hat(7), 0;...
        Theta_Hat(9), 0, -Theta_Hat(9)];

Bhat = [Theta_Hat(1), Theta_Hat(4), Theta_Hat(5);...
        Theta_Hat(6), 0, Theta_Hat(8);...
        0, 0, Theta_Hat(10)];

% Output states only (dummy variables, not used later)
C_dummy = eye(3);
D_dummy = 0;

% State space model
sys_hat = ss(Ahat, Bhat, C_dummy, D_dummy);

% Input vector from training data set
U_hat = [air_out, s, rad];

% Initial conditions
That0 = [air_in(1); mass_wall(1); mass_floor(1)];

% Simulate
[~,~,That] = lsim(sys_hat, U_hat, t, That0);

```

### 10.1.6 Model error calculation

```

%% Calculate Error

n = length(t);

for i = 1:n
    air_in_pe(i) = abs(air_in(i) - That(i,1))/air_in(i);
    mass_wall_pe(i) = abs(mass_wall(i) - That(i,2))/mass_wall(i);
    mass_floor_pe(i) = abs(mass_floor(i) - That(i,3))/mass_floor(i);
    air_in_e(i) = abs(air_in(i) - That(i,1));
    air_in_e_sq(i) = air_in_e(i)^2;
    mass_wall_e(i) = abs(mass_wall(i) - That(i,2));
    mass_wall_e_sq(i) = mass_wall_e(i)^2;
    mass_floor_e(i) = abs(mass_floor(i) - That(i,3));
    mass_floor_e_sq(i) = mass_floor_e(i)^2;
end

MAPE = mean([air_in_pe, mass_wall_pe, mass_floor_pe]);
SDAPE = std([air_in_pe, mass_wall_pe, mass_floor_pe]);
MAE = mean([air_in_e, mass_wall_e, mass_floor_e]);
SDAE = std([air_in_e, mass_wall_e, mass_floor_e]);
RMSE = sqrt(sum([air_in_e_sq, mass_wall_e_sq, mass_floor_e_sq])/(3*n));
fprintf(1, '\nRMSE: %1.4f\n', RMSE);
fprintf(1, 'MAPE: %1.4f, SDAPE: %1.4f\n', MAPE, SDAPE);
fprintf(1, 'MAE: %1.4f, SDAPE: %1.4f\n', MAE, SDAE);

air_in_RMSE = sqrt(sum(air_in_e_sq)/n);
mass_wall_RMSE = sqrt(sum(mass_wall_e_sq)/n);
mass_floor_RMSE = sqrt(sum(mass_floor_e_sq)/n);
air_in_CV_RMSE = sqrt(sum(air_in_e_sq)/n)/mean(air_in);
mass_wall_CV_RMSE = sqrt(sum(mass_wall_e_sq)/n)/mean(mass_wall);
mass_floor_CV_RMSE = sqrt(sum(mass_floor_e_sq)/n)/mean(mass_floor);
fprintf(1, 'Second floor indoor air RMSE: %1.4f, CV(RMSE): %1.4f\n', ...
    air_in_RMSE, air_in_CV_RMSE);
fprintf(1, 'Second floor mass wall RMSE: %1.4f, CV(RMSE): %1.4f\n', ...
    mass_wall_RMSE, mass_wall_CV_RMSE);
fprintf(1, 'Second floor mass floor RMSE: %1.4f, CV(RMSE): %1.4f\n', ...
    mass_floor_RMSE, mass_floor_CV_RMSE);

air_in_MAPE = mean(air_in_pe); air_in_SDAPE = std(air_in_pe);
fprintf(1, 'Second floor indoor air MAPE: %1.4f, SDAPE: %1.4f\n', ...
    air_in_MAPE, air_in_SDAPE);
mass_wall_MAPE = mean(mass_wall_pe); mass_wall_SDAPE = std(mass_wall_pe);
fprintf(1, 'Second floor mass wall MAPE: %1.4f, SDAPE: %1.4f\n', ...
    mass_wall_MAPE, mass_wall_SDAPE);
mass_floor_MAPE = mean(mass_floor_pe); mass_floor_SDAPE =
std(mass_floor_pe);
fprintf(1, 'Second floor mass floor MAPE: %1.4f, SDAPE: %1.4f\n', ...
    mass_floor_MAPE, mass_floor_SDAPE);

air_in_MAE = mean(air_in_e); air_in_SDAE = std(air_in_e);
fprintf(1, 'Second floor indoor air MAE: %1.4f, SDAE: %1.4f\n', air_in_MAE,
air_in_SDAE);
mass_wall_MAE = mean(mass_wall_e); mass_wall_SDAE = std(mass_wall_e);
fprintf(1, 'Second floor mass wall MAE: %1.4f, SDAE: %1.4f\n', mass_wall_MAE,
mass_wall_SDAE);
mass_floor_MAE = mean(mass_floor_e); mass_floor_SDAE = std(mass_floor_e);

```

```
fprintf(1,'Second floor mass floor MAE: %1.4f, SDAE:
%1.4f\n',mass floor MAE, mass floor SDAE);
```

## 10.1.7 K-fold cross validation

### LEES

```
%% K-Fold Cross Validation

months = 1;
days = 30*months;
hours = days*24/10;
starting_hour = 720;

for j = 1:10
    %load training data
    data = data_full(starting_hour+hours*(j-1):starting_hour+hours*j,:);
    t_train = data(:,1); %time vector [hr]
    t_train = (0:(length(t_train)-1))'; %resample vector to start at 0

    air_out_train = data(:,2); %outdoor air temperature, T_A [deg F]
    air_supply_train = data(:,3); %supply temperature, T_V [deg F]
    air_in_train = data(:,4); %indoor air temperature, T_Z [deg F]
    mass_wall_train = data(:,5); %wall mass temperature, T_W [deg F]
    mass_floor_train = data(:,6); %floor mass temperature, T_F [deg F]
    air_flow_train = data(:,7); %air flow, V [CFM]
    sol_train = data(:,11); %radiation [BTU]

    %load initial p-values
    load('./gradient_descent_values_1story_vent_1month_A1.mat')

    % Options for for the algorithm
    optim_options = optimset('Display', 'iter',...
    'TolFun', 1e-10,... %default: 1e-4
    'TolX', 1e-6... %default: 1e-4
    );

    % Input vector & initial conditions from training data
    U_hat_train = [air_out_train, air_flow_train, air_supply_train,
    sol_train];
    That0_train = [air_in_train(1); mass_wall_train(1);
    mass_floor_train(1)];

    % Nonlinear optimization of parameters
    [p,resnorm,residual] = lsqnonlin(@mle_error_vent, Theta_Hat,...
    [-30,0,0,0,-30,0,0,0,-30,0,0,0,-30,0],...
    [0,30,30,30,1,30,30,30,0,30,30,30,0,30],...
    optim_options,t_train, U_hat_train, That0_train, air_in_train,...
    mass_wall_train, mass_floor_train);
    Theta_Hat = p;

    % Simulate parameters
    Ahat = [Theta_Hat(1), Theta_Hat(2), Theta_Hat(3);...
    Theta_Hat(8), Theta_Hat(9), 0;...
    Theta_Hat(12), 0, Theta_Hat(13)];
```



```

Bhat = [Theta_Hat(4), Theta_Hat(5), Theta_Hat(6), Theta_Hat(7);...
        Theta_Hat(10), 0, 0, Theta_Hat(11);...
        0, 0, 0, Theta_Hat(14)];
C_dummy = eye(3);
D_dummy = 0;

% State space model
sys_hat = ss(Ahat, Bhat, C_dummy, D_dummy);

%load validation data
if j == 1
    data = data_full(starting_hour+hours:starting_hour+hours*10,:);
elseif j == 10
    data = data_full(starting_hour:starting_hour+hours*9,:);
else
    data = [data_full(starting_hour:starting_hour+hours*(j-1),:);...
            data_full(starting_hour+hours*j:starting_hour+hours*10,:)];
end
t_val = data(:,1);           %time vector [hr]
t_val = (0:(length(t_val)-1))'; %resample vector to start at 0

air_out_val = data(:,2);      %outdoor air temperature, T_A [deg F]
air_supply_val = data(:,3);   %supply temperature, T_V [deg F]
air_in_val = data(:,4);       %indoor air temperature, T_Z [deg F]
mass_wall_val = data(:,5);     %wall mass temperature, T_W [deg F]
mass_floor_val = data(:,6);    %floor mass temperature, T_F [deg F]
air_flow_val = data(:,7);      %air flow, V [CFM]
sol_val = data(:,11);          %radiation [BTU]

% Input vector & initial conditions from training data
U_hat_val = [air_out_val, air_flow_val, air_supply_val, sol_val];
That0_val = [air_in_val(1); mass_wall_val(1); mass_floor_val(1)];

% Simulate
[~,~,That] = lsim(sys_hat, U_hat_val, t_val, That0_val);
end

```

## BH

```
%% K-Fold Cross Validation
```

```

months = 8;
days = 30*months;
hours = days*24/10;
starting_hour = 720;

for j = 1:10
    %load training data
    data = data_full(starting_hour+hours*(j-1):starting_hour+hours*j,:);
    t_train = data(:,6);           %time vector [hr]
    t_train = (0:(length(t_train)-1))'; %resample vector to start at 0

    air_out_train = data(:,9);      %outdoor air temperature, T_A [deg C]
    air_in_train = data(:,7);       %indoor air temperature, T_Z [deg C]
    mass_wall_train = data(:,8);    %wall mass temperature, T_W [deg C]

```

```

mass_floor_train = data(:,8);      %floor mass temperature, T_F [deg C]
rad_train = data(:,11);           %solar radiation [J]
s_train = data(:,14);             %window state [0,1]

%load initial p-values
load('./gradient_descent_values_sol_-100.mat')

% Options for for the algorithm
optim_options = optimset('Display', 'iter',...
'TolFun', 1e-10,... %default: 1e-4
'TolX', 1e-6... %default: 1e-4
);

% Input vector & initial conditions from training data
U_hat_train = [air_out_train, s_train, rad_train];
That0_train = [air_in_train(1); mass_wall_train(1);
mass_floor_train(1)];

% Nonlinear optimization of parameters
[p,resnorm,residual] = lsqnonlin(@mle_error_novent, Theta_Hat,...
[0, 0, 0, -100, 0, 0, 0, 0, 0, 0],...
[30, 30, 30, 0, 10, .1, .1, 10, .1, 10],...
optim_options,t_train, U_hat_train, That0_train, air_in_train,...
mass_wall_train, mass_floor_train);
Theta_Hat = p;

% Simulate parameters
Ahat = [(-Theta_Hat(1)-Theta_Hat(2)-Theta_Hat(3)), Theta_Hat(2),
Theta_Hat(3);...
Theta_Hat(7), -Theta_Hat(6)-Theta_Hat(7), 0;...
Theta_Hat(9), 0, -Theta_Hat(9)];

Bhat = [Theta_Hat(1), Theta_Hat(4), Theta_Hat(5);...
Theta_Hat(6), 0, Theta_Hat(8);...
0, 0, Theta_Hat(10)];
C_dummy = eye(3);
D_dummy = 0;

% State space model
sys_hat = ss(Ahat, Bhat, C_dummy, D_dummy);

%load validation data
if j == 1
    data = data_full(starting_hour+hours:starting_hour+hours*10,:);
elseif j == 10
    data = data_full(starting_hour:starting_hour+hours*9,:);
else
    data = [data_full(starting_hour:starting_hour+hours*(j-1),:);...
data_full(starting_hour+hours*j:starting_hour+hours*10,:)];
end
t_val = data(:,6);                %time vector [hr]
t_val = (0:(length(t_val)-1))';  %resample vector to start at 0

air_out_val = data(:,9);          %outdoor air temperature, T_A [deg C]
air_in_val = data(:,7);          %indoor air temperature, T_Z [deg C]
mass_wall_val = data(:,8);       %wall mass temperature, T_W [deg C]

```

```

mass_floor_val = data(:,8);      %floor mass temperature, T_F [deg C]
rad_val = data(:,11);           %solar radiation [J]
s_val = data(:,14);             %window state [0,1]

% Input vector & initial conditions from training data
U_hat_val = [air_out_val, s_val, rad_val];
That0_val = [air_in_val(1); mass_wall_val(1); mass_floor_val(1)];

% Simulate
[~,~,That] = lsim(sys_hat, U_hat_val, t_val, That0_val);
end

```

## IND

```

%% K-Fold Cross Validation

months = 1;
days = 30*months;
hours = days*24/10;
starting_hour = 1;

for j = 1:10
    %load training data
    data = data_full(starting_hour+hours*(j-1):starting_hour+hours*j,:);
    t_train = data(:,1);           %time vector [hr]
    t_train = (0:(length(t_train)-1))'; %resample vector to start at 0

    air_out_train = data(:,2);      %outdoor air temperature, T_A [deg C]
    air_in_train = data(:,3);      %indoor air temperature, T_Z [deg C]
    mass_wall_train = data(:,4);   %wall mass temperature, T_W [deg C]
    mass_floor_train = data(:,4);  %floor mass temperature, T_F [deg C]
    s_train = data(:,5);           %window state [0,1]
    rad_train = data(:,6);         %radiation [BTU]

    %load initial p-values
    load('./gradient_descent_values_2.mat')

    % Options for the algorithm
    optim_options = optimset('Display', 'iter',...
        'TolFun', 1e-10,... %default: 1e-4
        'TolX', 1e-6... %default: 1e-4
    );

    % Input vector & initial conditions from training data
    U_hat_train = [air_out_train, s_train, rad_train];
    That0_train = [air_in_train(1); mass_wall_train(1);
mass_floor_train(1)];

    % Nonlinear optimization of parameters
    [p,resnorm,residual] = lsqnonlin(@mle_error, Theta_Hat,...
    [0,0,0,-30,0,0,0,0,0,0],...
    [10,10,10,0,10,1,1,10,1,10],...
    optim_options,t_train, U_hat_train, That0_train, air_in_train,...
    mass_wall_train, mass_floor_train);
    Theta_Hat = p;

```

```

% Simulate parameters
Ahat = [(-Theta_Hat(1)-Theta_Hat(2)-Theta_Hat(3)), Theta_Hat(2),
Theta_Hat(3);...
        Theta_Hat(7), -Theta_Hat(6)-Theta_Hat(7), 0;...
        Theta_Hat(9), 0, -Theta_Hat(9)];

Bhat = [Theta_Hat(1), Theta_Hat(4), Theta_Hat(5);...
        Theta_Hat(6), 0, Theta_Hat(8);...
        0, 0, Theta_Hat(10)];
C_dummy = eye(3);
D_dummy = 0;

% State space model
sys_hat = ss(Ahat, Bhat, C_dummy, D_dummy);

%load validation data
if j == 1
    data = data_full(starting_hour+hours:starting_hour+hours*10,:);
elseif j == 10
    data = data_full(starting_hour:starting_hour+hours*9,:);
else
    data = [data_full(starting_hour:starting_hour+hours*(j-1),:);...
            data_full(starting_hour+hours*j:starting_hour+hours*10,:)];
end
t_val = data(:,1); %time vector [hr]
t_val = (0:(length(t_val)-1))'; %resample vector to start at 0

air_out_val = data(:,2); %outdoor air temperature, T_A [deg C]
air_in_val = data(:,3); %indoor air temperature, T_Z [deg C]
mass_wall_val = data(:,4); %wall mass temperature, T_W [deg C]
mass_floor_val = data(:,4); %floor mass temperature, T_F [deg C]
s_val = data(:,5); %window state [0,1]
rad_val = data(:,6); %radiation [BTU]

% Input vector & initial conditions from training data
U_hat_val = [air_out_val, s_val, rad_val];
That0_val = [air_in_val(1); mass_wall_val(1); mass_floor_val(1)];

% Simulate
[~,~,That] = lsim(sys_hat, U_hat_val, t_val, That0_val);

%Calculate error
n = length(t_val);

for i = 1:n
    air_in_pe(i) = abs(air_in_val(i) - That(i,1))/air_in_val(i);
    mass_wall_pe(i) = abs(mass_wall_val(i) -
That(i,2))/mass_wall_val(i);
    mass_floor_pe(i) = abs(mass_floor_val(i) -
That(i,3))/mass_floor_val(i);
    air_in_e(i) = abs(air_in_val(i) - That(i,1));
    air_in_e_sq(i) = air_in_e(i)^2;
    mass_wall_e(i) = abs(mass_wall_val(i) - That(i,2));
    mass_wall_e_sq(i) = mass_wall_e(i)^2;
    mass_floor_e(i) = abs(mass_floor_val(i) - That(i,3));
    mass_floor_e_sq(i) = mass_floor_e(i)^2;

```

```

end

MAPE(j) = mean([air_in_pe, mass_wall_pe, mass_floor_pe]);
SDAPE(j) = std([air_in_pe, mass_wall_pe, mass_floor_pe]);
MAE(j) = mean([air_in_e, mass_wall_e, mass_floor_e]);
SDAE(j) = std([air_in_e, mass_wall_e, mass_floor_e]);
RMSE(j) = sqrt(sum([air_in_e_sq, mass_wall_e_sq,
mass_floor_e_sq])/(3*n));
end

MAPE_avg = mean(MAPE);
SDAPE_avg = mean(SDAPE);
MAE_avg = mean(MAE);
SDAE_avg = mean(SDAE);
RMSE_avg = mean(RMSE);
fprintf(1, 'Average MAPE\n%1.4f\nAverage SDAPE\n%1.4f\nAverage
MAE\n%1.4f\nAverage SDAE\n%1.4f\nAverage RMSE\n%1.4f\n', ...
MAPE_avg, SDAPE_avg, MAE_avg, SDAE_avg, RMSE_avg);

```

### 10.1.8 LEES Optimization with comfort as constraint

```

%% Load Data for room
data = xlsread('VAV_A-1_opt.xlsx');

months = 1;
days = 30*months;
hours = days*24;
starting_hour = 720;
data = data(starting_hour:starting_hour+hours,:);

%time variable
t = data(:,1); %time vector [hr]
t = (0:(length(t)-1))'; %resample vector to start at 0

%original state variables & controllable inputs
air_in_orig = data(:,2); %indoor air temperature, T_Z [deg F]
mass_wall_orig = data(:,3); %wall mass temperature, T_W [deg F]
mass_floor_orig = data(:,4); %floor mass temperature, T_F [deg F]
air_flow_orig = data(:,5); %air flow, V [CFM]
air_supply_orig = data(:,6); %supply temperature, T_V [deg F]

%uncontrollable inputs
air_out = data(:,7); %outdoor air temperature, T_A [deg F]
air_supply = data(:,7); %supply temperature, T_V [deg F]
sol = data(:,8); %radiation [BTU]

% Decide whether time is unoccupied or occupied
hour = data(:,9); %time of day in [HH]
weekday = data(:,10); %weekday [1-7]
occ = hour > 8 & hour <= 16 & weekday > 1 & weekday < 7; %occupancy [0/1]

%Find daily average outdoor air temp
temp = 0;
for i = 1:length(t)
    if i < 14

```

```

        air_out_daily_avg(i,1) = 66.62;
    elseif i > 1428-720
        air_out_daily_avg(i,1) = 63.17;
    else
        if hour(i) == 0
            temp = mean(air_out(i:i+23));
        end
        air_out_daily_avg(i,1) = temp;
    end
end

%Set max and min temperatures & airflow
oper_max = zeros(length(t),1);
oper_min = zeros(length(t),1);
air_flow_max = zeros(length(t),1);
air_flow_min = zeros(length(t),1);
for i = 1:length(t)
    if occ(i) == 1
        if i < 7*24+1
            oper_max(i) = .31*air_out_daily_avg(i)+60.5;
            oper_min(i) = .31*air_out_daily_avg(i)+47.9;
        else
            oper_max(i) = .31*mean(air_out_daily_avg(i-7*24+1:i))+60.5;
            oper_min(i) = .31*mean(air_out_daily_avg(i-7*24+1:i))+47.9;
        end
        air_flow_max(i) = 215;
        air_flow_min(i) = 215;
    else
        oper_max(i) = 90;
        oper_min(i) = 50;
        air_flow_max(i) = 1800;
        air_flow_min(i) = 0;
    end
end

%% Define vectors and matrices for linear programming

len = length(t);

%set optimization variables
air_in = sdpvar(len, 1);
mass_wall = sdpvar(len, 1);
mass_floor = sdpvar(len, 1);
air_flow = sdpvar(len, 1);
oper = sdpvar(len, 1);

%set objective function
Objective = sum(air_flow);

%convert continuous p-values to discrete
load('./p_values_vent_A1_correctsign.mat')
Ahat = [p(1), p(2), p(3);...
        p(8), p(9), 0;...
        p(12), 0, p(13)];
Bhat = [p(4), p(5), p(6), p(7);...
        p(10), 0, 0, p(11)];...

```

```

0, 0, 0, p(14)];
C_dummy = eye(3);
D_dummy = 0;
sys_hat = ss(Ahat, Bhat, C_dummy, D_dummy);
sys_hat = c2d(sys_hat,1);
Ahat_dis = sys_hat.A;
Bhat_dis = sys_hat.B;

p =
[Ahat_dis(1,:),Bhat_dis(1,:),Ahat_dis(2,:),Bhat_dis(2,:),Ahat_dis(3,:),Bhat_
dis(3,:)];

%Set constraints
delta_T = 1;
A_wall = 38*12.5*2 + 49.5*12.5*2;
A_floor = 38*49.5;
constraints = [air_in(1) == air_in_orig(1),...
    mass_wall(1) == mass_wall_orig(1),...
    mass_floor(1) == mass_floor_orig(1)];

for k = 1:len-1
constraints = [constraints,...
    air_in(k+1) == p(1)*air_in(k)+p(2)*mass_wall(k)+p(3)*mass_floor(k)+...
    p(4)*air_out(k)+p(5)*air_flow(k)+p(6)*air_supply(k)+p(7)*sol(k),...
    mass_wall(k+1) ==
p(8)*air_in(k)+p(9)*mass_wall(k)+p(10)*mass_floor(k)+...
p(11)*air_out(k)+p(12)*air_flow(k)+p(13)*air_supply(k)+p(14)*sol(k),...
    mass_floor(k+1) ==
p(15)*air_in(k)+p(16)*mass_wall(k)+p(17)*mass_floor(k)+...
p(18)*air_out(k)+p(19)*air_flow(k)+p(20)*air_supply(k)+p(21)*sol(k)];
end

for k=1:len
    constraints = [constraints,...
        oper(k) ==
(air_in(k)+(A_wall*mass_wall(k)+A_floor*mass_floor(k))/(A_wall+A_floor))/2,...
        ..
        oper_min(k) <= oper(k) <= oper_max(k),...
        air_flow_min(k) <= air_flow(k) <= air_flow_max(k)];
end

%% Optimization
optimize(constraints, Objective)

```

### 10.1.9 LEES Optimization with comfort as objective

```

%% Load Data for room
data = xlsread('VAV_A-1_opt.xlsx');

months = 1;
days = 30*months;
hours = days*24;

```

```

starting_hour = 720;
data = data(starting_hour:starting_hour+hours,:);

%time variable
t = data(:,1);           %time vector [hr]
t = (0:(length(t)-1))'; %resample vector to start at 0

%original state variables & controllable inputs
air_in_orig = data(:,2); %indoor air temperature, T_Z [deg F]
mass_wall_orig = data(:,3); %wall mass temperature, T_W [deg F]
mass_floor_orig = data(:,4); %floor mass temperature, T_F [deg F]
air_flow_orig = data(:,5); %air flow, V [CFM]
air_supply_orig = data(:,6); %supply temperature, T_V [deg F]

%uncontrollable inputs
air_out = data(:,7); %outdoor air temperature, T_A [deg F]
air_supply = data(:,7); %supply temperature, T_V [deg F]
sol = data(:,8); %radiation [BTU]

% Decide whether time is unoccupied or occupied
hour = data(:,9); %time of day in [HH]
weekday = data(:,10); %weekday [1-7]
occ = hour > 8 & hour <= 16 & weekday > 1 & weekday < 7; %occupancy [0/1]

%Find daily average outdoor air temp
temp = 0;
for i = 1:length(t)
    if i < 14
        air_out_daily_avg(i,1) = 66.62;
    elseif i > 1428-720
        air_out_daily_avg(i,1) = 63.17;
    else
        if hour(i) == 0
            temp = mean(air_out(i:i+23));
        end
        air_out_daily_avg(i,1) = temp;
    end
end

%Set max and min temperatures & airflow
oper_max = zeros(length(t),1);
oper_min = zeros(length(t),1);
air_flow_max = zeros(length(t),1);
air_flow_min = zeros(length(t),1);
for i = 1:length(t)
    if occ(i) == 1
        if i < 7*24+1
            oper_max(i) = .31*air_out_daily_avg(i)+60.5;
            oper_min(i) = .31*air_out_daily_avg(i)+47.9;
        else
            oper_max(i) = .31*mean(air_out_daily_avg(i-7*24+1:i))+60.5;
            oper_min(i) = .31*mean(air_out_daily_avg(i-7*24+1:i))+47.9;
        end
        air_flow_max(i) = 215;
        air_flow_min(i) = 215;
    else

```



```

        oper_max(i) = 90;
        oper_min(i) = 50;
        air_flow_max(i) = 1800;
        air_flow_min(i) = 0;
    end
end

%% Define vectors and matrices for linear programming

len = length(t);

%set optimization variables
air_in = sdpvar(len, 1);
mass_wall = sdpvar(len, 1);
mass_floor = sdpvar(len, 1);
air_flow = sdpvar(len, 1);
oper = sdpvar(len, 1);
comf = sdpvar(len,1);

%convert continuous p-values to discrete
load('./p_values_vent_A1_correctsign.mat')
Ahat = [p(1), p(2), p(3);...
        p(8), p(9), 0;...
        p(12), 0, p(13)];
Bhat = [p(4), p(5), p(6), p(7);...
        p(10), 0, 0, p(11);...
        0, 0, 0, p(14)];
C_dummy = eye(3);
D_dummy = 0;
sys_hat = ss(Ahat, Bhat, C_dummy, D_dummy);
sys_hat = c2d(sys_hat,1);
Ahat_dis = sys_hat.A;
Bhat_dis = sys_hat.B;

p =
[Ahat_dis(1,:), Bhat_dis(1,:), Ahat_dis(2,:), Bhat_dis(2,:), Ahat_dis(3,:), Bhat_
dis(3,:)];

%Set objective and constraint
delta_T = 1;
A_wall = 38*12.5*2 + 49.5*12.5*2;
A_floor = 38*49.5;
constraints = [air_in(1) == air_in_orig(1), ...
              mass_wall(1) == mass_wall_orig(1), ...
              mass_floor(1) == mass_floor_orig(1)];
Objective = 0;

for k = 1:len-1
    constraints = [constraints, ...
                  air_in(k+1) == p(1)*air_in(k)+p(2)*mass_wall(k)+p(3)*mass_floor(k)+...
                  p(4)*air_out(k)+p(5)*air_flow(k)+p(6)*air_supply(k)+p(7)*sol(k), ...
                  mass_wall(k+1) ==
                  p(8)*air_in(k)+p(9)*mass_wall(k)+p(10)*mass_floor(k)+...
                  p(11)*air_out(k)+p(12)*air_flow(k)+p(13)*air_supply(k)+p(14)*sol(k), ...

```

```

    mass_floor(k+1) ==
p(15)*air_in(k)+p(16)*mass_wall(k)+p(17)*mass_floor(k)+...

p(18)*air_out(k)+p(19)*air_flow(k)+p(20)*air_supply(k)+p(21)*sol(k)];
end

for k =1:len
    Objective = Objective + air_flow(k)/1800 + comf(k)/5;
    constraints = [constraints,...
        oper(k) ==
(air_in(k)+(A_wall*mass_wall(k)+A_floor*mass_floor(k))/(A_wall+A_floor))/2,...
        ..
        air_flow_min(k) <= air_flow(k) <= air_flow_max(k),...
        comf(k) >= oper(k)-oper_max(k),...
        comf(k) >= oper_min(k)-oper(k),...
        comf(k) >= 0];
end

%% Optimization

optimize(constraints, Objective)

```

### 10.1.10 BH & IND Optimization

#### BH

```

%% Load Data
data = xlsread('Danya_Room.xlsx');
window = xlsread('Window_State.xlsx');

%time vector
t = data(:,6);           %time vector [hr]
t = (0:(length(t)-1))'; %resample vector to start at 0

%Calculate airflow and window state
d_year = data(:,1);
d_month = data(:,2);
d_day = data(:,3);
d_hour = data(:,4);
d_minute = data(:,5);
w_year = window(:,3);
w_month = window(:,4);
w_day = window(:,5);
w_hour = window(:,6);
w_state = window(:,8);

s(1) = 1;
for i = 2:length(t)
    k = 0;
    for j = 1:length(w_state)
        if d_year(i) == w_year(j)
            if d_month(i) == w_month(j)
                if d_day(i) == w_day(j)
                    if d_hour(i) == w_hour(j)
                        if w_state(j) == 1
                            s(i) = 0;

```

```

                                k = 1;
                                else
                                    s(i) = 1;
                                    k = 1;
                                end
                            end
                        end
                    end
                end
            end
        if k == 0
            if s(i-1) == 1
                s(i) = 1;
            else
                s(i) = 0;
            end
        end
    end
end

data = [data,s'];

%original outputs & controllable inputs
air_in_orig = data(:,7);           %indoor air temperature, T_Z [deg C]
mass_wall_orig = data(:,8);        %wall mass temperature, T_W [deg C]
mass_floor_orig = data(:,8);       %floor mass temperature, T_F [deg C]
s_orig = data(:,13);               %window state [0,1]

%uncontrollable inputs
air_out = data(:,9);               %outdoor air temperature, T_A [deg C]
rad = data(:,11);                  %radiation [J]

%Find daily average outdoor air temp
temp = 0;
air_out_daily_avg = zeros(length(t),1);
for i = 1:length(t)
    if i < 23
        air_out_daily_avg(i,1) = 26.92;
    elseif i > 8567
        air_out_daily_avg(i,1) = 28.73;
    else
        if d_hour(i) == 0
            temp = mean(air_out(i:i+23));
        end
        air_out_daily_avg(i,1) = temp;
    end
end

%Set max and min temperatures
oper_max = zeros(length(t),1);
oper_min = zeros(length(t),1);
for i = 1:length(t)
    if i < 7*24+1
        oper_max(i) = .31*air_out_daily_avg(i)+21.3;
        oper_min(i) = .31*air_out_daily_avg(i)+14.3;
    else
        oper_max(i) = .31*mean(air_out_daily_avg(i-7*24+1:i))+21.3;

```

```

        oper_min(i) = .31*mean(air_out_daily_avg(i-7*24+1:i))+14.3;
    end
end

%% Define vectors and matrices for linear programming

len = length(t);

%set optimization variables
air_in = sdpvar(len, 1);
mass_wall = sdpvar(len, 1);
mass_floor = sdpvar(len, 1);
s = sdpvar(len, 1);
s_change = sdpvar(len,1);
oper = sdpvar(len, 1);
comf = sdpvar(len,1);

%convert continuous p-values to discrete
load('./p_values_bounded_sol_2.mat')
Ahat = [(-p(1)-p(2)-p(3)), p(2), p(3);...
        p(7), -p(6)-p(7), 0;...
        p(9), 0, -p(9)];
Bhat = [p(1), p(4), p(5);...
        p(6), 0, p(8);...
        0, 0, p(10)];
C_dummy = eye(3);
D_dummy = 0;
sys_hat = ss(Ahat, Bhat, C_dummy, D_dummy);
sys_hat = c2d(sys_hat,1);
Ahat_dis = sys_hat.A;
Bhat_dis = sys_hat.B;

p =
[Ahat_dis(1,:),Bhat_dis(1,:),Ahat_dis(2,:),Bhat_dis(2,:),Ahat_dis(3,:),Bhat_
dis(3,:)];

%Set objective and constraint
delta_T = 1;
A_wall = 4.34*3.79*2 + 5.47*3.79*2;
A_floor = 4.34*5.47;
constraints = [air_in(1) == air_in_orig(1),...
              mass_wall(1) == mass_wall_orig(1),...
              mass_floor(1) == mass_floor_orig(1),...
              s_change(1) == 0];
Objective = 0;

for k = 1:len-1
    constraints = [constraints,...
                  air_in(k+1) == p(1)*air_in(k)+p(2)*mass_wall(k)+p(3)*mass_floor(k)+...
                      p(4)*air_out(k)+p(5)*s(k)+p(6)*rad(k),...
                  mass_wall(k+1) ==
p(7)*air_in(k)+p(8)*mass_wall(k)+p(9)*mass_floor(k)+...
                      p(10)*air_out(k)+p(11)*s(k)+p(12)*rad(k),...
                  mass_floor(k+1) ==
p(13)*air_in(k)+p(14)*mass_wall(k)+p(15)*mass_floor(k)+...
                      p(16)*air_out(k)+p(17)*s(k)+p(18)*rad(k),...

```

```

    s_change(k+1) == abs(s(k+1)-s(k))];
end

for k = 1:len
    Objective = Objective + comf(k);
    constraints = [constraints,...
        oper(k) ==
        (air_in(k)+(A_wall*mass_wall(k)+A_floor*mass_floor(k))/(A_wall+A_floor))/2,...
        ..
        s(k) == 0 | s(k) == 1,...
        comf(k) >= oper(k)-oper_max(k),...
        comf(k) >= oper_min(k)-oper(k),...
        comf(k) >= 0];
end

for k = 24:len
    constraints = [constraints,...
        sum(s_change(k-23:k)) <= 2];
end

%% Optimization
optimize(constraints, Objective)

```

## IND

```

%% Load Data
data = xlsread('Indio Data.xlsx');

months = 1;
days = 30*months;
hours = days*24;
starting_hour = 720;
data = data(starting_hour:end,:);

t = data(:,1);           %time vector [hr]
t = (0:(length(t)-1))'; %resample vector to start at 0

%original states and inputs
air_in_orig = data(:,3); %indoor air temperature, T_Z [deg C]
mass_wall_orig = data(:,4); %wall mass temperature, T_W [deg C]
mass_floor_orig = data(:,4); %floor mass temperature, T_F [deg C]
s_orig = data(:,5); %window state [0,1]

%uncontrollable inputs
air_out = data(:,2); %outdoor air temperature, T_A [deg C]
rad = data(:,6); %radiation [BTU]

%occupancy and time
occ = data(:,7); %daytime [0/1]
hour = data(:,8); %hour

%Find daily average outdoor air temp
temp = 0;
for i = 1:length(t)
    if hour(i) == 0

```

```

        temp = mean(air_out(i:i+23));
    end
    air_out_daily_avg(i,1) = temp;
end

%Set max and min temperatures & airflow
oper_max = zeros(length(t),1);
oper_min = zeros(length(t),1);
for i = 1:length(t)
    if occ(i) == 1
        if i < 7*24+1
            oper_max(i) = .31*air_out_daily_avg(i)+60.5;
            oper_min(i) = .31*air_out_daily_avg(i)+47.9;
        else
            oper_max(i) = .31*mean(air_out_daily_avg(i-7*24+1:i))+60.5;
            oper_min(i) = .31*mean(air_out_daily_avg(i-7*24+1:i))+47.9;
        end
    else
        oper_max(i) = 90;
        oper_min(i) = 50;
    end
end

%% Define vectors and matrices for linear programming

len = length(t);

%set optimization variables
air_in = sdpvar(len, 1);
mass_wall = sdpvar(len, 1);
mass_floor = sdpvar(len, 1);
s = sdpvar(len, 1);
s_change = sdpvar(len,1);
oper = sdpvar(len, 1);
comf = sdpvar(len,1);

%convert continuous p-values to discrete
load('./p_values_bounded_v2.mat')
Ahat = [(-p(1)-p(2)-p(3)), p(2), p(3);...
        p(7), -p(6)-p(7), 0;...
        p(9), 0, -p(9)];
Bhat = [p(1), p(4), p(5);...
        p(6), 0, p(8);...
        0, 0, p(10)];
C_dummy = eye(3);
D_dummy = 0;
sys_hat = ss(Ahat, Bhat, C_dummy, D_dummy);
sys_hat = c2d(sys_hat,1);
Ahat_dis = sys_hat.A;
Bhat_dis = sys_hat.B;

p =
[Ahat_dis(1,:),Bhat_dis(1,:),Ahat_dis(2,:),Bhat_dis(2,:),Ahat_dis(3,:),Bhat_
dis(3,:)];

%Set objective and constraint

```

```

delta_T = 1;
A_wall = 180*20*4;
A_floor = 180*180;
constraints = [air_in(1) == air_in_orig(1), ...
    mass_wall(1) == mass_wall_orig(1), ...
    mass_floor(1) == mass_floor_orig(1), ...
    s_change(1) == 0];
Objective = 0;

for k = 1:len-1
    constraints = [constraints, ...
        air_in(k+1) == p(1)*air_in(k)+p(2)*mass_wall(k)+p(3)*mass_floor(k)+...
            p(4)*air_out(k)+p(5)*s(k)+p(6)*rad(k), ...
        mass_wall(k+1) ==
            p(7)*air_in(k)+p(8)*mass_wall(k)+p(9)*mass_floor(k)+...
            p(10)*air_out(k)+p(11)*s(k)+p(12)*rad(k), ...
        mass_floor(k+1) ==
            p(13)*air_in(k)+p(14)*mass_wall(k)+p(15)*mass_floor(k)+...
            p(16)*air_out(k)+p(17)*s(k)+p(18)*rad(k), ...
        s_change(k+1) == abs(s(k+1)-s(k))];
end

for k = 1:len
    Objective = Objective + comf(k);
    constraints = [constraints, ...
        oper(k) ==
            (air_in(k)+(A_wall*mass_wall(k)+A_floor*mass_floor(k))/(A_wall+A_floor))/2, ...
        ..
        s(k) == 0 | s(k) == 1, ...
        comf(k) >= oper(k)-oper_max(k), ...
        comf(k) >= oper_min(k)-oper(k), ...
        comf(k) >= 0];
end

for k = 24:len
    constraints = [constraints, ...
        sum(s_change(k-23:k)) <= 2];
end

%% Optimization
optimize(constraints, Objective)

```

## 10.2 R code

### 10.2.1 Heatmap generation

```

#formatting
{
    theme_heatmap = theme(title = element_text(size = 45),
        axis.text.x = element_text(size =
45, colour="black"),

```

```

axis.text.y = element_text(size =
50,colour="black"),
axis.title.x = element_text(size = 55),
axis.title.y = element_text(size = 55),
axis.ticks.y = element_line(colour="black"),
axis.ticks.x = element_line(colour="black"),
legend.text = element_text(size = 45),
legend.title = element_text(size = 50),
legend.position = "right",
legend.key.height = unit(2,"line"),
axis.line = element_line(color = "black"),
strip.text.x = element_text(size = 55),
panel.grid.major.y = element_blank(),
panel.grid.minor.y = element_blank(),
panel.grid.major.x = element_blank(),
panel.grid.minor.x = element_blank(),
panel.background = element_blank()
}

#set color scale
color = scale_fill_gradient2(low = "blue", high = "red", mid =
"white", midpoint = 65, limits = c(30,100),name =
"Ambient\nTemperature\n(°F)\n")

#heatmap
heatmap = ggplot(data, aes(Day, Hour, fill = DB_F)) +
  geom_tile() +
  theme_heatmap +
  color +
  xlab("Day") +
  ylab("Hour")
heatmap
png("ambient_heatmap.png", width=2200, height=1000, units="px");
heatmap; dev.off()

```

## 10.2.2 Boxplot generation

```

#Boxplots
{
  #Formatting
  {

    #Boxplot theme
    theme_box = theme(title = element_text(size = 45),
axis.text.x = element_text(size =
35,colour="black"),
axis.text.y = element_text(size =
40,colour="black"),
axis.title.x = element_text(size = 45),
axis.title.y = element_text(size = 45),
axis.ticks.y = element_line(colour="black"),

```



```

axis.ticks.x = element_line(colour="black"),
legend.text = element_text(size = 45),
legend.title = element_blank(),
legend.position = "bottom",
legend.key = element_rect(fill = NA),
axis.line = element_line(color = "black"),
strip.text.x = element_text(size = 45),
panel.grid.major.y =
element_line(colour="black", size=0.25),
panel.grid.minor.y =
element_line(colour="gray", size=0.25),
panel.grid.major.x = element_blank(),
panel.grid.minor.x = element_blank(),
panel.background = element_blank()

}

#Define boxplot parameters
{
box = geom_boxplot(outlier.colour = "red",
outlier.shape = 16,
outlier.size = 1,
notch = FALSE)

}

#Tz,max
boxplot_tzmax = ggplot(data, aes(Vmode, TZ.max,size =2)) +
box +
theme_box +
xlab("Ventilation mode") +
ylab("Daily maximum indoor air temperature (°F)") +
guides(size = FALSE)
boxplot_tzmax
png("boxplot_tzmax.png", width=1600, height=1000, units="px");
boxplot_tzmax; dev.off()

#Max damping
boxplot_dampmax = ggplot(data, aes(Vmode, Dampmax,size =2)) +
box +
theme_box +
xlab("Ventilation mode") +
ylab("Daily maximum damping (°F)") +
guides(size = FALSE)
boxplot_dampmax
png("boxplot_dampmax.png", width=1600, height=1000, units="px");
boxplot_dampmax; dev.off()

#Tz,range
boxplot_tzrange = ggplot(data, aes(Vmode, TZ.range,size =2)) +
box +
theme_box +
xlab("Ventilation mode") +

```

```

    ylab("Daily indoor air temperature range (°F)") +
    guides(size = FALSE)
    boxplot_tzrange
    png("boxplot_tzrange.png", width=1600, height=1000, units="px");
    boxplot_tzrange; dev.off()

    #Decrement factor
    boxplot_f = ggplot(data, aes(Vmode, f,size =2)) +
    box +
    theme_box +
    xlab("Ventilation mode") +
    ylab("Daily decrement factor [ ]") +
    guides(size = FALSE)
    boxplot_f
    png("boxplot_f.png", width=1600, height=1000, units="px");
    boxplot_f; dev.off()

    #Time lag
    boxplot_tl = ggplot(data, aes(Vmode, TL,size =2)) +
    box +
    theme_box +
    xlab("Ventilation mode") +
    ylab("Daily time lag (h)") +
    guides(size = FALSE)
    boxplot_tl
    png("boxplot_tl.png", width=1600, height=1000, units="px");
    boxplot_tl; dev.off()

    #Heat loss
    boxplot_q = ggplot(data, aes(Vmode, QN.day,size =2)) +
    box +
    theme_box +
    xlab("Ventilation mode") +
    ylab("Energy removed (BTU)") +
    guides(size = FALSE)
    boxplot_q
    png("boxplot_q.png", width=1600, height=1000, units="px");
    boxplot_q; dev.off()

    #Potential energy efficiency
    boxplot_PEE = ggplot(data, aes(Vmode, QN.day.QF.day,size =2)) +
    box +
    theme_box +
    xlab("Ventilation mode") +
    ylab("Potential energy efficiency [ ]") +
    guides(size = FALSE)
    boxplot_PEE
    png("boxplot_PEE.png", width=1600, height=1000, units="px");
    boxplot_PEE; dev.off()

    #Discomfort Degree Hours (+)

```

```

boxplot_ddhp = ggplot(data, aes(Vmode, DDHp.day, size = 2)) +
  box +
  theme_box +
  xlab("Ventilation mode") +
  ylab("Discomfort degree hours (°F-h)") +
  guides(size = FALSE)
boxplot_ddhp
png("boxplot_ddhp.png", width=1600, height=1000, units="px");
boxplot_ddhp; dev.off()

#Discomfort Degree Hours (-)
boxplot_ddhn = ggplot(data, aes(Vmode, DDHn.day, size = 2)) +
  box +
  theme_box +
  xlab("Ventilation mode") +
  ylab("Discomfort degree hours (°F-h)") +
  guides(size = FALSE)
boxplot_ddhn
png("boxplot_ddhn.png", width=1600, height=1000, units="px");
boxplot_ddhn; dev.off()
}

```

### 10.2.3 T-tests

```

df = data.frame(matrix(NA, nrow=48, ncol=2))

#Tz,max
AnovaModel = aov(TZ.max ~ Vmode, data = data)
tuk = TukeyHSD(AnovaModel); tuk; plot(tuk)
tuk_list = unlist(tuk)
df[1,1] = tuk_list["Vmode1"]
df[2,1] = tuk_list["Vmode2"]
df[3,1] = tuk_list["Vmode3"]
df[4,1] = tuk_list["Vmode4"]
df[5,1] = tuk_list["Vmode5"]
df[6,1] = tuk_list["Vmode6"]
df[1,2] = tuk_list["Vmode19"]
df[2,2] = tuk_list["Vmode20"]
df[3,2] = tuk_list["Vmode21"]
df[4,2] = tuk_list["Vmode22"]
df[5,2] = tuk_list["Vmode23"]
df[6,2] = tuk_list["Vmode24"]

#Max Damping
AnovaModel = aov(Dampmax ~ Vmode, data = data)
tuk = TukeyHSD(AnovaModel); tuk; plot(tuk)
tuk_list = unlist(tuk)
df[7,1] = tuk_list["Vmode1"]
df[8,1] = tuk_list["Vmode2"]
df[9,1] = tuk_list["Vmode3"]

```

```

df[10,1] = tuk_list["Vmode4"]
df[11,1] = tuk_list["Vmode5"]
df[12,1] = tuk_list["Vmode6"]
df[7,2] = tuk_list["Vmode19"]
df[8,2] = tuk_list["Vmode20"]
df[9,2] = tuk_list["Vmode21"]
df[10,2] = tuk_list["Vmode22"]
df[11,2] = tuk_list["Vmode23"]
df[12,2] = tuk_list["Vmode24"]

#Tz,range
AnovaModel = aov(TZ.range ~ Vmode, data = data)
tuk = TukeyHSD(AnovaModel); tuk; plot(tuk)
tuk_list = unlist(tuk)
df[13,1] = tuk_list["Vmode1"]
df[14,1] = tuk_list["Vmode2"]
df[15,1] = tuk_list["Vmode3"]
df[16,1] = tuk_list["Vmode4"]
df[17,1] = tuk_list["Vmode5"]
df[18,1] = tuk_list["Vmode6"]
df[13,2] = tuk_list["Vmode19"]
df[14,2] = tuk_list["Vmode20"]
df[15,2] = tuk_list["Vmode21"]
df[16,2] = tuk_list["Vmode22"]
df[17,2] = tuk_list["Vmode23"]
df[18,2] = tuk_list["Vmode24"]

#Decrement factor
AnovaModel = aov(f ~ Vmode, data = data)
tuk = TukeyHSD(AnovaModel); tuk; plot(tuk)
tuk_list = unlist(tuk)
df[19,1] = tuk_list["Vmode1"]
df[20,1] = tuk_list["Vmode2"]
df[21,1] = tuk_list["Vmode3"]
df[22,1] = tuk_list["Vmode4"]
df[23,1] = tuk_list["Vmode5"]
df[24,1] = tuk_list["Vmode6"]
df[19,2] = tuk_list["Vmode19"]
df[20,2] = tuk_list["Vmode20"]
df[21,2] = tuk_list["Vmode21"]
df[22,2] = tuk_list["Vmode22"]
df[23,2] = tuk_list["Vmode23"]
df[24,2] = tuk_list["Vmode24"]

#Heat loss
AnovaModel = aov(QN.day ~ Vmode, data = data)
tuk = TukeyHSD(AnovaModel); tuk; plot(tuk)
tuk_list = unlist(tuk)
df[25,1] = tuk_list["Vmode1"]
df[26,1] = tuk_list["Vmode2"]
df[27,1] = tuk_list["Vmode3"]

```

```

df[28,1] = tuk_list["Vmode4"]
df[29,1] = tuk_list["Vmode5"]
df[30,1] = tuk_list["Vmode6"]
df[25,2] = tuk_list["Vmode19"]
df[26,2] = tuk_list["Vmode20"]
df[27,2] = tuk_list["Vmode21"]
df[28,2] = tuk_list["Vmode22"]
df[29,2] = tuk_list["Vmode23"]
df[30,2] = tuk_list["Vmode24"]

#DDH (+)
AnovaModel = aov(DDHp.day ~ Vmode, data = data)
tuk = TukeyHSD(AnovaModel); tuk; plot(tuk)
tuk_list = unlist(tuk)
df[31,1] = tuk_list["Vmode1"]
df[32,1] = tuk_list["Vmode2"]
df[33,1] = tuk_list["Vmode3"]
df[34,1] = tuk_list["Vmode4"]
df[35,1] = tuk_list["Vmode5"]
df[36,1] = tuk_list["Vmode6"]
df[31,2] = tuk_list["Vmode19"]
df[32,2] = tuk_list["Vmode20"]
df[33,2] = tuk_list["Vmode21"]
df[34,2] = tuk_list["Vmode22"]
df[35,2] = tuk_list["Vmode23"]
df[36,2] = tuk_list["Vmode24"]

#DDH (-)
AnovaModel = aov(DDHn.day ~ Vmode, data = data)
tuk = TukeyHSD(AnovaModel); tuk; plot(tuk)
tuk_list = unlist(tuk)
df[37,1] = tuk_list["Vmode1"]
df[38,1] = tuk_list["Vmode2"]
df[39,1] = tuk_list["Vmode3"]
df[40,1] = tuk_list["Vmode4"]
df[41,1] = tuk_list["Vmode5"]
df[42,1] = tuk_list["Vmode6"]
df[37,2] = tuk_list["Vmode19"]
df[38,2] = tuk_list["Vmode20"]
df[39,2] = tuk_list["Vmode21"]
df[40,2] = tuk_list["Vmode22"]
df[41,2] = tuk_list["Vmode23"]
df[42,2] = tuk_list["Vmode24"]

#PEE
AnovaModel = aov(QN.day.QF.day ~ Vmode, data = data_q)
tuk = TukeyHSD(AnovaModel); tuk; plot(tuk)
tuk_list = unlist(tuk)
df[43,1] = tuk_list["Vmode1"]
df[44,1] = tuk_list["Vmode2"]
df[45,1] = tuk_list["Vmode3"]

```

```
df[46,1] = tuk_list["Vmode4"]
df[47,1] = tuk_list["Vmode5"]
df[48,1] = tuk_list["Vmode6"]
df[43,2] = tuk_list["Vmode19"]
df[44,2] = tuk_list["Vmode20"]
df[45,2] = tuk_list["Vmode21"]
df[46,2] = tuk_list["Vmode22"]
df[47,2] = tuk_list["Vmode23"]
df[48,2] = tuk_list["Vmode24"]

write.csv(df,file = "df.csv")
```